

Plutonic Rocks of the Santa Rita Mountains, Southeast of Tucson, Arizona

GEOLOGICAL SURVEY PROFESSIONAL PAPER 915



Plutonic Rocks of the Santa Rita Mountains, Southeast of Tucson, Arizona

By HARALD DREWES

GEOLOGICAL SURVEY PROFESSIONAL PAPER 915

A petrographic description, augmented by many modal and chemical analyses and radiometric age determinations, of a series of plutonic rocks and related hypabyssal intrusive rocks, and remarks on their relation to some mineral deposits



UNITED STATES DEPARTMENT OF THE INTERIOR

THOMAS S. KLEPPE, *Secretary*

GEOLOGICAL SURVEY

V. E. McKelvey, *Director*

Library of Congress Cataloging in Publication Data

Drewes, Harold, 1927–

Plutonic rocks of the Santa Rita Mountains, southeast of Tucson, Arizona.

(Geological Survey Professional Paper 915)

Bibliography: p.

Includes index.

Supt. of Docs. no.: I 19.16:915

1. Rocks, Igneous. 2. Petrology—Arizona—Santa Rita Mountains. 3. Intrusions (Geology)—Arizona—Santa Rita Mountains.

I. Title. II. Series: United States Geological Survey Professional Paper 915.

QE461.D65 552'.3 75-619358

For sale by the Superintendent of Documents, U.S. Government Printing Office

Washington, D.C. 20402

Stock Number 024-001-02865-4

CONTENTS

	Page		Page
Metric-English equivalents	V	Cretaceous rocks—Continued	
Abstract	1	Josephine Canyon Diorite—Continued	
Introduction	1	Modal and chemical summary	37
Objectives	2	Age and correlation	39
Acknowledgments	3	Madera Canyon Granodiorite	40
Geologic setting	3	Petrography	41
Precambrian rocks	6	Granodiorite	41
Pinal Schist	6	Porphyritic granodiorite	42
Granite gneiss	7	Melanocratic granodiorite	42
Continental Granodiorite	9	Modal and chemical summary	43
Petrography	9	Age and correlation	44
Granodiorite	9	Elephant Head Quartz Monzonite	47
Aplitic rocks	11	Petrography	48
Lamprophyre	13	Quantrell stock, coarse-grained quartz monzonite ..	49
Modal and chemical summary	13	Quantrell stock, fine-grained quartz monzonite	49
Age and correlation	15	Yoas stock, coarse-grained quartz monzonite	50
Triassic and Jurassic rocks	17	Modal and chemical summary	51
Piper Gulch Monzonite	17	Age and correlation	51
Quartz diorite	23	Tertiary rocks	54
Squaw Gulch Granite	24	Rocks of the Gringo Gulch pluton and other rocks	55
Petrography	25	Granitoid rocks of the Helvetia stock	57
Granite and quartz monzonite	26	Petrography	58
Aplite and lamprophyre	27	Modal and chemical summary	60
Modal and chemical summary	28	Age and correlation	61
Age and correlation	28	Quartz latite porphyry of the Greaterville plugs	62
Cretaceous rocks	29	Petrography	65
Granitoid rocks of the Corona stock	29	Modal and chemical summary	66
Josephine Canyon Diorite	33	Age and correlation	67
Petrography	34	Granodiorite of the San Cayetano stock	67
Dioritic rocks	34	References cited	71
Fine-grained quartz monzonite	36	Index	73

ILLUSTRATIONS

	Page
FIGURE 1. Index map showing location of Sahuarita and Mount Wrightson quadrangles and the Santa Rita Mountains	2
2. Index map of the Santa Rita Mountains	4
3. Map showing distribution of Precambrian rocks and specimen collection sites	8
4. Photograph of specimen 17, Continental Granodiorite	10
5. Photomicrograph of specimen 19, slightly metamorphosed Continental Granodiorite	10
6. Photomicrograph of specimen 12, Continental Granodiorite	12
7. Photomicrograph of specimen 17, Continental Granodiorite	12
8. Isometric diagram of a modal tetrahedron	13
9. Modified triangular diagram showing the modal quartz, potassium feldspar, plagioclase, and femic minerals of Continental Granodiorite	14
10. Histograms showing average chemical composition of each group of plutonic rocks	18
11. Map showing distribution of Triassic rocks and specimen collection sites	20
12. Photograph of specimen 37, Piper Gulch Monzonite	21
13. Photomicrograph of specimen 37, Piper Gulch Monzonite	21

	Page
FIGURE 14. Modified triangular diagram showing the modal quartz, potassium feldspar, plagioclase, and femic minerals of Piper Gulch Monzonite and related rocks	22
15. Map showing distribution of Squaw Gulch Granite and sample collection sites	25
16. Photograph of specimen 45, Squaw Gulch Granite	26
17. Photomicrographs of specimen 45, Squaw Gulch Granite	27
18. Photomicrograph of specimen 48, Squaw Gulch Granite	28
19. Modified triangular diagram showing modal quartz, potassium feldspar, plagioclase, and femic minerals of Squaw Gulch Granite ..	30
20. Map showing distribution of granitoid rocks of the Corona stock and specimen collection sites	32
21. Photomicrograph of specimen 64, quartz monzonite of the Corona stock	32
22. Modified triangular diagram showing modal quartz, potassium feldspar, plagioclase, and femic minerals of granitoid rocks of the Corona stock	33
23. Map showing distribution of Josephine Canyon Diorite and specimen collection sites	35
24. Photograph of specimen 80, Josephine Canyon Diorite	36
25. Photomicrographs of specimen 81, Josephine Canyon Diorite	37
26. Modified triangular diagram showing modal quartz, potassium feldspar, plagioclase, and femic minerals of Josephine Canyon Diorite	38
27. Map showing distribution of Madera Canyon Granodiorite and specimen collection sites	41
28. Photograph of specimen 113, nonporphyritic type of Madera Canyon Granodiorite	42
29. Photomicrographs of specimen 113, nonporphyritic type of Madera Canyon Granodiorite	43
30. Photograph of Specimen 127 of the melanocratic type of Madera Canyon Granodiorite	44
31. Modified triangular diagram showing modal quartz, potassium feldspar, plagioclase, and femic minerals of Madera Canyon Granodiorite	45
32. Map showing distribution of Elephant Head Quartz Monzonite and specimen collection sites	47
33. Photograph of Elephant Head	49
34. Photograph of specimen 134, Elephant Head Quartz Monzonite	50
35. Photomicrograph of specimen 132, coarse-grained Elephant Head Quartz Monzonite	50
36. Modified triangular diagram showing modal quartz, potassium feldspar, plagioclase, and femic minerals of Elephant Head Quartz Monzonite	52
37. Modified triangular diagram comparing the range of distribution of the modes of the Josephine Canyon Diorite, Madera Canyon Granodiorite, and Elephant Head Quartz Monzonite	53
38. Map showing distribution of rocks of the Gringo Gulch pluton and other rocks and specimen collection sites	56
39. Modified triangular diagram showing modal quartz, potassium feldspar, plagioclase, and femic minerals of rocks of the Gringo Gulch pluton and of the San Cayetano stock	58
40. Map showing distribution of granitoid rocks of the Helvetia stocks and porphyry of the Greaterville plugs and specimen collection sites	60
41. Photograph of specimen 174, quartz monzonite of the Helvetia stocks	61
42. Photomicrograph of specimen 174, quartz monzonite of the Helvetia stocks	61
43. Modified triangular diagram showing modal quartz, potassium feldspar, plagioclase, and femic minerals of the granitoid rocks of the Helvetia stocks	63
44. Photomicrograph of specimen 185, quartz latite porphyry of the Greaterville plugs	66
45. Modified triangular diagram showing modal quartz, potassium feldspar, plagioclase, and femic minerals of quartz latite porphyry of the Greaterville plugs	68

TABLES

	Page
TABLE 1. Stratigraphic summary of rocks of the Santa Rita Mountains	5
2. Modes of Continental Granodiorite	14
3. Chemical and spectrographic analyses and CIPW norms of Continental Granodiorite	16
4. Summary of radiometric age determinations	17
5. Modes of Piper Gulch Monzonite	22
6. Chemical and spectrographic analyses and CIPW norms of Piper Gulch Monzonite	23
7. Modes of Squaw Gulch Granite	30
8. Chemical and spectrographic analyses and CIPW norms of Squaw Gulch Granite	31
9. Modes of granitoid rocks of the Corona stock	33
10. Chemical and spectrographic analyses and CIPW norms of granitoid rocks of the Corona stock	33
11. Modes of Josephine Canyon Diorite	38
12. Chemical and spectrographic analyses and CIPW norms of Josephine Canyon Diorite	40
13. Modes of Madera Canyon Granodiorite	44
14. Chemical and spectrographic analyses and CIPW norms of Madera Canyon Granodiorite	46
15. Modes of Elephant Head Quartz Monzonite	52

	Page
TABLE 16. Chemical and spectrographic analyses and CIPW norms of Elephant Head Quartz Monzonite	54
17. Modes of the Gringo Gulch pluton	59
18. Chemical and spectrographic analyses and CIPW norms of rocks of the Gringo Gulch pluton	59
19. Modes of granitoid rocks of the Helvetia stocks	62
20. Chemical and spectrographic analyses and CIPW norms of granitoid rocks of the Helvetia stocks	64
21. Modes of quartz latite porphyry of the Greaterville plugs	68
22. Chemical and spectrographic analyses and CIPW norms of quartz latite porphyry of the Greaterville plugs	69
23. Modes of granodiorite of the San Cayetano stock	70
24. Chemical and spectrographic analyses and CIPW norms of granodiorite of the San Cayetano stock	70

METRIC-ENGLISH EQUIVALENTS

Metric unit	English equivalent	
Length		
millimetre (mm)	=	0.03937 inch (in)
metre (m)	=	3.28 feet (ft)
kilometre (km)	=	.62 mile (mi)
Area		
square metre (m ²)	=	10.76 square feet (ft ²)
square kilometre (km ²)	=	.386 square mile (mi ²)
hectare (ha)	=	2.47 acres
Volume		
cubic centimetre (cm ³)	=	0.061 cubic inch (in ³)
litre (l)	=	61.03 cubic inches
cubic metre (m ³)	=	35.31 cubic feet (ft ³)
cubic metre	=	.00081 acre-foot (acre-ft)
cubic hectometre (hm ³)	=	810.7 acre-feet
litre	=	2.113 pints (pt)
litre	=	1.06 quarts (qt)
litre	=	.26 gallon (gal)
cubic metre	=	.00026 million gallons (Mgal or 10 ⁶ gal)
cubic metre	=	6.290 barrels (bbl) (1 bbl=42 gal)
Weight		
gram (g)	=	0.035 ounce, avoirdupois (oz avdp)
gram	=	.0022 pound, avoirdupois (lb avdp)
tonne (t)	=	1.1 tons, short (2,000 lb)
tonne	=	.98 ton, long (2,240 lb)
Specific combinations		
kilogram per square centimetre (kg/cm ²)	=	0.96 atmosphere (atm)
kilogram per square centimetre	=	.98 bar (0.9869 atm)
cubic metre per second (m ³ /s)	=	35.3 cubic feet per second (ft ³ /s)

Metric unit	English equivalent	
Specific combinations—Continued		
litre per second (l/s)	=	.0353 cubic foot per second
cubic metre per second per square kilometre [(m ³ /s)/km ²]	=	91.47 cubic feet per second per square mile [(ft ³ /s)/mi ²]
metre per day (m/d)	=	3.28 feet per day (hydraulic conductivity) (ft/d)
metre per kilometre (m/km)	=	5.28 feet per mile (ft/mi)
kilometre per hour (km/h)	=	.9113 foot per second (ft/s)
metre per second (m/s)	=	3.28 feet per second
metre squared per day (m ² /d)	=	10.764 feet squared per day (ft ² /d) (transmissivity)
cubic metre per second (m ³ /s)	=	22.826 million gallons per day (Mgal/d)
cubic metre per minute (m ³ /min)	=	264.2 gallons per minute (gal/min)
litre per second (l/s)	=	15.85 gallons per minute
litre per second per metre [(l/s)/m]	=	4.83 gallons per minute per foot [(gal/min)/ft]
kilometre per hour (km/h)	=	.62 mile per hour (mi/h)
metre per second (m/s)	=	2.237 miles per hour
gram per cubic centimetre (g/cm ³)	=	62.43 pounds per cubic foot (lb/ft ³)
gram per square centimetre (g/cm ²)	=	2.048 pounds per square foot (lb/ft ²)
gram per square centimetre	=	.0142 pound per square inch (lb/in ²)
Temperature		
degree Celsius (°C)	=	1.8 degrees Fahrenheit (°F)
degrees Celsius (temperature)	=	[(1.8×°C) + 32] degrees Fahrenheit

PLUTONIC ROCKS OF THE SANTA RITA MOUNTAINS, SOUTHEAST OF TUCSON, ARIZONA

By HARALD DREWES

ABSTRACT

Plutonic masses and some related hypabyssal bodies were intruded into the rocks of the Santa Rita Mountains during Precambrian, Triassic, Jurassic, Cretaceous (2 episodes), Paleocene (3 episodes), and Oligocene times. The plutonic rocks range in composition from diorite to granite; most of them are granodiorite or quartz monzonite. The intrusive masses range in size from a small batholith to plugs and related dikes; most of them underlie areas of 1 to 10 square miles. Some of the intrusive masses are locally associated with contact metamorphic mineral deposits, and plugs of quartz latite porphyry of late Paleocene age are closely associated with hydrothermal deposits of base and noble metals in the Helvetia and Greaterville mining districts.

Petrographic descriptions of the plutonic rocks are augmented by nearly 200 modal analyses, more than 50 chemical and spectrographic analyses, and more than 25 radiometric age determinations.

The oldest of the plutonic rocks, the Continental Granodiorite, of Precambrian Y age, is a coarse-grained, very coarsely porphyritic, partly metamorphosed and much-altered granodiorite and quartz monzonite that forms a mass of unknown size. Its host rocks are intensely metamorphosed, but they are not mineralized near the intrusive mass.

During Triassic time, the Piper Gulch Monzonite was intruded, probably along a major northwest-trending fault zone. It consists mainly of very coarse grained, dark-gray, anorthositic-looking rock in large inclusions, septa, and wallrock to younger intrusive masses. Its host rocks are metamorphosed and locally mineralized; the mineralization in the host is probably related to nearby younger intrusive masses.

Squaw Gulch Granite forms a partly concealed batholith or very large stock of Jurassic age. The rock is coarse grained and pinkish gray, and it ranges in composition from granite to quartz monzonite. At least some of its host rocks are contact metamorphosed, and those which are Paleozoic limestone, near the Glove mine, contain contact metamorphic ore deposits, chiefly of base metals and silver.

Magmatic activity was particularly widespread during the Laramide Orogeny extending through much of Late Cretaceous time and through Paleocene time. Quartz monzonite and granodiorite of the Corona stock were intruded into the rocks of the northern end of the Santa Rita Mountains about 73 to 74 m.y. (million years) ago. Three composite stocks were emplaced in the central and southern part of the mountains about 67 to 69 m.y. ago. Of these three, the Josephine Canyon Diorite ranges widely in composition from diorite, syenodiorite, and quartz diorite to granodiorite and quartz monzonite. It is generally a fine- to medium-grained light- to dark-gray rock, and locally it may be associated with base-metal mineral deposits. The Madera Canyon Granodiorite is a coarse-grained light- to medium-gray porphyritic and locally metamorphosed rock not obviously associated with mineral deposits. The Elephant Head Quartz Monzonite is also coarse grained, is pinkish gray, and is only locally associated with a little mineralization.

Scattered small stocks and plugs, such as the Gringo Gulch pluton, were intruded into rocks of the southern part of the Santa Rita Mountains, at least in part during the early Paleocene. They include some

hypabyssal rocks of uncertain composition, age, and geologic association, some hornblende dacite porphyry plugs, and a small micro-granodiorite plug.

During the late Paleocene, one group of small barren stocks and a group of ore-associated plugs were intruded into complexly faulted rocks of the Helvetia and Greaterville mining districts of the northern part of the Santa Rita Mountains. The stocks of Helvetia are mainly of granodiorite and quartz monzonite; they are elliptical in plan, their position and shape is only slightly controlled by faults, and the host rocks are widely metamorphosed. The plugs of Greaterville are of quartz latite porphyry, are commonly irregular in plan, and are strongly controlled by faults. Hydrothermal fluids associated with these plugs deposited base and noble metals in favorable host rocks along faults near the plugs.

A small stock of granodiorite, of late (?) Oligocene age, was intruded into the rocks of the San Cayetano Mountains. This stock is believed to occupy part of a magma chamber associated with an extensive volcanic pile in the nearby Grosvenor Hills area.

INTRODUCTION

Plutonic rocks and related hypabyssal intrusive rocks underlie much of the Santa Rita Mountains and adjacent mountains of southeastern Arizona. Significant intrusive events are recorded during the Precambrian, Triassic, Jurassic, Late Cretaceous, Paleocene, and Oligocene. The plutonic rocks intrude sequences of Precambrian metamorphic rocks, Paleozoic sedimentary rocks, and several sequences of Mesozoic and Cenozoic sedimentary and volcanic rocks. As a result of this extensive geologic record, the Santa Rita Mountains are the best reference area from which to develop the regional geologic history. The plutonic rocks deserve special attention not only because they are closely related to the depositional and tectonic development of the area, but also because they provide most of the radiometrically datable rocks, and because some of them seem to be genetically related to mineral deposits.

The Santa Rita Mountains are the first range southeast of Tucson (fig. 1). They extend more than 25 miles southward from Pantano Wash, along which the main railroad and highway east of Tucson lie, to Sonoita Creek, about 12 miles from the Mexican border. The mountains commonly reach heights of 6,000 to 7,000 feet and the highest, Mount Wrightson, is 9,453 feet high. The broad

valley east of the mountains lies at an elevation of about 4,500 feet, whereas the valley west of the mountains is only 3,000 feet high. The mountains are high enough to receive an amount of precipitation adequate to support an extensive, though largely scrubby, forest, which contrasts strikingly with grasslands in the high valley to the east and with the thorn brush and cactus vegetation typical of the Sonoran Desert plant assemblage in the low valley to the west.

OBJECTIVES

A geologic investigation of the Santa Rita Mountains was carried out by the U.S. Geological Survey during 1962–68 to help determine the geologic history of a part

of southeastern Arizona having the potential of being one of the major sources of copper in the country. Several mountain ranges were studied during part of the 1950's and 1960's by eight geologists, J. R. Cooper, S. C. Creasey, T. L. Finnel, P. T. Hayes, E. R. Landis, R. B. Raup, F. S. Simons, and the author. The results of the investigation in the Santa Rita Mountains are presented mainly on two geologic maps (Drewes, 1971b, c) and in a report on the structural geology of the area (Drewes, 1972b). Details on field and laboratory observations and analyses that support the main interpretations and the results of subordinate studies on particular topical problems are presented in separate reports, referred to

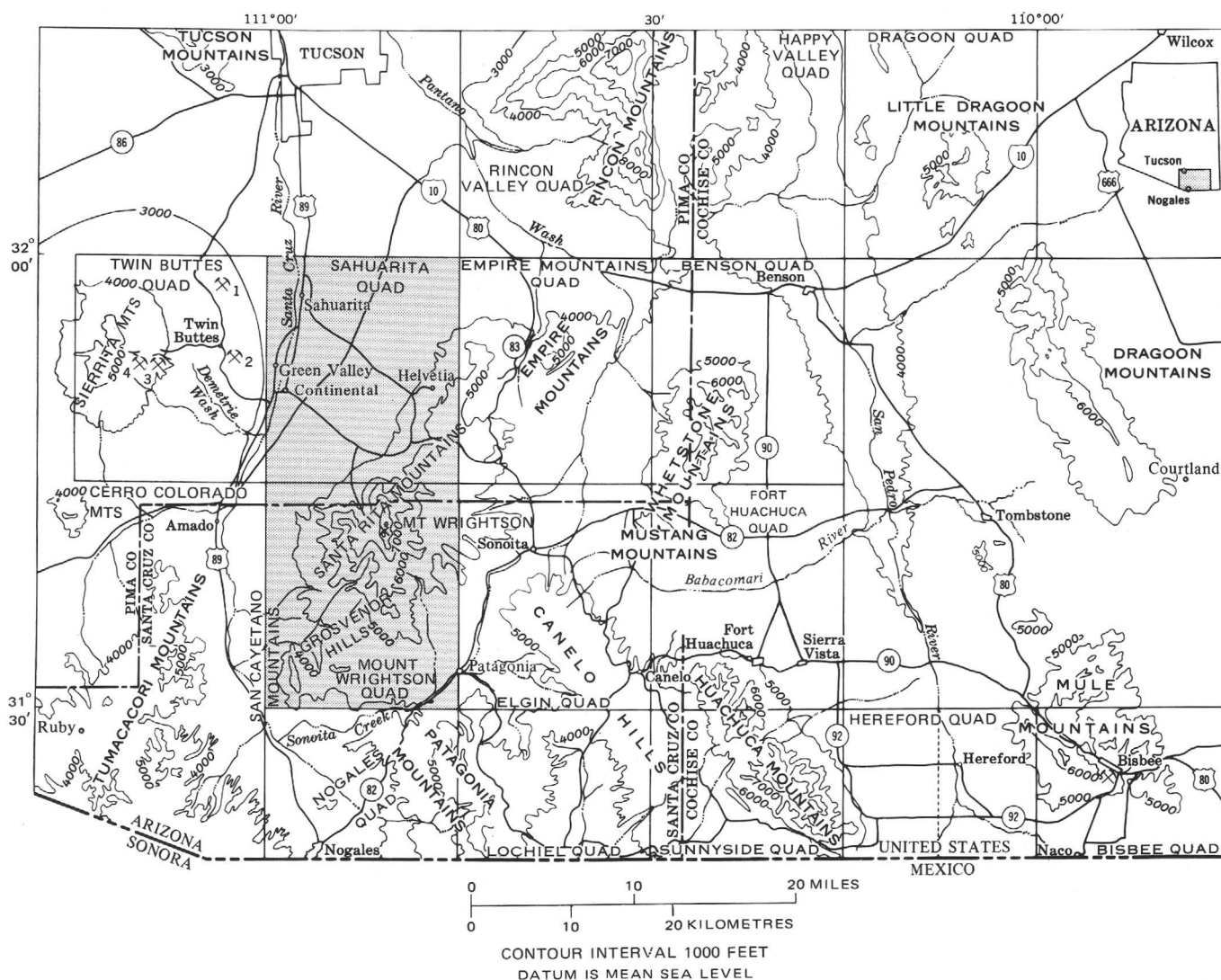


FIGURE 1.—Location of the Sahuarita and Mount Wrightson quadrangles and the Santa Rita Mountains, southeastern Arizona. Major copper mines: 1, Mission-Pima; 2, Twin Buttes; 3, Esperanza; 4, Sierrita. Published geologic maps: Twin Buttes quadrangle (Cooper, 1974), Empire Mountains quadrangle (Finnel, 1973), Benson

quadrangle (Creasey, 1967), Happy Valley quadrangle (Drewes, 1974), Nogales and Lochiel quadrangles (Simons, 1974), Sunnyside quadrangle and parts of Hereford and Fort Huachuca quadrangles (Hayes and Raup, 1968), Bisbee quadrangle (Hayes and Landis, 1964), and Driagoon quadrangle (Cooper and Silver, 1964).

herein where pertinent. The objective of the present report is to support and augment the study of the structural history of the Santa Rita Mountains by presenting abundant data on the plutonic and related rocks.

The petrographic studies of the plutonic rocks of the Santa Rita Mountains include both field and laboratory observations. Almost 200 modal analyses were made by petrographic microscope. More than 50 chemical analyses of the major constituents of rocks and spectrographic analyses of the trace constituents of the rocks are presented, and 27 radiogenic age determinations are included.

This considerable effort in describing and defining the plutonic rocks of the area was made for two reasons. First, the evidence was clear early during the field investigations that the area contained plutonic rocks of many ages, among them some new additions to the then-available geologic knowledge of the region. Second, some plutonic rocks were more closely related to mineralization than others, which suggested that distinguishing between the plutonic rocks was desirable for purposes of mineral exploration. Furthermore, the conditions of emplacement of the plutons and their subsequent alteration are also of potential economic interest.

For the purpose of this report, the area referred to as the Santa Rita Mountains coincides with the Mount Wrightson and Sahuarita 15-minute quadrangles (fig. 2). A small part of the northern end of the mountains is therefore omitted; it lies in the Empire Mountains quadrangle mapped by T. L. Finnell (1971). At the southwest flank of the Santa Rita mountains the outlying hills named the Grosvenor Hills and the San Cayetano Mountains are included in this study.

Included in this study of plutonic rocks are some granitoid rocks believed to be intruded near the surface and some fine-grained hypabyssal intrusive rocks believed to be genetically related to the plutonic rocks. Precambrian regionally metamorphosed rocks are also mentioned herein simply for convenience and in order to complete the general description of the rocks of the Santa Rita Mountains. Hereafter in this report general references to plutonic rocks of the area are used in the sense of including these few hypabyssal granitoid rocks and aphanitic rocks and the Precambrian metamorphic rocks, unless specifically stated otherwise.

ACKNOWLEDGMENTS

The geologic investigation of the Santa Rita Mountains was carried out approximately simultaneously with the other studies of the larger program of the U.S. Geological Survey, mentioned in the preceding section. As a result, the investigation benefited through field consultations and from frequent discussions with my colleagues during the preparation of all the reports. I am particularly grateful for the benefits derived from the colleagues who have worked

in the adjoining areas (fig. 1)—J. C. Cooper for the Sierrita Mountains, T. L. Finnell for the Empire Mountains, R. B. Raup for the Canelo Hills, and F. S. Simons for the Patagonia Mountains. Undoubtedly some geologic interpretations were developed jointly with them, yet the following presentation of these ideas and their validity in the context of the geology of the Santa Rita Mountains remain my own responsibility.

The success of the field study was facilitated by many people. Invaluable assistance in mapping and sampling was provided by G. C. Cone, Bruce Hansen, C. W. Norton, F. W. Plut, J. R. Riele, R. A. Rohrbacker, F. Sutheimer, and W. M. Swartz. Discussions in the field benefited from the experience of R. E. Wallace, M. D. Crittenden, Jr., J. H. Courtright, and many others. The courtesies of George and Sis Bradt, Roy Green, Dewey Kieth, and George Yakobian, all residents near the Santa Rita Mountains, and those of Professors John Anthony, Evans Mayo, and P. E. Damon of the University of Arizona are appreciated.

Invaluable support was obtained from many laboratories. One radiometric age determination was obtained from P. E. Damon before its publication, and the others were provided by R. F. Marvin, T. W. Stern, Z. E. Peterman, S. C. Creasey, and their many colleagues. Chemists and spectrographers who have contributed are acknowledged in the tables of analytical data. G. C. Cone also assisted in many phases of the preparatory work on samples.

Previous geologic studies of the Santa Rita Mountains are few, and most of them consider very local areas or topical problems. The study by Schrader (1915) represents the pioneer effort at geologic mapping in the area and the influence of his work is still noticeable on the latest edition of the geologic map of Arizona (Wilson and others, 1969). Several Master of Science theses on file at the University of Arizona were also consulted. The present geologic study is thus most accurately viewed as a second-generation effort, even though in some respects this is an overstatement.

GEOLOGIC SETTING

The geologic setting of the plutonic rocks of the Santa Rita Mountains has been extensively described in earlier reports (Drewes, 1972a, b), but for convenience of the reader, the geologic history is briefly summarized here. The names, stratigraphic positions, and ages of the plutonic rocks and the other rocks of the area are shown in table 1.

The oldest known rocks of the area are regionally metamorphosed rocks conventionally assigned to the Pinal Schist. In most nearby areas the formation is a muscovite-chlorite or muscovite-biotite schist, but locally this formation consists largely of biotite gneiss and granite gneiss and of only a small amount of schist, which are described in the following section of this report. These rocks were deformed, metamorphosed, and intruded,

PLUTONIC ROCKS, SANTA RITA MOUNTAINS, SOUTHEAST OF TUCSON, ARIZONA

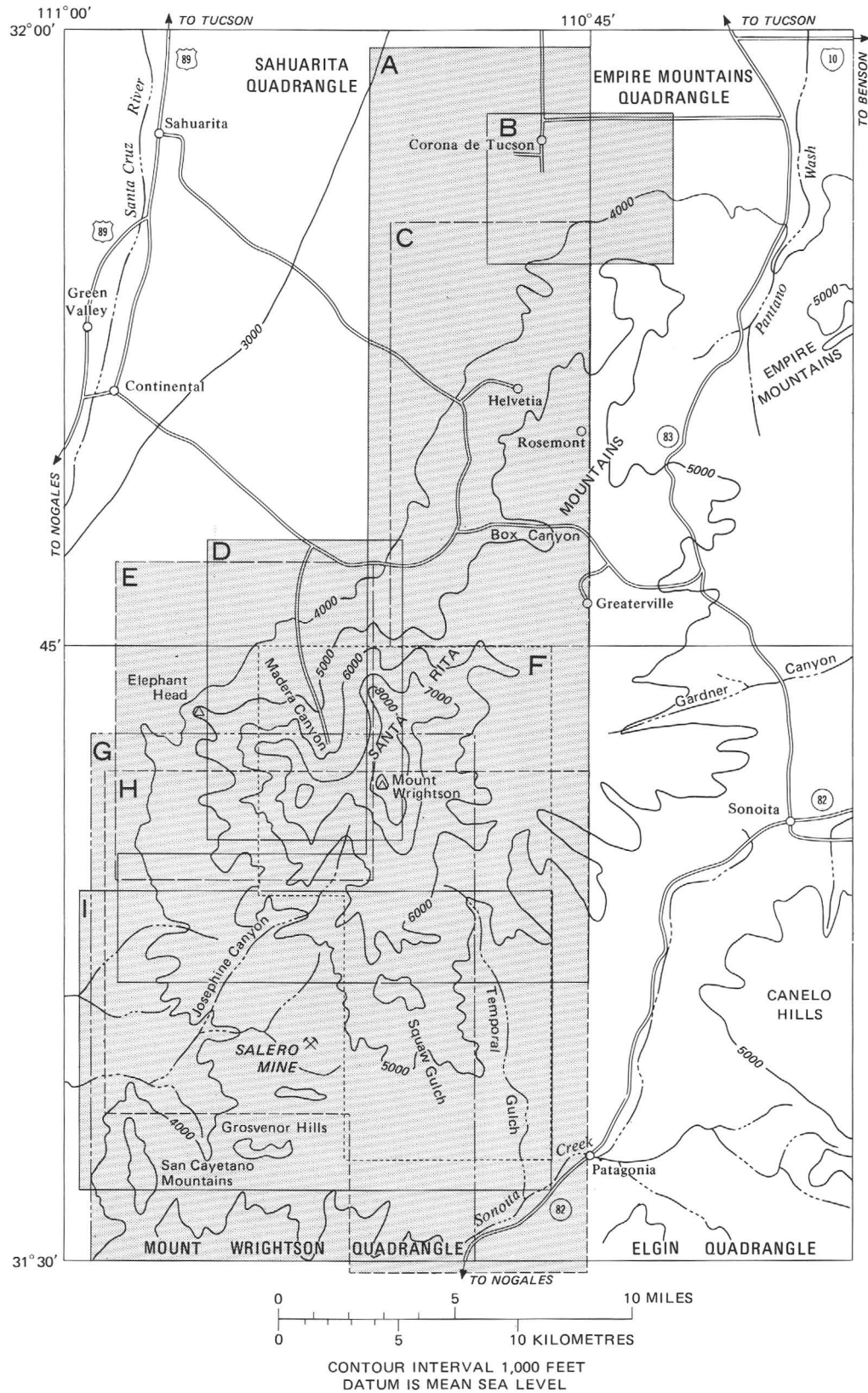


FIGURE 2.—The Santa Rita Mountains, showing areas covered by geologic maps in this report: A, figure 3; B, figure 20; C, figure 40; D, figure 27; E, figure 32; F, figure 11; G, figure 23; H, figure 15; I, figure 38.

TABLE 1.—*Stratigraphic summary of rocks of the Santa Rita Mountains, indicating the rocks described in this report*

Age	Rocks described in this report (mainly plutonic rocks)	Other rocks
Quaternary and Tertiary		Gravel.
Tertiary: Miocene and Pliocene		Nogales Formation. ¹
Oligocene	Granodiorite of San Cayetano Mountains.	Grosvenor Hills Volcanics, laccoliths, and dike swarms. ¹
Paleocene to Oligocene		Rhyolite, andesite, and quartz veins. ¹
Paleocene	Aphanitic rocks, Greaterville intrusives; granitic rocks, Helvetia stocks; rocks of Gringo Gulch pluton.	
Paleocene(?)		Gringo Gulch Volcanics, volcanics of Red Mountain. ¹
Tertiary or Cretaceous	Quartz latite porphyry intrusives.	
Late Cretaceous	Elephant Head Quartz Monzonite.	
Do	Madera Canyon Granodiorite.	
Do	Josephine Canyon Diorite.	
Do	Granitoid rocks of Corona stock.	Salero Formation. ¹
Do		Fort Crittenden Formation. ¹
Early Cretaceous		Bisbee Group.
Do		Bathtub Formation. ¹
Do		Temporal Formation. ¹
Jurassic	Squaw Gulch Granite.	
Triassic	Piper Gulch Monzonite.	
Do		Gardner Canyon Formation. ¹
Do		Mount Wrightson Formation. ¹
Permian		Rainvalley Formation.
Do		Concha Limestone.
Do		Scherrer Formation.
Do		Epitaph Dolomite.
Do		Colina Limestone.
Permian and Pennsylvanian		Earp Formation.
Pennsylvanian		Horquilla Limestone.
Mississippian		Escabrosa Limestone.
Late Devonian		Martin Formation.
Late and Middle Cambrian		Abrigo Formation.
Middle Cambrian		Bolsa Quartzite.
Precambrian Y	Continental Granodiorite.	
Precambrian X	Pinal Schist and granite gneiss.	

¹ Formation that contains volcanic rocks.

either during one geologic event or separately in the given sequence, by a large pluton of Continental Granodiorite (Drewes, 1968). The rocks were uplifted and deeply eroded before the deposition of a sequence of Paleozoic rocks; indeed, considering evidence from the Rincon Mountains (fig. 1) 10 miles north of the Santa Rita Mountains, this uplift predates the deposition of the Apache Group of Precambrian Y age.

The Paleozoic rocks of the Santa Rita Mountains are believed to have lain unconformably on the Precambrian crystalline rocks, although they are now invariably faulted upon them. The Paleozoic rocks form a concordant marine sequence that begins with the Bolsa Quartzite of Middle Cambrian age, contains several disconformities, and ends

with the Rainvalley Formation, of late Early Permian or slightly younger age. Nearby areas have no Permian rocks younger than the Rainvalley Formation. This marine sequence was deposited in a shallow continental sea and its internal disconformities mark a succession of epeirogenic fluctuations of an otherwise tectonically stable region.

Moderate tectonic activity marked the interval between the deposition of Permian rocks and the onset of the Laramide orogeny in mid-Cretaceous time. Toward the end of the Permian the region was uplifted and the sea retreated; in Early Triassic time, the area now occupied by the Santa Rita Mountains was faulted, an uplifted block was deeply eroded, and a thick pile of volcanic and sedimentary rocks of the Mount Wrightson and Gardner

Canyon Formations were deposited in a fault-block basin (Drewes, 1971a). Near the end of Triassic time a stock of the Piper Gulch Monzonite was intruded, perhaps along an old fault zone, the Santa Rita fault scar (Drewes, 1972b). During the Jurassic Period a large stock or small batholith of granite intruded the southern part of the area. Faulting and erosion followed, and during Early Cretaceous time the Temporal Formation, Bathtub Formation and Bisbee Group were deposited in a continental environment. Both the local relief and tectonic activity decreased during this interval and, before its close, a shallow sea briefly encroached upon the area for the last time.

The initial impulse of the Laramide orogeny occurred during mid-Cretaceous time, for the Upper Cretaceous Fort Crittenden Formation was deposited unconformably upon the Lower Cretaceous Bisbee. The deposition of coarse clastic rocks and resumption of volcanism mark the upper part of the Fort Crittenden and widespread volcanism is recorded in the succeeding Salero Formation. During this time, the Corona stock was emplaced in the northern part of what is now the Santa Rita Mountains. Major northeastward-directed thrust faulting marked the tectonic climax of the Piman phase of the Laramide orogeny during the time of deposition of the Salero Formation (probably Campanian time). The Piman phase culminated a few million years later with a series of multiple intrusions of rocks known as the Josephine Canyon Diorite, Madera Canyon Granodiorite, and Elephant Head Quartz Monzonite.

During early Paleocene time, about 63 to 58 m.y. (million years) ago, the area was tectonically fairly quiet. The Josephine Canyon stock, a large epizonal body, was partly exposed by erosion and the volcanic and sedimentary rocks of the Gringo Gulch Volcanics and the volcanic rocks of Red Mountain were deposited in the southern part of the area. The Gringo Gulch pluton and other small bodies were probably emplaced during that time.

In late Paleocene time, tectonic and volcanic activity was renewed in the northern part of the area to record the Helvetian phase of the Laramide orogeny (Drewes, 1972b). Minor northwestward-directed thrust faulting was penecontemporaneous with the emplacement of a group of small stocks named the Helvetia stocks. Quartz latite porphyry intrusives that are locally referred to as "ore porphyry" because of their association with mineralization (Drewes, 1970) were intruded at the close of the Helvetian phase of the Laramide orogeny.

During the time between the Paleocene and Oligocene the local geologic record is fragmentary. Mineralized quartz veins were emplaced in the southern part of the area and some rhyolite volcanic rocks and andesitic intrusive rocks were emplaced in the northern part. The area was strongly eroded and possibly block faulted to form the ancestral Santa Rita Mountains.

During late Oligocene time magmatic activity was renewed in the southern part of the area. Rhyolite and rhyodacite of the Grosvenor Hills Volcanics were extruded as flows and tuffs. Vitric laccoliths and dikes were intruded into these tuffs (Drewes, 1972a), and at a considerably greater depth the feeder dikes of the volcanic rocks and hypabyssal intrusive rocks are believed to have emanated from small stocks such as that of the granodiorite of the San Cayetano Mountains, the youngest pluton of the area.

The area was block faulted several times during the late Tertiary and Quaternary, and gravel of several formations filled the basins next to the raised and gently southeastward tilted Santa Rita Mountains. The latest magmatic activity is recorded by basalt flows, of Miocene or Pliocene age that are intercalated in the oldest unit of gravel along the Santa Cruz River a few miles south and west of the Mount Wrightson quadrangle.

In the above review of the geologic setting of the plutonic rocks, as well as in the summary in table 1, the association of plutonic events with volcanic and tectonic events seems clear. Likewise, some of the magmatic events are shown to be related, at least in time if not also in origin, to mineralization.

PRECAMBRIAN ROCKS

Rocks of Precambrian age compose an older group of regionally metamorphosed granite, gneiss, and schist and a younger granodiorite pluton. As mentioned before, the metamorphic rocks are described with the plutonic rocks because they have not been previously described in the topical papers on the Mesozoic or Cenozoic rocks of the area. The metamorphic rocks include rocks assigned to the Pinal Schist and to an associated granite gneiss, and they are intruded by the Precambrian Continental Granodiorite.

PINAL SCHIST

The oldest rocks of the Santa Rita Mountains are foliated rocks that sufficiently resemble the Pinal Schist of some nearby areas to be assigned to that formation. The Pinal Schist, as it has been used in southeastern Arizona in recent decades, includes a wide variety of metasedimentary, metavolcanic, and other metaigneous rock types, probably of significantly different ages from place to place. Cooper and Silver (1964, p. 23, 24) described in detail a variety of these rocks that are extensively exposed 30 miles east-northeast of the north end of the Santa Rita Mountains. Somewhat more gneissic varieties are being studied in the Rincon Mountains (Drewes, 1974).

In the Santa Rita Mountains, Pinal Schist appears in a few small widely scattered areas, shown in detail on the geologic map of the Sahuarita quadrangle (Drewes, 1971b) and shown in a more general way, as rocks older than the Continental Granodiorite, in figure 3 of this report. Biotite gneiss and schist are the most common lithology, and

chlorite schist and phyllite appear in a few localities. The Pinal Schist in the large outcrop areas, lying athwart the crest of the mountains west of Greaterville, is biotite gneiss and schist that is intruded to the north and east by the Continental Granodiorite and is faulted against younger rocks to the southwest. The intrusive contact is broad and gradational, and inclusions of Pinal Schist occur in the granodiorite as far north as Box Canyon (fig. 3).

The rocks of the main outcrop areas consist of alternating layers, typically a half an inch to many inches thick, of biotite gneiss or biotite schist and of feldspathic rock. Less commonly the rocks also include hornblende-biotite gneiss and some pegmatite bodies and lamprophyre dikes that may be related to the Continental Granodiorite. Weathered outcrops of biotite gneiss are dark grayish brown and have the sheen of a micaceous surface. The relatively unweathered outcrops, such as those along the bottom of Sawmill Canyon, are medium dark gray and the gneissic layers are more conspicuous. In places these layers are strongly deformed on a small scale, in the manner of pygmy folds. Elsewhere the layers are cut by many small faults and intrusives that are internal features of the formation which may be related to the emplacement of the nearby Continental Granodiorite. Locally the attitude of the foliation appears to be erratic, but over the outcrop area foliation strikes northwesterly and dips steeply southwest.

Under the microscope, the grains of a typical dark or micaceous layer are seen to be about 0.5 mm long and those of the adjacent light-colored felsic layers 0.5 to 1.5 mm. Aligned grains of biotite control the strong schistosity of the rock; grain alignment is fairly subtle in the felsic layers. Dark layers have an estimated mode of: quartz, 5; andesine plagioclase, 65; biotite, 30; ilmenitic magnetite, 3; and traces each of sphene, apatite, zircon, and allanite(?). Light layers have an estimated mode of: quartz, 50; andesine, 40; biotite, 5; and traces each of magnetite, sphene, and apatite. Alteration minerals are scarce and they consist of a little chlorite and epidote. The anorthite content of plagioclase ranges from 38 to 42 percent. Biotite is pleochroic in pale yellow brown to moderate brown.

Chlorite schist and phyllite are mapped (Drewes, 1971b) as small slivers along a northwest-trending tear fault about half a mile east of Helvetia. The rocks crop out on dark-gray low knolls or ledges in many places surrounded by slopes of light-brownish-gray Continental Granodiorite. The schist consists of microscopic layers of aligned mica and of quartz and feldspar with a cataclastic texture. Biotite, plagioclase, and quartz each make up about 30 percent of the rock, sericite and chlorite each almost 5 percent of the rock, and ilmenitic magnetite, zircon, and apatite trace amounts. The chlorite- and biotite-rich layers have a felty texture, indicative of recrystallization after shearing. The quartz forms mosaic-textured or

interlocking aggregates of crystals, also indicative of postcataclasis recrystallization.

The origin and metamorphic development of the biotite gneiss and schist and of the chlorite schist and phyllite are uncertain. The biotite gneiss may have been a sedimentary rock, whose alternating beds of siltstone and arkosic sandstone were transformed by dynamothermal (load?) metamorphism into a rock in the biotite-chlorite subfacies of the greenschist facies (Turner and Verhoogen, 1951, p. 446). Many of the aplitic sheets intruded subparallel to the foliation could be orogenic features, perhaps related to metamorphism itself. These events may have occurred during the Mazatzal Revolution (Wilson, 1939, p. 1161). The chlorite schist and phyllite were tectonically deformed by movement along the tear faults in which the slivers lie. These faults were active during the Helvetian phase of the Laramide orogeny (Drewes, 1972b). The posttectonic recrystallization was probably concomitant with the emplacement of the youngest quartz latite porphyry plugs toward the end of the Paleocene. Alternatively, the recrystallization may be still younger and related to the mid-Tertiary thermal event recorded mainly in the Rincon Mountains.

GRANITE GNEISS

Granite gneiss crops out over an area of about 3 square miles near Cottonwood Canyon on the west flank of the southern part of the Santa Rita Mountains; it is shown as schist and granite gneiss in figure 3 and is shown in greater detail on the geologic map of the Mount Wrightson quadrangle (Drewes, 1971c). The gneiss is intruded by granitoid rocks that resemble the Continental Granodiorite or a strongly metamorphosed equivalent of that granodiorite. The foliation of the gneiss and the geologic relation with the granodiorite suggest that the gneiss is probably of the same general age as the Pinal Schist. Rocks of Paleozoic or younger age overlie, or are faulted against, the granite gneiss.

The granite gneiss underlies low hills, which are uniformly colored a pale brownish gray, that contrast subtly with the more varicolored hills of volcanic rocks to the east and west. A northwest-trending grain, reflecting the strike of the foliation, helps to distinguish this terrain from the nearby hills of Jurassic granite. Although generally striking northwestward, the foliation of the gneiss is arcuate, concave to the northeast, and dips moderately to the southwest.

In detail, the lithology of the granite gneiss varies as much as does that of the Pinal Schist. In the northeastern part of the outcrop area the rock is a faintly gneissic quartz monzonite. The central part of the area contains the typical granite gneiss, and the southwestern part contains a biotite-granite gneiss. Shearing and chemical alteration of the rocks increases toward the north and northeast, where faults bound the gneiss.

The granite gneiss has a hypidiomorphic-granular to tabular microscopic texture that is modified by an alignment of mineral grains and by a slight zoning of light- and dark-colored grains. In this section, some specimens show a seriate texture. Mineral grains are commonly 0.2–3.0 mm long, and in some specimens the grain size distribution is bimodal with the smaller grains included in larger poikilitic grains.

Essential minerals of the gneiss typically are quartz, microcline, plagioclase, and biotite, but some rocks have only one of the feldspars. The microcline contains very fine perthitic intergrowths and indistinct grid twinning that appears to be partly obliterated. The plagioclase commonly has a calcic oligoclase composition, but in some rocks it has an albite composition, presumable as a result of albitization. Biotite forms discrete subhedral plates that are pleochroic in yellowish brown to moderate brown and that are partly chloritized. In addition, the rock contains 0.5 to 3 percent each of ilmenitic magnetite and apatite and trace amounts of sphene and zircon. This entire mineral assemblage is slightly to moderately altered to epidote, chlorite, sericite, kaolinite, and leucoxene.

The granite gneiss presumably was formed by the metamorphism of granitoid rock. This metamorphism probably is part of the regional metamorphism affecting the Pinal Schist, for it is associated with a well-developed foliation and shows no increase in intensity near the contact with younger plutonic rocks. This rock, then, may well be the oldest plutonic rock of the Santa Rita Mountains.

CONTINENTAL GRANODIORITE

The Continental Granodiorite is a coarse-grained and coarsely porphyritic rock that forms part of a single large stock (or batholith?) in the northern part of the Santa Rita Mountains; it also forms some small intrusive bodies on the southwest flank of the mountains (fig. 3). The formation was defined and was briefly described by Drewes (1968); further details on its distribution are shown on the geologic maps of the area (Drewes, 1971b and 1971c). The granodiorite is generally massive, but locally it is faintly foliated. Dark minerals are fairly abundant in this rock, and they typically form aggregates that form a meshwork around the light-colored minerals.

The Continental Granodiorite intrudes the Pinal Schist, which forms roof pendants or remnants of wallrock, as well as some scattered inclusions. Small bodies of granodiorite also intrude the granite gneiss of the southwestern flank of the mountains. Bolsa Quartzite, of Cambrian age, is the oldest rock overlying the granodiorite, but, inasmuch as these rocks seem to be separated everywhere by a fault, the geologic relations have been variously interpreted as a depositional contact and as an intrusive one. The fault separating the

granodiorite from the Bolsa is believed to be a regional thrust fault of the Piman phase of the Laramide orogeny (Drewes, 1972b), which followed a major unconformity. The complexities of this contact led to conflicting interpretations on the age of the granodiorite, as reviewed in the section on the age of that rock.

PETROGRAPHY

The Continental Granodiorite is made up mainly of granodiorite, but it includes small aplitic dikes and sills and small lamprophyre dikes. These small intrusive bodies presumably are genetically related to the granodiorite pluton because they are virtually coextensive with it and are absent in the younger rocks around it. The included dikes and sills are too small to be shown in figure 3 but the distribution of some of the larger aplitic masses are shown on the geologic maps of the northern part of the mountains (Drewes, 1971b; 1972b, pl. 5).

GRANODIORITE

The dominant rock type of the Continental Granodiorite is mostly biotite granodiorite, but in places it grades into biotite quartz monzonite, and it includes some biotite-hornblende granodiorite. The rock of the main outcrop area in the northern part of the mountains (fig. 3) is almost free of hornblende and grades, seemingly at random, from the biotite granodiorite to the biotite quartz monzonite. The rock of the small outcrop areas, to the southwest, contains several percent of hornblende.

Slopes underlain by the granodiorite are somber colored and mostly a light brownish gray. Outcrops are small and irregular; even in the deepest canyons, such as Box Canyon, they rarely form extensive cliffs because the rock is abundantly fractured and disaggregates readily. As a result of these internal weaknesses, the local relief on slopes underlain by granodiorite is generally more subdued than that on nearby slopes underlain by Paleozoic rocks or by some of the younger plutonic rocks. In areas of low relief the granodiorite is covered thickly by grus and in all areas the freshest exposures are in the narrowest and deepest gullies or canyons. The one exception to this weak weathering habit occurs along the crest of the mountains southeast of Helvetia, where the granodiorite is very massive and less friable than elsewhere, and so it forms large rounded knobs and bosses which dominate the landscape.

Unweathered specimens of granodiorite (fig. 4) are dark gray, commonly with a slight greenish tinge in rocks having perhaps as much as 20 percent dark minerals, but with a pinkish cast in rocks having only about 10 percent dark minerals. Biotite and chlorite, most abundant of the dark minerals, form clusters between or around the quartz and feldspars. Phenocrysts, which in part are actually porphyroblasts, are of potassium feldspar and are as much

as 4 cm long. In most rocks they make up about 5 percent of the volume, but they are scarce or absent in some of the small intrusive masses on the southwest flank of the mountains. Compared to the phenocrysts in the younger plutonic rocks, they are mostly smaller and less abundant. The large phenocrysts of the Continental Granodiorite are found in the grus mantle on weathered terrane, and they persist as clasts in some Mesozoic conglomerates that overlie the granodiorite.

The granodiorite locally contains small widely scattered xenoliths that are mostly of uncertain origin. A few of them shown in the areas of Box Canyon and Enzenberg Canyon (Drewes, 1971c; and about 1 mile south of collection site 3, fig. 3, this report) are from the Pinal Schist. Elsewhere the granodiorite contains smaller xenoliths that resemble the granite gneiss unit. Still others may be remnants of a hornblende gneiss or an amphibolite not known at the surface.

Zones of sheared rock and veinlets of aplitic material and of quartz are also common features of the granodiorite. Some of the sheared zones are obviously related to mapped faults, but most of them are small and so widely scattered and randomly oriented as to indicate little more than that the rocks apparently have had a long and involved geologic history. The aplitic veinlets may be genetically related to the larger mapped bodies of aplite, which are described in the following section of this report.

In thin section, the granodiorite is seen to have a hypidiomorphic-granular texture in which the groundmass

grains are 3 to 7 mm in diameter. A cataclastic texture is superposed on the hypidiomorphic-granular texture of those specimens from the eastern bodies of hornblende-biotite granodiorite, which occur near the fault that bounds the Precambrian rocks. The samples from in, and north of, the Box Canyon area have a mosaic to sutured or seriate texture superposed on the granular one. Traces of microgranophytic texture appear in some specimens and the rims of many large crystals are poikilitic. Poikilitic grains and a bimodal distribution of groundmass grain size are particularly common in the southern part of the outcrop area of hornblende-biotite granodiorite, which appears to be metamorphosed by the nearby pluton of Squaw Gulch Granite.

Modes of 24 samples of Continental Granodiorite, grouped to show the mineral composition of the unmetamorphosed and slightly metamorphosed rocks of the main granodiorite stock separately from the other rocks, are listed in table 2. The collection sites of the

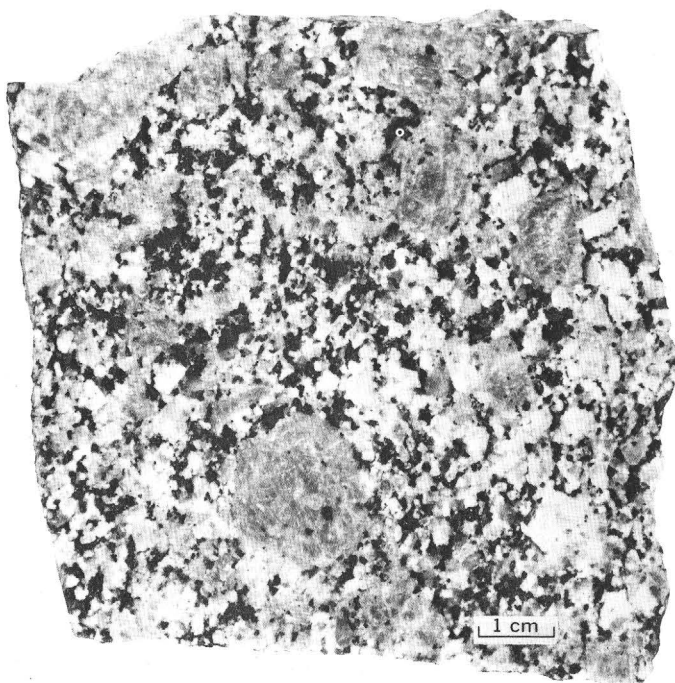


FIGURE 4.—Specimen 17. Continental Granodiorite, showing porphyritic texture and clustered dark minerals.

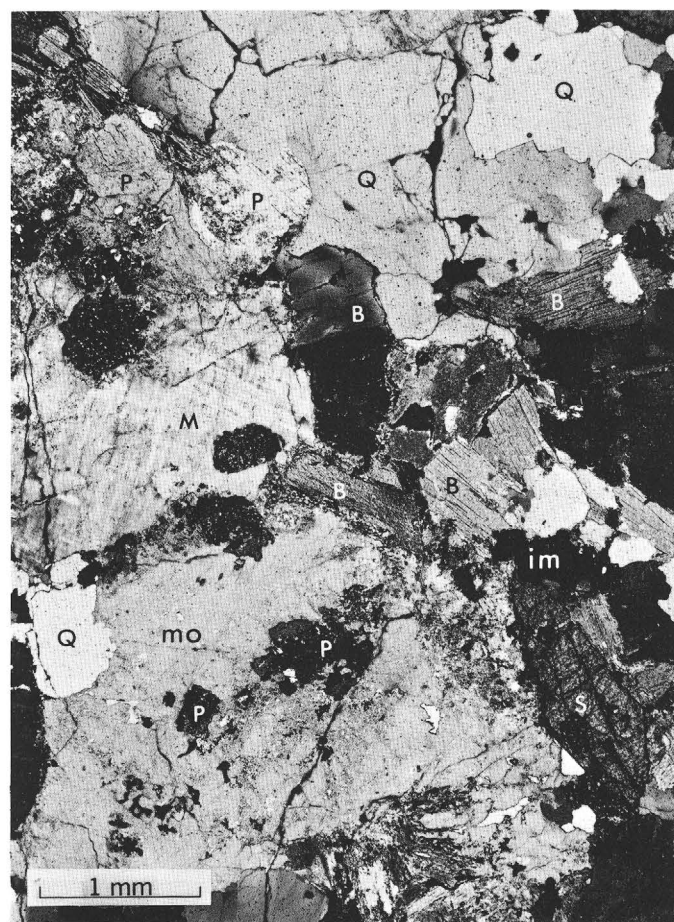


FIGURE 5.—Specimen 19. Slightly metamorphosed Continental Granodiorite showing indistinct grid twinning in microcline. Crystals: microcline (M), microcline or orthoclase (mo), plagioclase (P), quartz (Q), biotite (B), ilmenitic magnetite (im), and sphene (S). Crossed nicols; $\times 20$.

samples are shown in figure 3; and additional data in field notes and maps, filed in the U.S. Geological Survey Records Center in Denver, are keyed to this report through the field numbers.

Standard techniques were used in moding the plutonic rocks of the area; many thin sections were preferred to a few rock slabs. In such coarsely porphyritic rocks as the Continental Granodiorite modal data involving potassium feldspar are most reliably obtained by using the mean of many counts, and even then the relatively large value of the standard deviation suggests that the data are insufficient. Point counting, using an 0.5-mm grid, was done on thin sections that were stained with sodium cobaltinitrate, as needed. Separate counts of 1,000 points each were made of the top and bottom halves of thin sections in an attempt to check the modal uniformity over a thin section area of 7 to 8 square centimetres. The relative abundance of quartz between the halves of a moded thin section, reported as the quartz index, gives an approximate measure of the mineralogic uniformity of a rock at this scale. Thus, a quartz index of 1 implies perfect mixing, and the smaller the value of the index, the poorer the mixing. To some extent, of course, variations in grain size between rock types interfere with this attempt, the finer grained rocks giving the visual impression of being better mixed. However, the mean quartz index of rock types having similar grain size varies sufficiently to suggest that the degree of mixing is an intrinsic feature of the rock.

The main mineral constituents of the granodiorite are quartz, two feldspars, biotite, and, in some specimens, hornblende. Among the light-colored grains, quartz is anhedral and bimodally sized in those rocks which have the mosaic or seriate texture. Its undulatory extinction is commonly large, but that of quartz of the strongly metamorphosed granodiorite of the southwest flank of the mountains is faint or absent. Plagioclase forms subhedral tabular crystals. The anorthite content of plagioclase from the biotite granodiorite is 0 to 30 percent; in about half the specimens crystal cores are of oligoclase and the rims albite, whereas in the other specimens only albite is present, suggesting that the granodiorite is incompletely albitized. The anorthite content of plagioclase from the hornblende-biotite granodiorite is 35 to 50 percent, in the range of andesine. The plagioclase of most specimens is moderately to intensely altered to sericite and clay minerals, which are stained by some iron oxide; the specimens from the strongly metamorphosed hornblende-biotite granodiorite are relatively unaltered. The potassium feldspar of most specimens forms anhedral subequant grains. In the unmetamorphosed rocks the potassium feldspar is microcline; in the other rocks it is either orthoclase or microcline or possibly both. Typically the microcline grid twinning is indistinct or blurred and discontinuous through a crystal (fig. 5) of the slightly

metamorphosed rock. Most orthoclase and microcline is perthitic, with lace and patch perthite types and coarse and fine perthite sizes equally common (fig. 6). The albite phase of the perthitic crystals are moded separately; in this report such albite is considered to be part of the plagioclase component, but its abundance is tabulated independently to permit an alternate grouping. Albite in perthitic grains makes up only 2 to 3 percent of most specimens but ranges from 0.8 to 8.4 percent. Kaolinite alteration of potassium feldspar is ubiquitous and in many specimens is intense.

Dark minerals are more abundant in the Continental Granodiorite than in most other plutonic rocks of the area; the color index of the rock ranges from 10 to 20 percent. Biotite, or its chlorite alteration mineral, is the most abundant dark mineral. It forms clusters of relatively large subequant grains in unmetamorphosed rocks (fig. 6) or felty aggregates of relatively small tabular grains in metamorphosed rocks (fig. 7). Biotite is pleochroic in yellowish brown to moderate brown. The alteration of biotite to chlorite is a common feature; relatively unaltered biotite is most common in the metamorphosed rocks, and the more intense the metamorphism, the more abundant the biotite seems to be, no doubt as recrystallized or secondary micas. Hornblende is pleochroic in pale yellowish green to pale olive green to pale bluish green. Some hornblende grains are poikilitic, containing quartz and biotite. Magnetite is invariably ilmenitic and commonly is clustered with biotite and sphene. The abundance of zircon is generally greater in this granodiorite than in other plutonic rocks of the area, and the zircon of specimen 19 (fig. 5) is probably hyacinth zircon.

Alteration minerals are chiefly sericite, clay minerals, and chlorite; epidote, uraltite, calcite, iron oxide, leucosene, and penninite are also present in smaller amounts and in various combinations.

APLITIC ROCKS

Aplite, alaskite, and fine-grained leucocratic quartz monzonite bodies in the Continental Granodiorite are hereinafter collectively referred to as aplitic rocks of the granodiorite. The aplitic rocks form many intrusive masses too small to be shown either in figure 3 of this report or on the geologic maps, but the larger masses are shown on the map of the Sahuarita quadrangle (Drewes, 1971b). The quartz veinlets that were mentioned in the preceding section of this report as being scattered throughout the granodiorite may be related to the aplitic rocks but are unmapped because of their small size.

The intrusive masses of aplitic rocks commonly are lenticular or tabular, a few feet to a few tens of feet thick, and hundreds of feet long. Some of the masses are pluglike(?) and are irregular in plan; others resemble closely spaced dikelets. Many of the tabular intrusive



FIGURE 6.—Specimen 12. Continental Granodiorite showing a cluster of large chloritized biotite crystals and part of a perthitic microcline phenocryst that has a coarse-textured lace to patch perthite. Crystals: microcline (M) and altered albite (ab) of the perthitic phenocryst, quartz (Q), chloritized biotite (cb), ilmenitic magnetite (im), calcite (ca) derived from alteration of biotite, apatite (ap) leucoxene (L) derived from sphene, and possible zircon (Z). Crossed nicols; $\times 20$.

masses are clustered in belts of subparallel-striking sheets in which gently inclined masses are as abundant as steeply inclined ones. The contact of most of the aplitic rocks with the granodiorite is sharp, but in a few places, such as the hills a mile southwest of the cemetery below Helvetia and around the large aplitic mass 1 to 1.5 miles south of Box Canyon (Drewes, 1971b), the contact is apparently gradational.

The aplitic rocks weather yellowish gray rather than the more somber brownish gray of the granodiorite, and outcrops of aplitic rocks are more resistant to weathering and hence are more abundant and somewhat more rugged than those of the granodiorite. Outcrops of aplitic rocks commonly form narrows and falls where they cross the bottoms of canyons. Small angular blocks of aplitic rocks are strewn around the outcrops, along with a grus that does not contain large chips of feldspar phenocrysts.

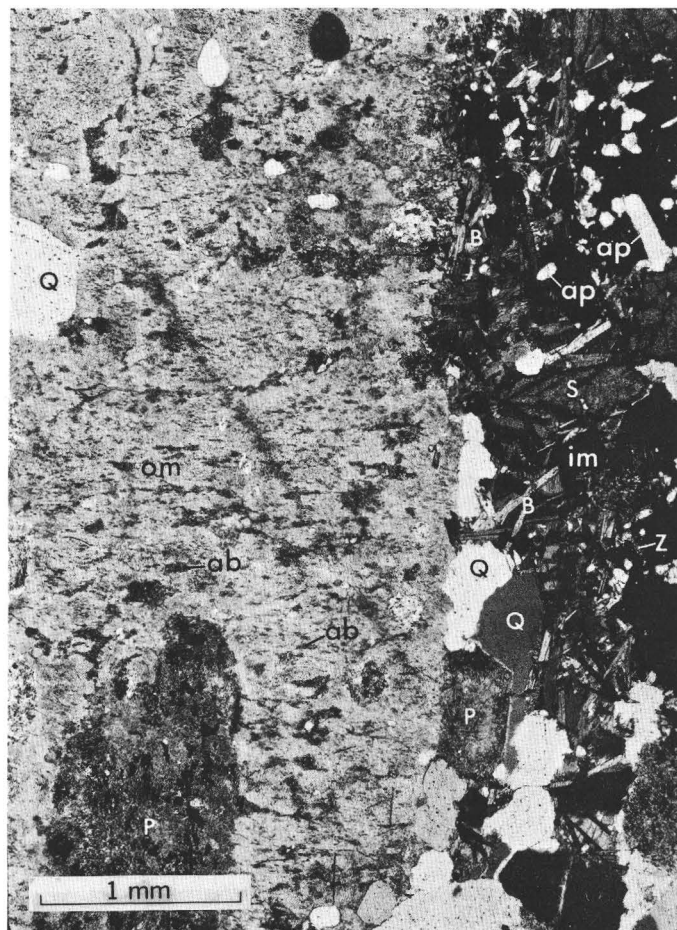


FIGURE 7.—Specimen 17. Continental Granodiorite showing part of a phenocryst or porphyroblast and small felty-textured recrystallized biotite. Crystals: orthoclase or microcline (om), quartz (Q), plagioclase (P), biotite (B), and altered albite (ab) in fine lacy perthitic intergrowths, ilmenitic magnetite (im), sphene (S), apatite (ap), and zircon (Z). Crossed nicols; $\times 25$.

Mineral grains of the aplitic rocks are mostly 1 to 2 mm in diameter and are arranged in an idiomorphic-granular texture. Most of the aplitic masses have a felty or granular nonporphyritic texture; some have a few phenocrysts, which are generally less than 7 mm long.

The assemblage and abundance of minerals in the aplitic rocks differ slightly from those of its granodiorite host. Modal analyses of two rocks, specimens 23 and 24, are given in table 2. Estimated modes of three additional rocks, not presented in the table, show some variations from the tabulated modes; the mica of one rock is biotite, that of another is muscovite, and the third contains both micas. Likewise, apatite and zircon are in only some of the rocks and not consistently together. And finally, the potassium feldspar is orthoclase in some rocks and microcline in others. Throughout the aplitic rocks, though, the plagioclase is either albite or oligoclase. The albite in perthitic grains is finely lacy and rarely exceeds a few

percent by volume. Biotite occurs either as widely scattered chloritized flakes or as unaltered inclusions in quartz. Felty aggregates of small biotite crystals, typical of recrystallized rocks, are found in the aplitic rocks 1 to 2 miles southwest of Helvetia. Sericite and clay minerals are abundant alteration products in the aplitic rocks.

LAMPROPHYRE

Small dikes of dark-greenish-gray rock are sparsely scattered throughout the Continental Granodiorite. Some dikes occupy dilation fractures as much as 3 feet wide and are a fine-grained dioritic rock. Other dikes form short tabular bodies as much as 10 feet wide and are a finely porphyritic dacite or andesite. The outcrops of both rock types are inconspicuous and generally lie in small sags and low areas.

A few specimens of lamprophyre have an ophitic to subophitic texture, with crystals 0.1 to 0.3 mm long. A few acicular crystals and rare phenocrysts are as much as 4 mm long. Plagioclase, potassium feldspar, and an amphibole are the most abundant minerals; quartz and pyroxene(?) are present in small amounts, and magnetite, apatite, and zircon occur in trace amounts. The plagioclase has a composition of albite, probably as a result of diagenetic(?) albitization. Alteration minerals, such as sericite, clay minerals, chlorite, and epidote, are abundant.

In the Santa Rita Mountains, many of the plutons and their host rocks contain lamprophyre dikes. Although slightly variable in habit, texture, and phenocryst mineralogy from dike to dike, the lamprophyre dikes of some plutons are uniform. In the absence of a considerably more detailed study of these dikes, they are considered simply as lamprophyres from late-phase magmas of the plutons with which they are associated, rather than as the result of distinctly later and genetically unassociated magmatic events.

MODAL AND CHEMICAL SUMMARY

For ease of comparison of the abundant analytical data on the plutonic rocks, the tables of analyses are augmented by a series of modified triangular diagrams summarizing the modes and by a series of histograms summarizing the chemical analyses.

The triangular diagram summarizing the modes consists of two parts (fig. 9): the left half is part of a standard quartz-potassium feldspar-plagioclase diagram, following the general method of Johannsen (1939, p. 152) and as used by Bateman (1961, p. 1524) and by Ross (1969, p. 7). The quartz-rich corner is eliminated, as it is unoccupied by analyses of the plutonic rocks of the Santa Rita Mountains suite; and the right half is a similar but smaller segment of a quartz-plagioclase-femic mineral triangular diagram. Together, these two parts of the diagram represent the front and right side of a tetrahedron (fig. 8) showing the

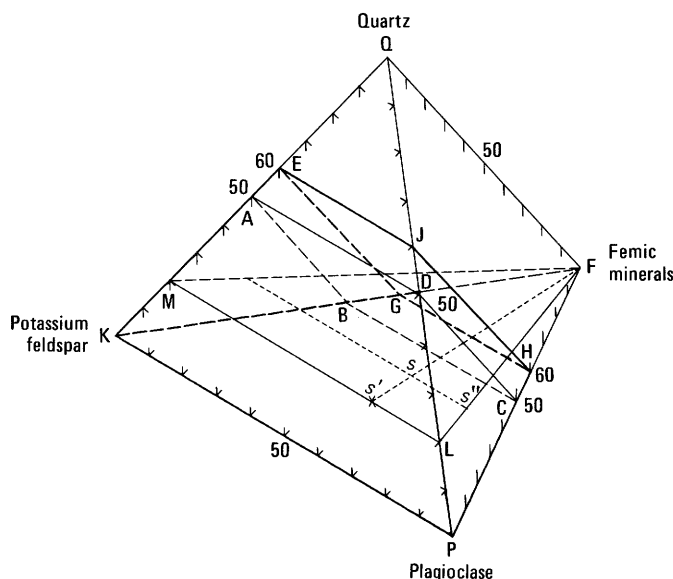


FIGURE 8.—Isometric diagram of a modal tetrahedron whose apices QKPF represent, respectively, the quartz, potassium feldspar, plagioclase, and femic minerals. The solid ABCDKP is a hemitetrahedron. The solid EGHJKP is the body whose front face, EKPJ, and right side, JPH, are projected into the plane of the modified triangular diagrams, such as that of figure 9. The true mode of hypothetical specimen, *s*, (having 16 percent quartz, 16 percent orthoclase, 48 percent plagioclase, and 20 percent femic minerals) is first plotted as *s'* on the leucocratic face, QKP, of the tetrahedron in the usual manner, the femic component having been subtracted and the others recalculated to 100 percent. The projection of the true mode on the right face, QPF, of the tetrahedron is then plotted as *s* along the edge, LF, of plane LFM, on which *s*, *s'*, and *s''* all lie.

three major leucocratic components of granitoid rocks plus the combined femic mineral component. The method of plotting the femic component is illustrated in figure 8; the resulting diagram slightly exceeds in size a hemitetrahedron in the example shown in figure 9 but equals a hemitetrahedron in all following examples. In figure 9 the right side of the oversized hemitetrahedron is rotated into the plane of its front face. Each mode is represented by two points on the diagram, one showing the relative abundance of the leucocratic components and the other the actual abundance of the femic component. The true composition, in terms of these four components, must be visualized as a projection within the tetrahedron controlled by the two points shown. The method of projection shown in figure 8 gives both the recomputed data shown on the conventional triangular diagram plus actual data on the femic component, which the recomputed data on a triangular diagram showing quartz, plagioclase, and femic end members would not.

A composite of the modal analyses of the Continental Granodiorite (fig. 9) shows the unmetamorphosed rocks to be scattered in a fairly compact subspherical body centered

TABLE 2.—*Mode (in percent)*

[Field numbers are abbreviated, symbols showing year of collection and collector's initial omitted. Full field number of specimen 1 thus

Rock type	Granodiorite (includes quartz monzonite)													Slightly (regionally?) metamorphosed granodiorite and quartz monzonite				
Specimen No.	1	2	3	4	5	6	7	8	9	10	11	12	1 ¹³	1—13 Mean ^s	14	15	16	
Field No.	914	1034	1014	997	1022	913	994	899b	898	100	897	104	627		1220	1191	1142 _i	
Quartz	15.8	28.1	19.9	30.5	21.5	24.4	24.5	22.8	29.0	32.2	25.1	16.4	20.5	23.9	5.1	28.2	32.8	46.3
Plagioclase, total	32.8	35.1	52.6	43.4	46.9	41.0	45.8	42.2	39.6	39.4	42.8	26.7	56.5	41.9	7.9	35.4	32.9	27.6
(plagioclase in perthite)	(8.4)	(1.0)	(0.2)	0	(1.2)	(0.8)	(0.8)	(3.5)	(2.6)	0	(1.5)	0	0	(1.5)	(2.3)	0	(5.1)	(2.0)
Microcline	36.0	19.8	12.4	8.1	19.1	25.0	12.7	21.8	15.3	13.7	11.1	38.6	9.0	18.7	9.7	0	17.5	17.4
Orthoclase	0	0	0	0	0	0	0	0	0	0	0	0	0	0	...	15.2	0	0
Biotite	12.4	12.8	13.2	13.0	9.1	7.8	13.2	9.8	12.1	10.7	16.2	11.7	10.1	11.7	2.2	15.4	14.0	6.6
Hornblende	0	0	0	0	0	0	0	0	0	0	0	0	0	Tr.	...	0	0	0
Magnetite	1.5	2.0	1.7	3.9	1.4	.4	1.5	1.7	.9	3.0	2.4	2.9	2.2	2.0	.9	4.4	1.9	1.6
Apatite6	.4	Tr.	.6	.4	.4	.5	.4	.6	.8	1.0	1.0	.4	.5	.3	1.0	.9	.15
Sphene7	1.8	0	Tr.	1.6	.5	1.8	1.2	2.4	0	1.4	0	.9	.9	.8	.05	Tr.	.4
Zircon	0	.05	.2	.05	.05	Tr.	Tr.	.05	.05	.1	.05	.2	.2	.1	.1	.4	Tr.	Tr.
Allanite	0	0	0	0	0	.5	0	0	.05	0	0	0	0	Tr.	...	0	0	0
Rutile05	0	0	0	0	0	0	0	0	0	0	0	0	Tr.	...	0	0	0
Muscovite	0	0	0	.5	0	0	0	0	0	0	0	0	0	Tr.	0	0	0	0
Pyrite1	0	0	0	0	0	0	0	0	0	0	0	0	Tr.	...	0	0	0
Total	99.95	100.05	100.0	100.05	100.05	100.0	100.0	99.95	100.0	99.9	100.05	97.5	100.0	99.7	...	100.05	100.0	100.05
Femic	15.4	17.0	15.1	18.1	12.5	9.6	17.0	13.2	16.1	14.6	21.0	16.8	14.0	15.2	2.9	21.2	16.8	8.7
Percent anorthite in plagioclase	5—10	0—10	5—10	5—10	0	0	0—5	0—5	0	0—5	5—10	3	27—30	0—10	...	0	0—5	...
Quartz mixing index (see text)88	.79	.92	.86	.77	.89	.91	.93	.91	.82	.9592	.88	.06	.89	.86	.77

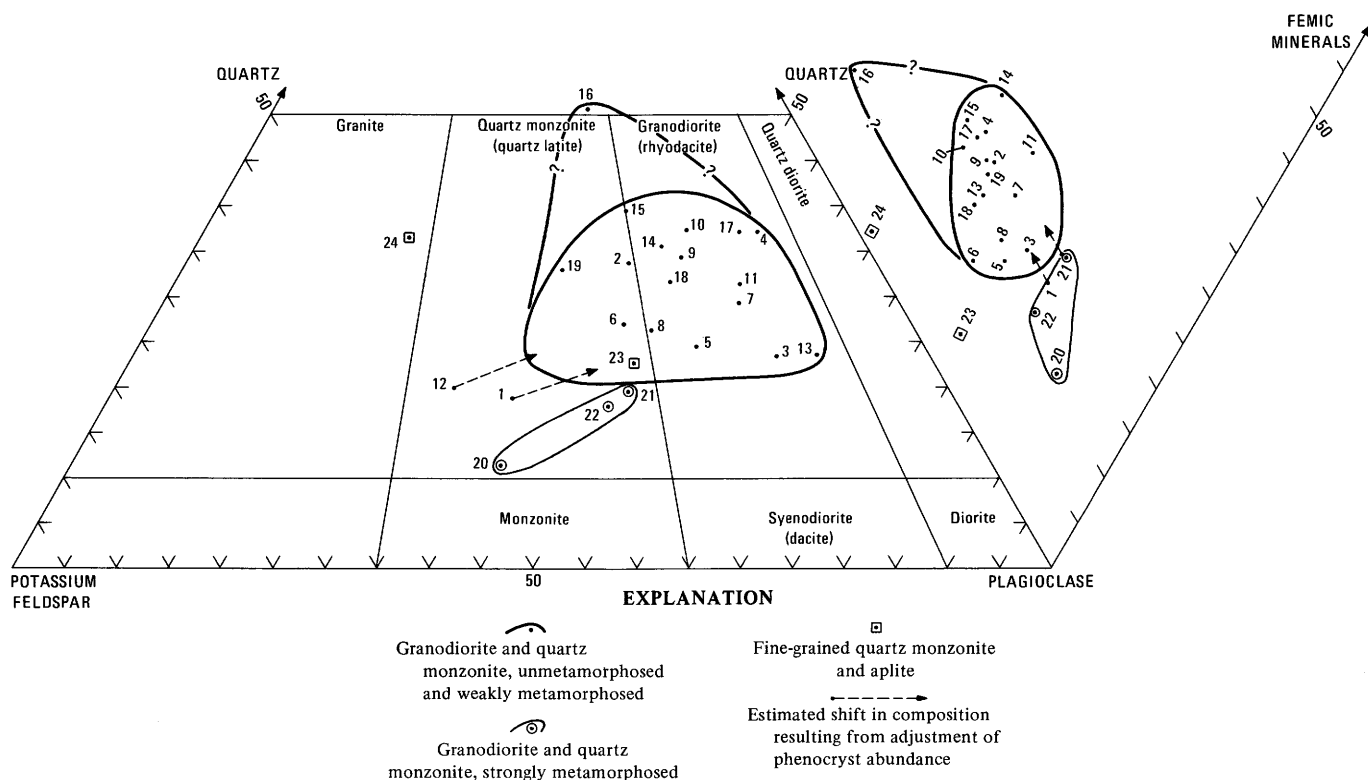
¹Mode of specimen 13 has affinity to metagranodiorite.

FIGURE 9.—Modified triangular diagram showing modal quartz, potassium feldspar, plagioclase, and femic minerals of Continental Granodiorite. Abundance of quartz in specimen 16 may be anomalously large.

near a point about 15 percent of the distance from the granodiorite field toward the femic point of the tetrahedron. The body circumscribing the modal analyses

of the metamorphosed rocks is larger and less regular. In subsequent sections of this report the skewness of the modal bodies thus represented will vary considerably.

of Continental Granodiorite

is 65D914. Symbols s, standard deviation; Tr., trace; ..., not determined]

Slightly (regionally?) metamorphosed granodiorite and quartz monzonite—Continued						Strongly contact metamorphosed metagranodiorite			Fine-grained quartz monzonite and aplite phase	
17	18	19	14—19		1—19	20	21	22	23	24
1152	1043	1046	Mean	s	Mean	620	611,686	614	1106	1104
31.0	27.7	27.8	32.3	6.8	26.8	10.2	4.3	15.8	21.8	36.0
42.8	41.5	31.0	35.2	7.8	39.8	36.3	55.4	42.4	46.4	19.8
(1.2)	(Tr.)	(4.9)	(2.2)	(2.3)	(1.7)	(2.4)	0	(2.5)	(5.4)	(9.0)
9.4	0	7.6	8.7	10.1	15.5	42.0	0	0	27.5	42.7
0	18.0	18.0	8.5	6.4	2.7	0	.5	29.4	0	0
13.0	9.4	11.6	11.7	2.5	11.7	9.3	5.6	7.5	3.5	.7
0	0	0	0	...	Tr.9	29.2	.1	0
1.9	1.8	1.9	2.3	1.0	2.1	1.0	2.5	3.4	.4	.5
.9	.6	.9	.7	.3	.6	Tr.	.7	.6	.2	Tr.
1.0	.9	1.1	.6	.7	.8	.1	1.8	.8	.2	.1
.05	.1	.1	.1	.2	.1	.1	0	Tr.	.05	Tr.
0	0	Tr.	Tr.	Tr.	Tr.	0	0	0	0	.15
0	0	0	0	...	0	0	0	0	0	0
0	0	0	0	...	0	0	0	0	0	0
0	0	0	0	...	0	0	0	0	0	0
100.05	100.0	100.0	100.1	...	100.1	99.9	100.0	100.0	100.05	99.95
16.8	12.8	15.6	15.4	4.2	15.3	11.4	39.8	12.4	4.3	1.5
5—15	0—5	5—10	0—10	...	0—10	37—40	28—31	5—35	0—5	0
.93	.92	.98	.89	.06	.88	.67	.58	.98	.83	.84

The chemical and spectrographic analyses and calculated CIPW norms are listed in table 3 and the chemical analyses of the Continental Granodiorite and of the other plutonic rocks are summarized in figure 10. Inasmuch as this study was part of a general geological investigation, rapid rock analytic techniques and semiquantitative spectrographic methods were used. Chemically, the Continental Granodiorite closely resembles the average granodiorites reported by Johannsen (1932, p. 344) and by Nockolds (1954, p. 1014). Most noteworthy of the spectrographic results is the decrease in the abundance of copper and lead in the metamorphosed granodiorite near Helvetia compared to the content in unmetamorphosed granodiorite near Greaterville. This change reflects the variations in the copper content of mica, described by Lovering and others, (1970), and studied in greater detail in some rocks of the nearby Sierrita Mountains by Banks (1974).

AGE AND CORRELATION

The Continental Granodiorite has not been precisely dated by radiometric means. Lead-alpha dates indicate an age of at least 1,450 m.y. (Drewes, 1968, p. C5); rubidium-strontium and potassium-argon dates are discordant with the lead-alpha date, and they suggest that later thermal events have modified at least many of the available radiometric ages. The granodiorite is thus considered to be at least 1,450 m.y. old and it may be 1,600 to 1,700 m.y. old.

Geologic means do not permit the dating of the granodiorite with complete confidence either, but the field

relations also suggest a Precambrian age. The fault separating the Cambrian Bolsa Quartzite from the granodiorite has been described in the introductory section on the Continental Granodiorite as following an unconformity. In addition, cobbles of granodiorite resembling the Continental occur in conglomerate lenses intercalated in the Triassic Mount Wrightson Formation (Drewes, 1971a, p. 12); if the cobbles are derived from the Continental, the pluton must be at least as old as Triassic. Furthermore, the granodiorite has a distinctly older appearance through its alteration, shear zones, and local areas of faint foliation, than the plutonic rocks of Triassic and younger ages in the Santa Rita Mountains.

Radiometric ages of 11 plutonic rocks of the Santa Rita Mountains are listed in table 4. The general locations from which the dated samples were collected are shown in figure 3; and detailed locations of two sample sites are shown on the geologic map of the Sahuarita quadrangle (Drewes, 1971b). The detailed collection site of the third sample is not shown on the geologic map of the Mount Wrightson quadrangle (Drewes, 1971c); it lies in the Mavis Wash area, just east of the middle one of three small areas mapped as Bolsa(?) Quartzite, in the larger outcrop area of contact-metamorphosed Continental(?) Granodiorite.

Three samples of granodiorite are radiometrically dated, two of them by two methods each. Sample 21 is probably thoroughly recrystallized and sample 19 is slightly recrystallized, features which were not initially recognized in the field. The lead-alpha ages of zircons of specimens 1 and 19, 1,360 m.y. and 1,450 m.y., are probably nearest to the true age of the rock, for the zircon would be among the minerals most refractory to change by thermal metamorphism. The rubidium-strontium whole-rock age, 800 m.y., only corroborates a Precambrian age of specimen 1; perhaps a very mild metamorphism, petrographically not noticeable and so not considered in tables 2—4, has resulted in loss of radiogenic strontium from this rock. The potassium-argon age of 55 m.y. of specimen 19 coincides closely with the ages of the Helvetia stocks, the nearest of which lies 2½ miles to the north, and the biotite of the rock of the intervening area is subtly recrystallized. The other potassium-argon age, 159 m.y. (sample 21), dates the age of crystallization of an anomalously fresh-looking granodiorite variety as Jurassic, in an area of rock otherwise resembling the Continental Granodiorite. The granodiorite lies within a few hundred feet of a concealed contact of Squaw Gulch Granite, of Jurassic age, and apparently was contact metamorphosed by that granite.

The laboratory measurements and constants used in calculating the ages shown in table 4 are listed by Marvin and others (1973).

Plutonic rocks resembling the Continental Granodiorite occur in the Rincon and Sierrita Mountains and possibly

TABLE 3.—*Chemical and spectrographic analyses and CIPW norms of Continental Granodiorite*

[Chemical analyses by rapid rock method (Shapiro and Brannock, 1962), with analyses of specimens 1, 11, 14, and 19 supplemented by atomic absorption method and others supplemented by X-ray fluorescence method. Chemical analyses by Lowell Artis, S. D. Botts, G. W. Chloe, P. L. D. Elmore, John Glenn, J. Kelsey, H. Smith, and Dwight Taylor. Spectrographic analyses (semiquantitative method) by W. B. Crandell, J. L. Finley, J. C. Hamilton, and A. L. Sutton. Elements looked for but not found: As, Au, B, Bi, Cd, Eu, Ge, Hf, Hg, In, Li, Pd, Pr, Pt, Re, Sb, Sm, Sn, Ta, Te, Th, Ti, U, W, and Zn. Symbols: s, standard deviation; <, less than;, not determined; Tr., trace; N, not detected]

Rock type	Granodiorite and quartz monzonite					Slightly metamorphosed granodiorite	Granodiorite and quartz monzonite	Strongly contact metamorphosed metagranodiorite
Specimen No.	1	11	12	13	14	1-14	19	20
Field No.	914	897	104	627	1220	Mean s	1046	Mean s
Chemical analyses (weight percent)								
SiO ₂	59.0	67.4	69.4	64.6	67.8	65.6 4.1	67.4	65.9 3.7
Al ₂ O ₃	17.4	14.4	12.4	17.6	14.0	15.2 2.3	14.3	15.0 2.1
Fe ₂ O ₃	3.4	2.2	3.6	1.0	1.8	2.4 1.1	3.0	2.5 1.0
FeO	3.0	2.1	1.3	1.2	3.0	2.1 .9	2.0	2.1 .8
MgO	1.2	1.2	.61	1.2	1.3	1.1 .3	.91	1.1 .3
CaO	2.9	2.7	1.7	5.2	2.0	2.9 1.4	3.3	3.0 1.2
Na ₂ O	3.7	2.8	3.8	4.2	2.3	3.4 .8	3.1	3.3 .7
K ₂ O	6.9	4.1	4.5	2.2	5.3	4.6 1.7	2.8	4.3 1.7
H ₂ O	.08	.11	.13	.33	.08	.15 .11	.14	.15 .09
H ₂ O+	1.0	1.2	1.2	1.0	.42	1.0 .32	.82	.95 .29
TiO ₂	.46	.18	.92	.74	.83	.63 .30	1.0	.69 .31
P ₂ O ₅	.42	.29	.34	.28	.27	.32 .06	.43	.34 .07
MaO	.12	.12	.12	.08	.13	.11 .02	.08	.11 .02
CO ₂	<.05	.36	.34	.11	.05	.16 .18	.05	.14 .17
Total	100	99	100	100	99	100 . . .	99	100 . . .
Spectrographic analyses (weight percent)								
Ag	0	0	0.0005	0	0	Tr. . . .	0	Tr. . . .
Ba	.2	.15	.2	.2	.1	.17 .04	.07	.15 .06
Be	.0001	.0002	0	.0002	.0003	.0002 .0001	0	.0001 .0007
Ce	.02	.02	.015	0	.05	.02 .02	N	N
Co	.002	.001	.001	.0007	.001	.001 .0004	.007	.002 .002
Cr	.0015	.002	.001	.0005	.01	.003 .004	.002	.003 .004
Cu	.003	.02	.1	.00015	.005	.03 .04	.007	.02 .04
Ga	.0015	.0015	.003	.002	.0015	.002 .001	N	N
La	.02	.01	.005	0	.01	.009 .007	.007	.009 .007
Mo	0	0	0	0	.0003	Tr. . . .	0	Tr. . . .
Nb	.0005	.0007	.0015	0	.002	.0009 .0008	0	.0008 .0008
Nd	.02	.015	.007	0	0	.008 .009	N	N
Ni	<.003	<.003	.0007	.0015	.002	.002 .003	.003	.002 .001
Pb	.007	.007	.07	.0015	.002	.02 .03	.0015	.01 .03
Sc	.002	.001	.001	.0015	.002	.0015 .0005	.007	.002 .002
Sn	.0005	.0007	0	0	0	.0001 .015	0	.0002 .0003
Sr	.03	.02	.03	.1	.02	.04 .03	.003	.03 .03
V	.007	.007	.007	.01	.007	.008 .001	.02	.01 .005
Y	.005	.005	.005	.002	.01	.005 .003	.0015	.005 .003
Yb	.0005	.0005	N	.0003	.001	.0005 .0003	N	N
Zr	.03	.05	.03	.015	.03	.03 .01	.007	.03 .01
CIPW norms								
Q	3.6	29.0	27.6	19.9	27.7	31.8	18.1	13.7
C	0	2.0	0	0	1.6	1.3	0	.4
or	40.9	24.4	26.6	13.0	31.5	16.7	13.0	17.1
ab	31.4	23.9	32.1	35.5	19.6	26.4	38.9	32.1
an	10.5	9.3	3.5	22.7	7.9	13.3	20.3	20.7
di	.35	0	.23	.24	0	0	.23	0
fs	.19	0	.20	.19	0	0	.12	0
hy	.11	0	0	.02	0	0	.10	0
en	2.8	3.0	1.3	2.8	3.3	2.3	2.1	5.0
fs	2.0	2.0	0	.28	2.9	0	1.8	1.9
mt	4.9	3.2	1.9	1.5	2.6	3.8	3.0	4.8
hm	0	0	2.3	0	0	.38	0	0
il	.87	.34	1.7	1.4	1.6	1.9	1.0	1.9
ap	1.0	.69	.80	.66	.64	1.0	.52	1.1
cc	.11	.82	.77	.25	.11	.11	0	.18
Total	98.7	98.7	99.0	98.4	99.5	99.0	99.2	98.9
Femic	12.3	10.1	9.2	7.3	11.2	9.5	8.9	14.9

also in the Empire and Patagonia Mountains (fig. 1). In the Rincon Mountains (Drewes, 1974) a gneissic granodiorite porphyry that intrudes Pinal Schist and is intruded by other less foliated rock of probable Precambrian age is believed to be a strongly metamorphosed equivalent of the Continental Granodiorite. In the Sierrita Mountains, rocks originally mapped by J. R. Cooper (written commun.,

1970) as granite and diorite of Precambrian age, and schist and gneiss of undetermined age resemble, respectively, the unfoliated and the foliated varieties of the Continental Granodiorite, with which I have correlated them (Cooper, 1974). On the northern flank of the Empire Mountains T. L. Finnell (oral commun., 1972) has mapped Precambrian plutonic rocks, some of which resemble a

TABLE 4.—Summary of radiometric age determinations of plutonic rocks of the Santa Rita Mountains

Specimen No.	Field No.	Formation (pluton)	Geologic age	Dating method	Radiometric age (m.y.)	Comment	Collection site shown ¹
197	65D687	Granodiorite of the San Cayetano Mountains.	(late?) Oligocene	K-Ar	27.6 ± 0.8	Genetically related to Grosvenor Hills Volcanics (Drewes, 1972).	Map I—614.
189 192 (2)	66D1185 67D1245 68D1472	Aphanitic rocks (Greaterville plugs).	(late?) Paleocene	K-Ar	55.8 ± 2.1 56.3 ± 2.1 55.7 ± 1.9	"Ore porphyry" quartz latite porphyry.	Map I—613. Map I—613. Fig. 40, this report.
163 163	66D1051 66D1051				53.5 ± 1.3 53.5 ± 2.0		Map I—613. Map I—613.
174	70D1612				53.9 ± 2.0		Fig. 40, this report.
160 158	63D281 64D660	(Gringo Gulch pluton)	Paleocene	K-Ar	60.3 ± 6.0 60.4 ± 6.0	Microgranodiorite Hornblende dacite porphyry	Map I—614. Map I—614.
132	65D754				68.2 ± 3.0 170 ± 20	Rock without recrystallization texture. Pb-alpha ages may reflect a Jurassic history, now nearly obliterated. Collected and dated by P. E. Damon (written commun., 1964).	Map I—614.
139	65D876	Elephant Head Quartz Monzonite (Quantrell stock).	Late Cretaceous	K-Ar Pb-alpha	69.0 ± 2.9 188 ± 40		Map I—614.
(2)	RM—6—63	Madera Canyon Granodiorite.	Late Cretaceous	K-Ar	67.9 ± 2.1		Map I—614.
80 83	63D316 63R292	Josephine Canyon Diorite.	Late Cretaceous	K-Ar Pb-alpha Pb-alpha	467.1 ± 7.0 62 ± 10 63 ± 10	Quartz diorite phase	Map I—614. Map I—614.
101 (2)	63D507 F—33—68			Pb-alpha K-Ar	61 ± 20 73.8 ± 2.6	Quartz monzonite phase Quartz diorite collected and correlated by T. L. Finnell.	Map I—614. Open-file map.
54 45	64D605 63D282	Squaw Gulch Granite	Jurassic	K-Ar Pb-alpha Pb-alpha	145 ± 4 160 ± 20 161 ± 20	Biotite has recrystallization texture; nearby stocks 53—55 m.y. old.	Map I—614. Map I—614.
34 1	63D280 65D914			Pb-alpha Pb-alpha Rb-Sr	184 ± 20 1450 ± 160 800 ± 80		Map I—614. Map I—613.
19	65D1046	Continental Granodiorite.	Precambrian	K-Ar Pb-alpha	55 ± 1.7 1360 ± 270		Map I—613.
21	65D686	Continental Granodiorite (?).	Precambrian (?)	K-Ar	159 ± 5	Nearby stock 145—161 m.y.	Map I—614.

¹ Map I—614 (Drewes, 1971c); map I—613 (Drewes, 1971b).² Not given a specimen number; no modal or chemical analyses available.³ Specimens 64D660 and 64D661 were collected from nearly the same outcrops; the dated rock has coarser phenocrysts than the moded one.⁴ Reported as 67 ± 3 by Marvin and others (1973, table 1, no. 3).⁵ Specimen 63D507 and 63D276, referred to in other tables, from same outcrop.⁶ Specimens 65D686 and 64D611, referred to in other tables, from same outcrop.

nonporphyritic and finer grained variety of Continental Granodiorite and others of which resemble different plutonic rocks like ones found in the Rincon and Whetstone Mountains. Precambrian plutonic rocks of the Patagonia Mountains (Simons, 1974) also include coarsely porphyritic granodiorite with a general resemblance to the Continental. Although rocks similar to the Continental Granodiorite seem to be fairly widespread, there is no evidence to suggest that all known occurrences are from the same pluton, or indeed are of identical age.

TRIASSIC AND JURASSIC ROCKS

Plutonic masses were intruded into the area of the Santa Rita Mountains during the Triassic and Jurassic Periods, approximately coinciding with times of abundant volcanic activity. This magmatic activity followed a long quiescent interval that began after the emplacement of the Continental Granodiorite in the Precambrian. The magmatic activity of the early Mesozoic began with the

locally prolific volcanism that formed the Mount Wrightson pile (Drewes, 1971a) and followed near the end of the Triassic with the intrusion of a stock of the Piper Gulch Monzonite and smaller masses of quartz diorite. About this time, or slightly later, volcanism is again recorded, in the Upper Triassic and Lower Jurassic Canelo Hills Volcanics. Near the middle of Jurassic time a batholith of Squaw Gulch Granite was emplaced in the southern part of the area. Finally, between the Middle Jurassic and the onset of the Laramide orogenic events in the mid-Cretaceous, magmatic activity dwindled; of three formations, only the oldest two contain volcanic rocks.

PIPER GULCH MONZONITE

The Piper Gulch Monzonite, defined by Drewes (1968), is a very coarse grained dark-gray rock almost unique in its Triassic age and monzonite to syenodiorite composition to this part of Arizona. The monzonite underlies many small areas and a larger one, together not exceeding 4 square

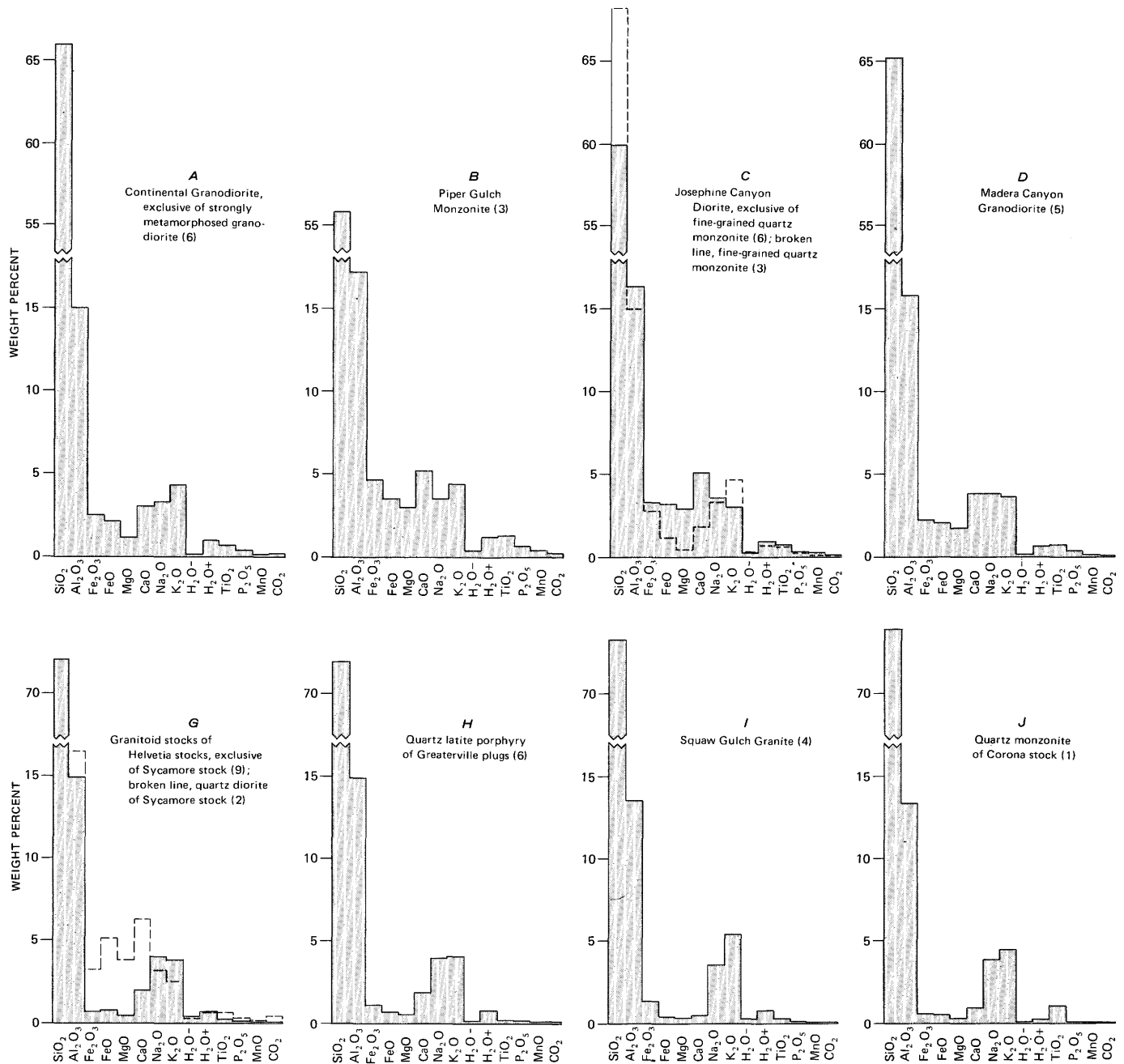
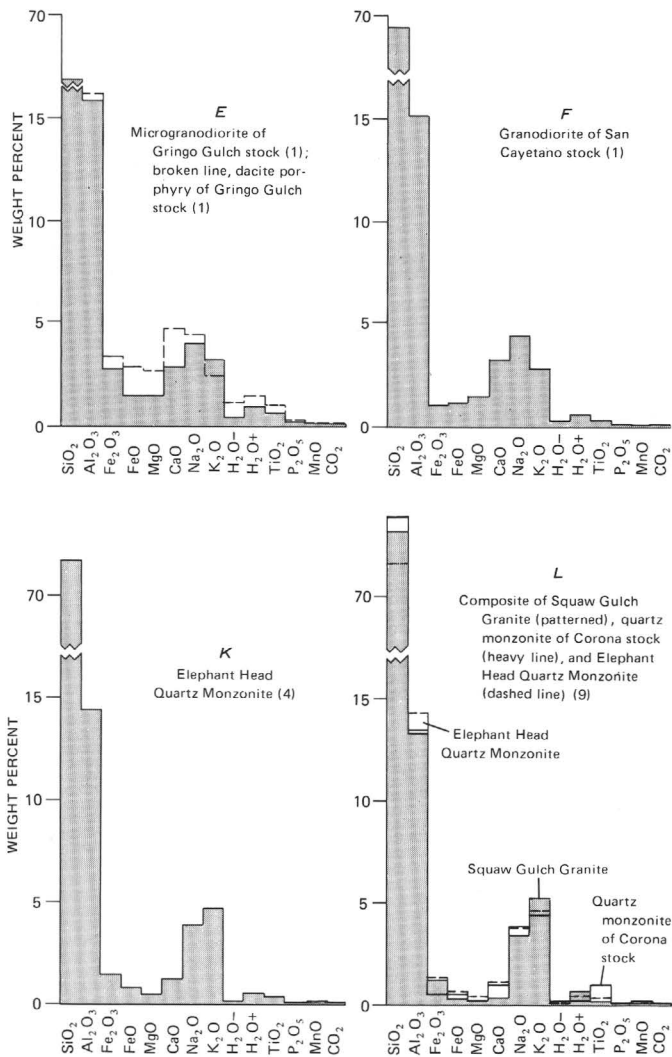


FIGURE 10.—Histograms showing average chemical composition of each group of plutonic rocks. Parenthetic figures

miles. These outcrop areas lie mainly in a belt that extends from the middle reaches of Temporal Gulch northwestward to the west wall of Madera Canyon, shown in general fashion in figure 11 and shown in greater detail on the geologic map of the Mount Wrightson quadrangle (Drewes, 1971c). Monzonite underlies part of the east wall of Madera Canyon, and very small masses of monzonite lie well southwest of the main belt of outcrops. The monzonite intrudes the Mount Wrightson Formation and is extensively intruded by the Squaw Gulch Granite and

some younger rocks. The masses of monzonite included within the younger intrusive bodies are elongated and oriented parallel to the northwest-trending belt of outcrops. Where the monzonite inclusions are abundant, as between specimen collection sites 38 and 30 in figure 11, they may once have formed a single elongate stock. Indeed, that stock may have extended the length of the outcrop belt to site 25.

The intrusive contact of the monzonite with older rocks is fairly sharp, but that of the younger rocks with the



show number of analyses averaged.

monzonite is broadly gradational in many places. For example, west of Madera Canyon the monzonite is gradually assimilated over a zone hundreds of feet wide. The attitudes of the monzonite contact with the host rocks is gentle along the upper reaches of Temporal Gulch and farther north, but it is steep to the southeast. The caps of host rock on the higher hills west of the upper reaches of Temporal Gulch even suggest that the top of this part of the monzonite stock lies at the level of the tops of these hills. The host rock near the contact with the monzonite is

strongly contact metamorphosed to a sugary-textured metavolcanic rock with intercalated quartzite. Secondary minerals, such as schorlite tourmaline, are fairly abundant in pockets and in rosettes along fractures in the metamorphosed rock. Mineralization of the host rock, such as that evident in the Mansfield Canyon area (Drewes, 1973), is probably related to younger intrusive rocks although some pyrite in and near the Piper Gulch could be related to the monzonite. Younger rocks not only intrude the monzonite, but, toward the south, rocks of Early Cretaceous age unconformably overlie it.

The appearance of the Piper Gulch Monzonite in outcrops varies, apparently largely as the result of a difference in the friability of the rock. In many of the southwestern areas the rock forms but few and small outcrops, and these typically occur in topographically low positions in which grus forms a fairly thick, though discontinuous, veneer. The grus that formed on a monzonite parent rock is distinctly darker than that formed on the neighboring granite. In many of the northern outcrop areas the monzonite underlies grayish-brown rounded outcrops and some fairly prominent bosses, as well as steep slopes strewn with coarse residual blocks and grus. A train of monzonite blocks that are as much as 20 feet long and 10 feet wide and thick lie along the Montosa Canyon at least as far as 5 miles from their source on Mount Hopkins. The dark-gray color, derived from both the calcic plagioclase and the abundance of femic minerals, and the very coarse grained texture distinguish the Piper Gulch Monzonite from the other plutonic rocks in the area (fig. 12). Superficially the rock resembles anorthosite, but on fresh surfaces a small amount of light-colored interstitial material is visible.

The prevalent texture of the monzonite is idiomorphic to hypidiomorphic tabular, but east of Madera Canyon the texture is porphyritic. Much of the rock is made up of plagioclase laths 7–15 mm long; the other minerals are considerably smaller. The phenocrysts of the one body of porphyritic monzonite east of Madera Canyon are also in the 10-mm-size range, but the groundmass has a grain size less than 5 mm. Much myrmekitic texture and some granophyric texture is superposed on the general idiomorphic tabular texture. Most rocks that are not obviously hybrid contain a very fine grained, nearly submicroscopic, fingerprintlike myrmekitic intergrowth of quartz in feldspar (fig. 13). These normal rock textures have been modified by recrystallization in specimens from near the contacts with the younger stocks. Recrystallization produces a bimodal distribution of grain size, seriate grain boundaries, bent and partly resorbed edges of plagioclase crystals, and it may enhance the development of poikilitic grains; granophyric and myrmekitic textures, however, seem to be unaffected.

The Piper Gulch Monzonite is made up of plagioclase

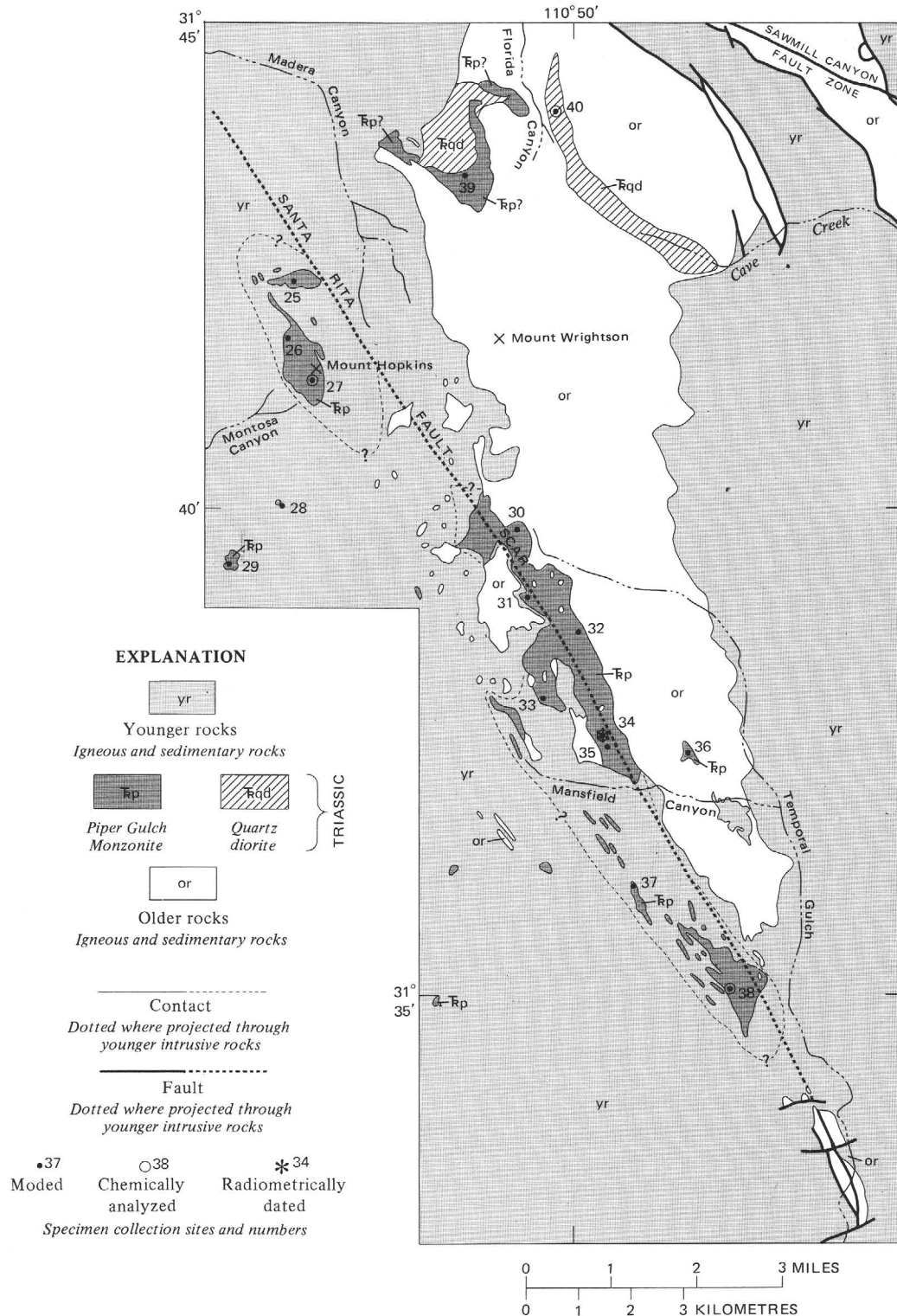


FIGURE 11.—Distribution of Triassic rocks and specimen collection sites.

(30–55 percent by estimate), orthoclase (10–40 percent), amphibole (2–20 percent), less than 10 percent each of quartz, pyroxene, biotite, and magnetite, and trace

amounts of apatite, sphene, zircon, rutile(?), and tourmaline. A few rocks, not including those moded (table 5), also contain primary(?) pyrite. Modal plagioclase,

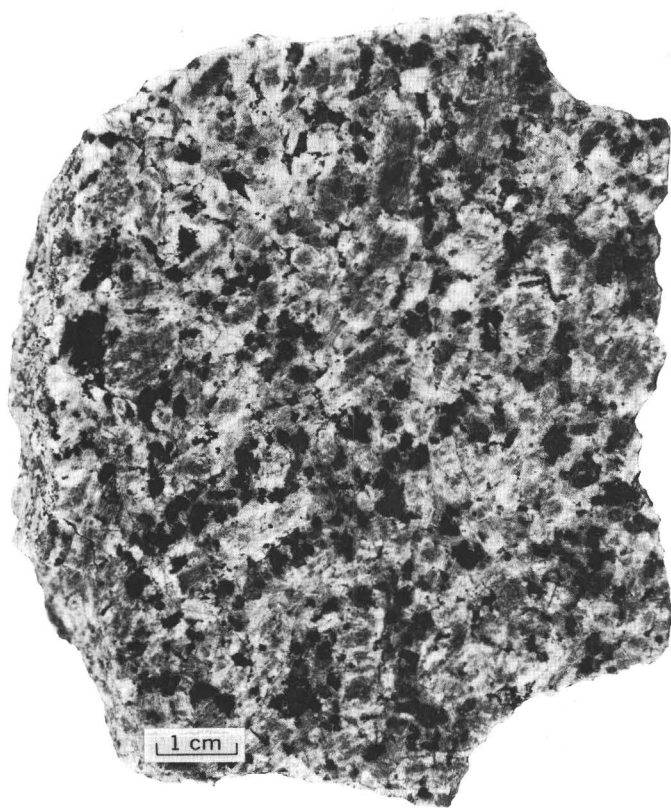


FIGURE 12.—Specimen 37. Piper Gulch Monzonite, showing abundant very coarse grained dark-gray plagioclase.

biotite, and sphene decrease in abundance southeastward and orthoclase and pyroxene increase. Most of the moded specimens contain insufficient quartz to bring the rock out of the monzonite or syenodiorite fields of the modified triangular diagram of figure 14, but the quartz content of specimen 34 is sufficient to place the analysis in the quartz-poor end of the granodiorite field. The solid figure circumscribed around the modes in figure 14 forms a highly flattened oblate spheroid centered roughly 20 percent of the way from the right-hand side of the monzonite field toward the femic apex.

Plagioclase forms large subhedral grains that are moderately to strongly altered to clay minerals and sericite, giving them a finely mottled gray to pale-brownish-gray appearance in clear transmitted light. The anorthite content of plagioclase of most specimens is 40 to 60 percent, placing it with calcic oligoclase or sodic labradorite. The plagioclase of a few specimens from near the contacts of monzonite masses is apparently albitized. The plagioclase crystals of a few other specimens are so severely altered that their estimated anorthite content of 0 to 40 percent is as likely to be unreliable as it is to be the results of incomplete albitization.

Orthoclase and quartz are generally anhedral and

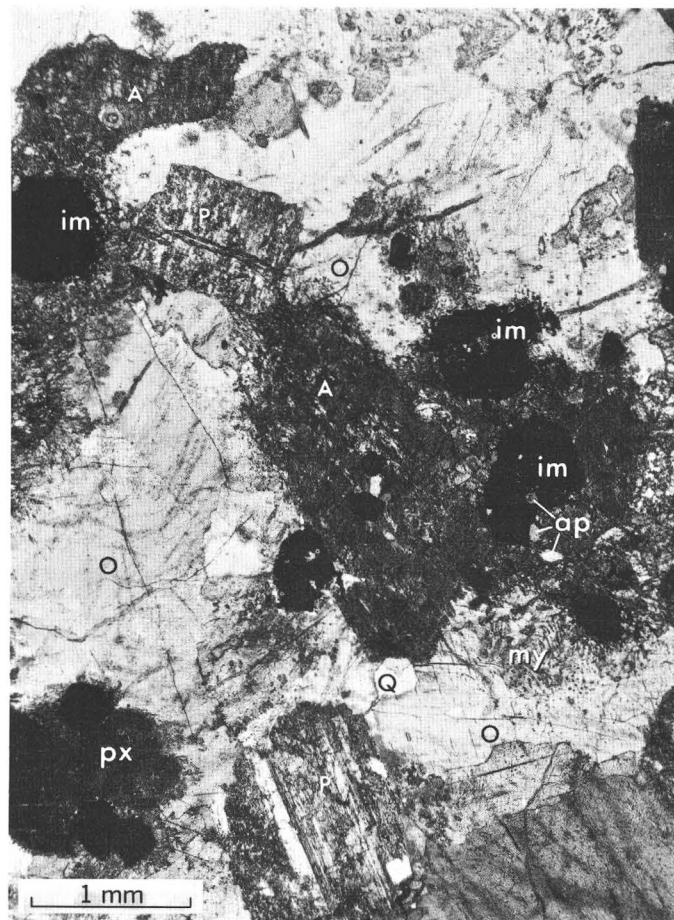


FIGURE 13.—Specimen 37. Piper Gulch Monzonite, showing finger-printlike myrmekitic texture (my). Crystals: orthoclase (O), plagioclase (P), amphibole (A), ilmenitic magnetite (im), and apatite (ap), pyroxene (px), and quartz (Q). Crossed nicols; $\times 20$.

interstitial to the other grains; only in the porphyritic variety of monzonite east of Madera Canyon does the orthoclase form subhedral grains in the groundmass. Strong kaolinite alteration gives orthoclase a smooth very pale brown appearance. The orthoclase is commonly finely perthitic with albite which forms lacy or banded patterns that make up only a few percent of the grains. Some orthoclase grains are poikilitic. Quartz grains show little or no undulatory extinction. The amphibole, probably a hornblende, forms subhedral to anhedral crystals which in most specimens are pleochroic in pale yellowish green to pale greenish gray but in some specimens are pleochroic in light green to pale olive green. It commonly is strongly altered to uralite and chlorite or penninitic chlorite. The clinopyroxene, possibly augite, is present in about half the specimens, generally those with scant amphibole. The biotite forms subhedral crystals that are pleochroic in pale yellowish brown to moderate brown and are strongly altered to chlorite and iron oxide. The magnetite is ilmenitic and in many specimens it is sheathed by sphene.

TABLE 5.—Modes of Piper Gulch Monzonite and related rocks

[Field numbers are abbreviated; year of collection and collector's initial omitted. Full field number of specimen 25 thus is 65D840, etc. (except R21, which was collected independently by R. Rohrbacher). s, standard deviation, Tr., trace; . . . , not determined]

Rock type	Monzonite and syenodiorite															Quartz diorite and diorite	
Specimen No.	25	26	27	28	29	30	31	32	33	34	35	36	37	38	25-38	39	40
Field No.	840	725	779	578	470	144	151	148	R21	280	160	156	185	212	Mean	1808	854
Quartz	2.8	1.9	3.3	2.9	5.6	0.8	2.7	3.1	4.8	8.6	4.2	6.1	1.3	7.3	3.8 2.4	0.7	3.5
Plagioclase, total	62.8	55.8	43.2	52.9	38.	51.0	57.4	55.9	29.5	57.8	42.4	40.5	46.7	49.3	48.9 9.2	54.9	71.2
(plagioclase in perthite)	0	(2.0)	(4.5)	0	(4.1)	(0.6)	0	(2.0)	0	0	0	0	0	0	(0.9) (1.6)	(1.9)	0
Orthoclase	13.1	26.3	31.7	29.2	26.4	35.0	22.2	21.4	39.7	14.5	31.4	27.6	34.6	24.4	27.0 7.6	27.0	9.2
Hornblende	10.3	7.6	3.8	11.4	17.6	7.8	12.9	7.8	21.5	14.4	11.0	11.6	2.8	9.8	10.7 5.0	8.7	11.6
Pyroxene	0	0	5.7	0	0	0	0	0	0	0	4.8	3.9	6.7	4.8	1.9 2.6	0	0
Biotite	36.3	.8	4.4	.5	6.2	.5	.6	8.2	0	Tr.	1.1	2.7	2.2	0	2.4 2.8	.5	0
Magnetite	2.7	3.9	5.9	3.8	4.6	3.9	3.3	2.5	3.3	4.0	3.8	6.3	3.9	3.7	4.0 1.1	6.9	3.7
Apatite	1.0	1.1	1.2	1.0	.5	.6	.4	.8	1.2	.7	1.1	.8	.9	.4	.8 .3	1.0	.5
Sphene	.9	.8	.6	.3	.4	.3	.4	.3	0	0	Tr.	.05	0	.05	.3 .3	.3	.3
Rutile	0	0	0	0	0	0	0	0	0	0	.1	.3	.1	0	Tr. .08	0	0
Tourmaline	.1	1.8	.2	0	0	.05	0	.05	0	Tr.	.05	.2	.8	.1	.2 .5	Tr.	0
Zircon	.05	0	0	0	0	0	0	0	0	Tr.	0	0	Tr.	0	Tr.	0	Tr.
Total	100.05	100.0	100.0	100.0	100.0	99.95	99.9	100.05	100.0	100.0	99.95	100.05	100.0	99.85	100.0	100.0	100.0
Femic	21.3	16.0	21.8	17.0	29.3	13.2	17.6	19.6	26.0	19.1	22.0	25.8	17.4	18.9	20.3 . . .	17.4	16.1
Percent plagioclase in anorthite	47-55	45-56	50-55	50-55	0-5	45-50	45-50	0	38-50	60	38-39	47-55	20-56	48-50	Common range 35-55	37-41	0-5
Quartz mixing index (see text)	.85	.90	.97	.80	.93	1.00	.50	.79	.62	.85	.45	.53	.55	.36	.72 .21	.30	.87

¹ Rock is metamorphosed.

² Quartz content may be as much as 0.5 percent higher, owing to presence of uncounted microgranophyre.

³ Modal sum of hornblende and biotite, 16.6 percent, is more reliable than these reported values.

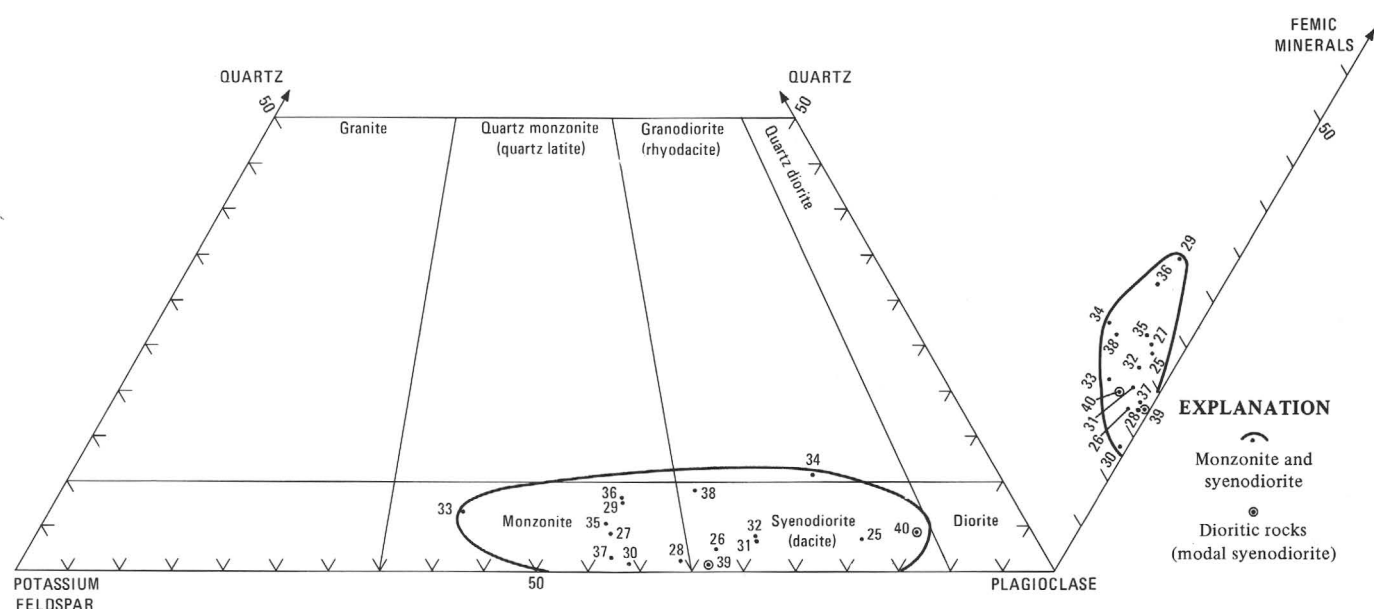


FIGURE 14.—Modified triangular diagram showing modal quartz, potassium feldspar, plagioclase, and femic minerals of Piper Gulch Monzonite and related rocks.

Of the trace minerals, apatite forms crystals that range in shape from stubby prismatic to highly acicular. Sphene is notably less abundant in the monzonite than in other rocks in the area that have a high color index, such as the Josephine Canyon Diorite. Rutile(?) forms acicular crystals along the cleavage planes of the orthoclase of several specimens. Schorlite tourmaline is a secondary

mineral in the border rocks, and it may be a primary mineral elsewhere in the monzonite.

The alteration minerals are, in addition to those already mentioned, epidote, leucosene, and calcite.

Chemical and spectrographic analyses and calculated CIPW norms of three specimens are shown in table 6. The mean composition of these specimens is similar to the

TABLE 6.—*Chemical and spectrographic analyses and CIPW norms of Piper Gulch Monzonite and related rocks*

[Chemical analyses by rapid rock method (Shapiro and Brannock, 1962), with sample 40 supplemented by atomic absorption method and all other specimens supplemented by X-ray fluorescence method. Chemical analysts: Lowell Artis, S. D. Botts, G. W. Chloe, P. L. D. Elmore, John Glenn, H. Smith, and Dwight Taylor. Spectrographic analyses by semiquantitative method. Spectrographic analysts: W. B. Crandell, J. L. Finley, and J. C. Hamilton. Elements looked for but not found: Ag, As, Au, Bi, Cd, Eu, Ge, Hf, Hg, In, Li, Pd, Pr, Pt, Re, Sb, Sm, Ta, Te, Th, Ti, U, W, and Zn. Symbols: s, standard deviation; <, less than; N, not detected; . . . , not determined]

Rock type	Monzonite and syenodiorite				Quartz diorite	
Specimen No.	27	34	38	27— 38	40	
Field No.	779	280	212	Mean s	854	
Chemical analyses (weight percent)						
SiO ₂	55.4	56.0	56.0	55.8	0.3	64.1
Al ₂ O ₃	18.2	15.8	17.2	17.1	1.2	16.8
Fe ₂ O ₃	4.2	5.0	4.5	4.6	.4	2.8
FeO	3.0	3.8	3.3	3.4	.4	2.1
MgO	3.1	2.7	3.0	2.9	.2	1.1
CaO	5.0	5.3	5.0	5.1	.2	4.3
Na ₂ O	3.8	3.0	3.4	3.4	.4	4.0
K ₂ O	4.3	4.2	4.5	4.3	.2	2.0
H ₂ O—	.30	.19	.19	.23	.06	.15
H ₂ O +	.80	1.4	1.1	1.1	.3	1.3
TiO ₂	.97	1.2	1.2	1.12	.1	.78
P ₂ O ₅	.57	.53	.42	.51	.08	.29
MnO	.14	.33	.18	.22	.1	.13
CO ₂	.11	.16	<.05	.09	.08	<.05
Total	100	100	100	100	...	100
Spectrographic analyses (weight percent)						
B	0.007	0.005	0.003	0.005	0.002	0
Ba	.1	.15	.01	.09	.07	.1
Be	.0001	.0002	.0003	.0002	.0001	0
Ce	.01	0	N	.005	.007	.01
Co	.002	.002	.003	.003	.0006	.0005
Cr	.001	.002	.0007	.001	.0007	0
Cu	.03	.015	.03	.03	.009	.0005
Ga	.001	.003	N	.002	.001	.0015
La	.007	.005	.005	.006	.001	.007
Mo	.0005	0	0	.0002	.0002	0
Nb	0	.0015	0	.0005	.0008	0
Nd	0	.007	N	.004	.005	.01
Ni	<.003	.0015	.003	.002	.0008	0
Pb	.0015	.0015	.001	.001	.0003	.0007
Sc	.005	.002	.007	.004	.003	.0005
Sn	.0003	0	0	.0001	.0002	0
Sr	.1	.1	.015	.07	.05	.07
V	.02	.015	.015	.02	.003	.002
Y	.003	.003	.015	.007	.007	.002
Yb	.0003	N	N	.00030002
Zr	.03	.02	.005	.02	.01	.02
CIPW norms						
Q	3.2	9.4	5.5			23.1
C	0	0	0			1.0
or	25.4	24.8	26.6			11.8
ab	32.1	25.4	28.8			33.9
an	19.9	17.2	18.4			19.1
di	{ wo	.20	1.9	1.5		0
		.16	1.4	1.2		0
hy	{ en	.01	.31	.12		0
		7.6	5.3	6.2		2.7
mt	{ fs	.68	1.2	.58		.50
		6.1	7.3	6.5		4.1
hm	0	0	0		0	
il	1.8	2.3	2.3		1.5	
ap	1.4	1.3	1.0		.69	
cc	.25	.36	0		.11	
Total	98.8	98.2	98.7			98.5
Femic	18.2	21.4	19.4			9.6

lead-alpha age determination (table 4; specimen 34). A Late Triassic or Early Jurassic age of this formation was also surmised from its geologic relations to other rocks: it postdates the Triassic Mount Wrightson Formation and predates the Jurassic Squaw Gulch Granite. The reliability of the lead-alpha age determination, which would be low if taken by itself, is considerably increased because that age determination is part of a series of determinations on Mesozoic rocks which are internally consistent with the geologic relations between the rocks.

Monzonite that resembles precisely the composition and age of the Piper Gulch is not known in other parts of southeastern Arizona. However, rocks that resemble the Piper Gulch in a general way include the Harris Ranch Monzonite of Damon (1965), in the Sierrita Mountains (fig. 1) and the Copper Belle Monzonite Porphyry (Gilluly, 1956, p. 63–65) in the Courtland area (fig. 1), 50 miles east of the Santa Rita Mountains. Neither of these formations is radiometrically dated, and the restraints in age imposed by the geologic relations of the Copper Belle to surrounding formations are fewer than those on the Piper Gulch or the Harris Ranch.

QUARTZ DIORITE

Two masses of strongly altered quartz diorite and other dioritic rocks underlie an area of about 2 square miles of the high central part of the Santa Rita Mountains (fig. 11) and are provisionally mapped as intrusive masses of Triassic age. One of these intrusive masses underlies a broadly arcuate area about 3½ miles long and ¼ mile wide between Cave Creek and Florida Canyon. The elongate shape of this mass and its parallelism to some faults 1–3 miles east of the mass (Drewes, 1971c) suggest that its emplacement was structurally controlled, but direct evidence supporting this notion has not been found in the thick and uniform pile of volcanic rocks into which the quartz diorite was intruded. The other intrusive mass of quartz diorite crops out in an irregular area high on the east wall of Madera Canyon.

The Triassic quartz diorite is generally a greenish-gray to bluish-gray rock that is poorly exposed because it is more friable than the Mount Wrightson volcanic host rocks. The quartz diorite typically underlies benches, saddles, and steep slopes thickly covered by colluvium derived from the volcanics. The available outcrops are small except along the bottom of a tributary on the south side of Cave Creek where the rock is an atypically fine grained border phase. The contact was not seen and the intrusive relations are inferred from the shapes of the masses and the suggestions of chilled fine-grained textures of rocks near some of the margins of the masses. Along the western side of the irregular-shaped mass the quartz diorite and its andesitic border-phase contain some small inclusions of hybridized

composition of the hornblende-biotite monzonite of Nockolds (1954, p. 1017).

The Piper Gulch Monzonite is dated as Triassic by one

porphyritic rock resembling the nearby body of Piper Gulch Monzonite. Toward the northern part of this contact area the quartz diorite itself appears to be recrystallized by the adjacent stock of Madera Canyon Granodiorite.

The quartz diorite has a sparsely porphyritic felty to granular texture and a mineral assemblage that is largely obscured by alteration. The felty laths of the groundmass are 0.1–2.0 mm long and the few phenocrysts are only about 4 mm long. The major mineral constituents and their estimated abundance are andesine plagioclase (50–75 percent), amphibole (8–20 percent) and quartz (0.5–15 percent). Some specimens contain potassium feldspar, pyroxene, and biotite in unknown but probably small quantities. Trace amounts of magnetite, zircon, apatite, and sphene are generally also present. The secondary minerals are very abundant and include chlorite, epidote, zoisite, leucoxene, penninite, calcite, sericite, iron oxide, and clay minerals. The plagioclase of most specimens is albitized.

The relatively large variation in the content of quartz among specimens and within a specimen suggests that quartz may be in part recrystallized or a secondary mineral. Note that the quartz content of the two moded specimens in table 5, the least altered rocks available, is as low as any recorded (0.5–15 percent), and the specimens are modal syenodiorites. The mixing index of specimen 39 (table 5) is also unusually small. Furthermore, that specimen has unusually large amounts of orthoclase, magnetite, and apatite. Other specimens too altered to be moded seem to be quartz diorites, which designation is applied to the entire suite of specimens. Assembling modal data on the Triassic quartz diorite will require additional detailed study.

Chemical and spectrographic analyses of a single specimen are listed in table 6. In view of the modal uncertainties, these analytical results must be evaluated cautiously.

The quartz diorite masses are dated only through their geologic relations to other rocks; it seems unlikely that the rock can be dated by radiometric methods because it is so strongly altered. Both dioritic masses intrude the Mount Wrightson Formation of Triassic age. The inclusions in one mass may be penecontemporaneous with, or younger than, the Piper Gulch Monzonite, which, in turn, appears to be altered by the Madera Canyon Granodiorite of Late Cretaceous age. The intensive alteration of the rock, which is so unlike that of the Jurassic and Cretaceous intrusive bodies, and the dioritic composition, which is also unlike that of the Jurassic body, are the reasons for assigning the quartz diorite to the older part (Triassic) of the age range available for the rock. Correlation of the quartz diorite is precluded by the uncertain age and original composition.

SQUAW GULCH GRANITE

Squaw Gulch Granite, defined by Drewes (1968), is a coarse-grained pink rock, mainly of granitic composition, that forms an intrusive mass almost batholithic in size. It underlies an outcrop area of only 12 square miles in the southern part of the Santa Rita Mountains (fig. 15), but at shallow depths the granite mass probably extends over an area of 40 square miles. About 3 miles south of the Squaw Gulch area, granite of similar appearance underlies a substantial part of the upfaulted block of the northern Patagonia Mountains (Simons, 1974). The granite of the Patagonia Mountains may be a direct extension of the Squaw Gulch Granite batholith, or it may be a separate cupola of that batholith. In addition, a shred of evidence, to be discussed in the section on the Elephant Head Quartz Monzonite, suggests that the Squaw Gulch Granite may have extended northwestward where it was thoroughly recrystallized during Late Cretaceous time.

In the Santa Rita Mountains the granite intruded igneous, sedimentary, and metamorphic rocks of Precambrian, Paleozoic, and Triassic ages. The contact with the Triassic Mount Wrightson is typically steep, and the nearby volcanic rocks are contact metamorphosed. (See geologic map, Drewes, 1971c.) Near the Glove mine (fig. 15) the granite intruded contact-metamorphosed Paleozoic formations along another steep contact. Some of the Continental Granodiorite immediately north of the collection site of specimen 54 was also recrystallized by the granite, and the concealed contact there is inferred to be steep and regular. The contact of the granite with other rocks, such as the Triassic Piper Gulch Monzonite and a few small masses of Paleozoic rock south of the Glove mine, is short and dips irregularly; there the host rock forms inclusions, roof pendants, or septa, rather than wallrock, to the batholith. Most of the intrusive contacts are fairly sharp, but the contacts with some of the inclusions of Piper Gulch Monzonite are gradational over distances of tens to hundreds of feet. The rocks in the transition zone are mottled and consist of patches of dark-gray monzonite surrounded by pinkish-gray granitic material.

Rocks of Early Cretaceous and younger ages unconformably overlie the granite. The oldest of these formations is the Temporal, a pre-Bisbee Group volcanic and sedimentary formation that contains wedges of granite-boulder conglomerate and that was deposited on a surface of rugged local relief carved on the granite as described by Drewes (1971a, figs. 18 and 19, and p. C35). Along the west flank of the mountains, the Upper Cretaceous Salero Formation overlies an extensive area of granite on a surface of moderate local relief, and some members of the Salero consist mainly of sediment derived from weathered Squaw Gulch Granite.

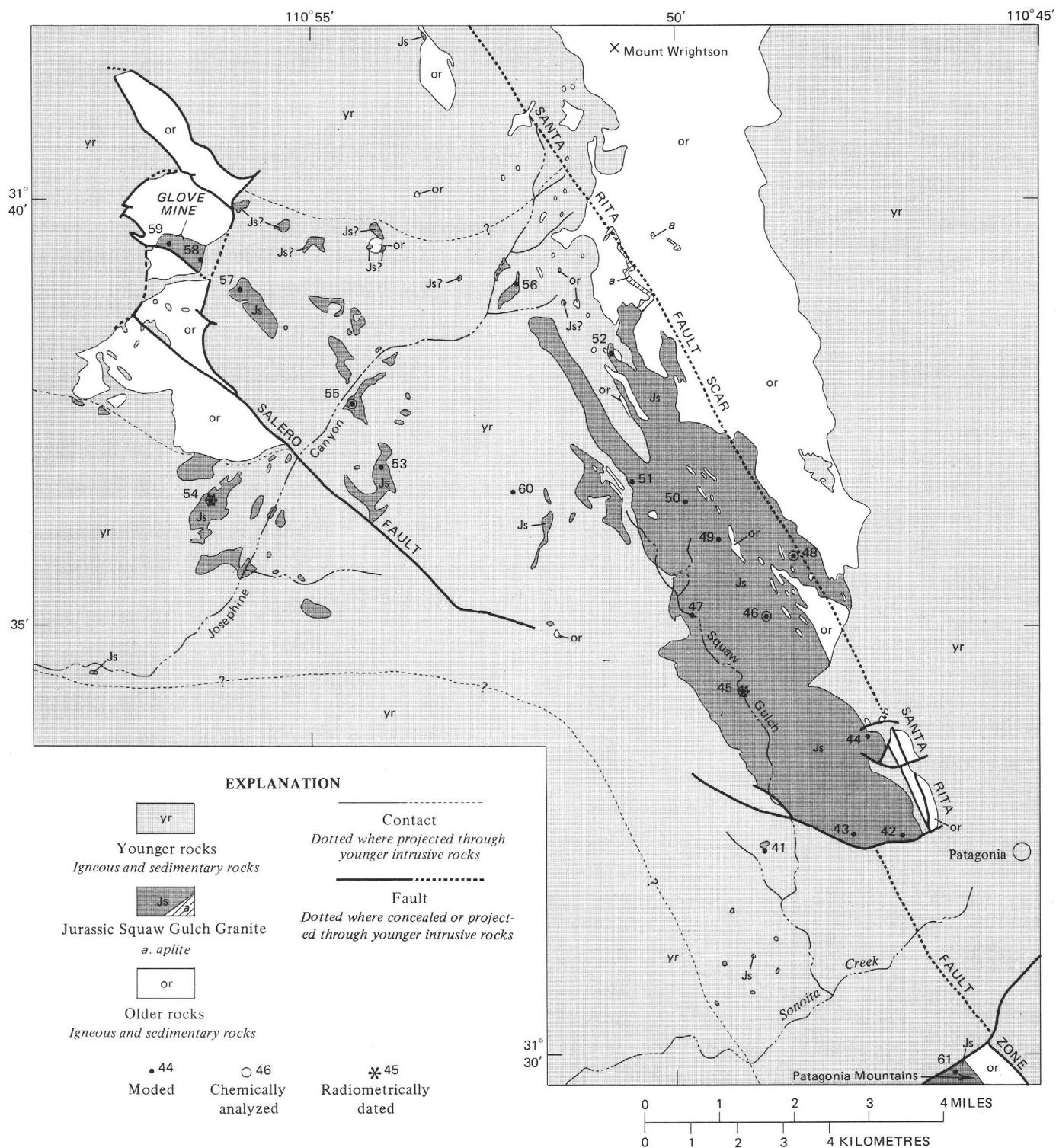


FIGURE 15.—Distribution of Squaw Gulch Granite and specimen collection sites.

PETROGRAPHY

The Squaw Gulch Granite is made up mainly of coarse-grained granitic rock intruded by some small masses of aplite and lamprophyre. In composition and appearance

the granitic rock is uniform over a distance of a mile or so but varies from a pinkish rock of granite composition in the southeast to a grayish rock of sodic quartz monzonite composition in the northwest. The term "granite" is emphasized in the name of the formation in order to

distinguish it from other formations whose composition is entirely of quartz monzonite. Aplite generally fills dilation fractures, forms small irregular bodies within the batholith, or has accumulated along parts of the northeastern margin of the batholith where it forms a sill-like tongue into the host rock. A few lamprophyre dikes that were plotted on the field sheets are too small to be shown on the published geologic maps.

GRANITE AND QUARTZ MONZONITE

The Squaw Gulch Granite (fig. 15) typically underlies a gently rolling terrain in which outcrops are fairly small, widely scattered, and deeply weathered. However, granite along the west flank of the mountains, particularly along the middle reaches of Josephine Canyon, forms prominent bosses and ledges and some small clusters of boulderlike residual masses. The granite of the type area, along Squaw Gulch, and that near Josephine Canyon is characteristically "salmon" colored, or moderate orange pink; the rock farther north is grayish orange pink. The granite along Squaw Gulch is generally more closely fractured than that near Josephine Canyon to the northwest, perhaps, thereby weathering to form the prominent bosses and massive outcrops. In all areas the least weathered granite is in outcrops along the deepest and narrowest canyons. A slab of typical granite is shown in figure 16. The rock has a hypidiomorphic-granular texture (fig. 17) and a grain size of 3 to 8 mm. Myrmekitic and granophyric textures occur throughout the batholith and are particularly abundant and coarse grained in the southern part of it. In some specimens the quartz intergrowths form conspicuous rosette patterns and alternate zones of differing grain size (fig. 18).

The modal compositions of 21 specimens of granite are shown in table 7. Two specimens (60, 61) are not from the batholith in the Santa Rita Mountains; specimen 60 is from a boulder in the Cretaceous Salero Formation where that formation lies directly on the granite, and specimen 61 is from the northern part of the Patagonia Mountains. The modes of specimen 58 and, to a lesser extent, specimen 59 resemble those of the Elephant Head Quartz Monzonite more closely than they do the average Squaw Gulch Granite. This observation will be referred to again in connection with the section on the age and origin of the Elephant Head Quartz Monzonite. The correlation of the granitic body represented by specimens 58 and 59 with the Squaw Gulch Granite is based on geologic relations that show the body to be older than the Elephant Head stock, for the stock intrudes the Salero Formation, which in turn, unconformably overlies the granitic body and its contact-metamorphosed host rocks. These field relations are illustrated on the geologic map (Drewes, 1971c) and are discussed in greater detail in the report on the structural geology of the area (Drewes, 1972b).



FIGURE 16.—Specimen 45. Squaw Gulch Granite.

The three main mineral constituents—quartz, orthoclase, and plagioclase—make up more than 93 percent of the Squaw Gulch Granite, and accessory biotite, magnetite, apatite, and zircon make up the remainder; some specimens also contain trace amounts of sphene and tourmaline. The quartz forms anhedral grains that have a moderately strong undulatory extinction. Orthoclase is also anhedral and is slightly kaolinitized to give the fine-textured light-gray appearance of the crystals in figure 17. Lace and patch perthite are common in the orthoclase; they produce the white blotches seen in figure 17 and the fine lacy patterns in the orthoclase of figure 18. The amount of albite in the perthitic orthoclase averages nearly 8 percent, and in specimen 43 it exceeds 24 percent. The plagioclase has the composition of albite, but its alteration to clay minerals and sericite obscures any evidence of albitization. Biotite is largely altered to chlorite and in some specimens to penninitic chlorite; only specimen 54 has enough unaltered biotite to be concentrated for radiometric dating. The magnetite is ilmenitic. Zircon is

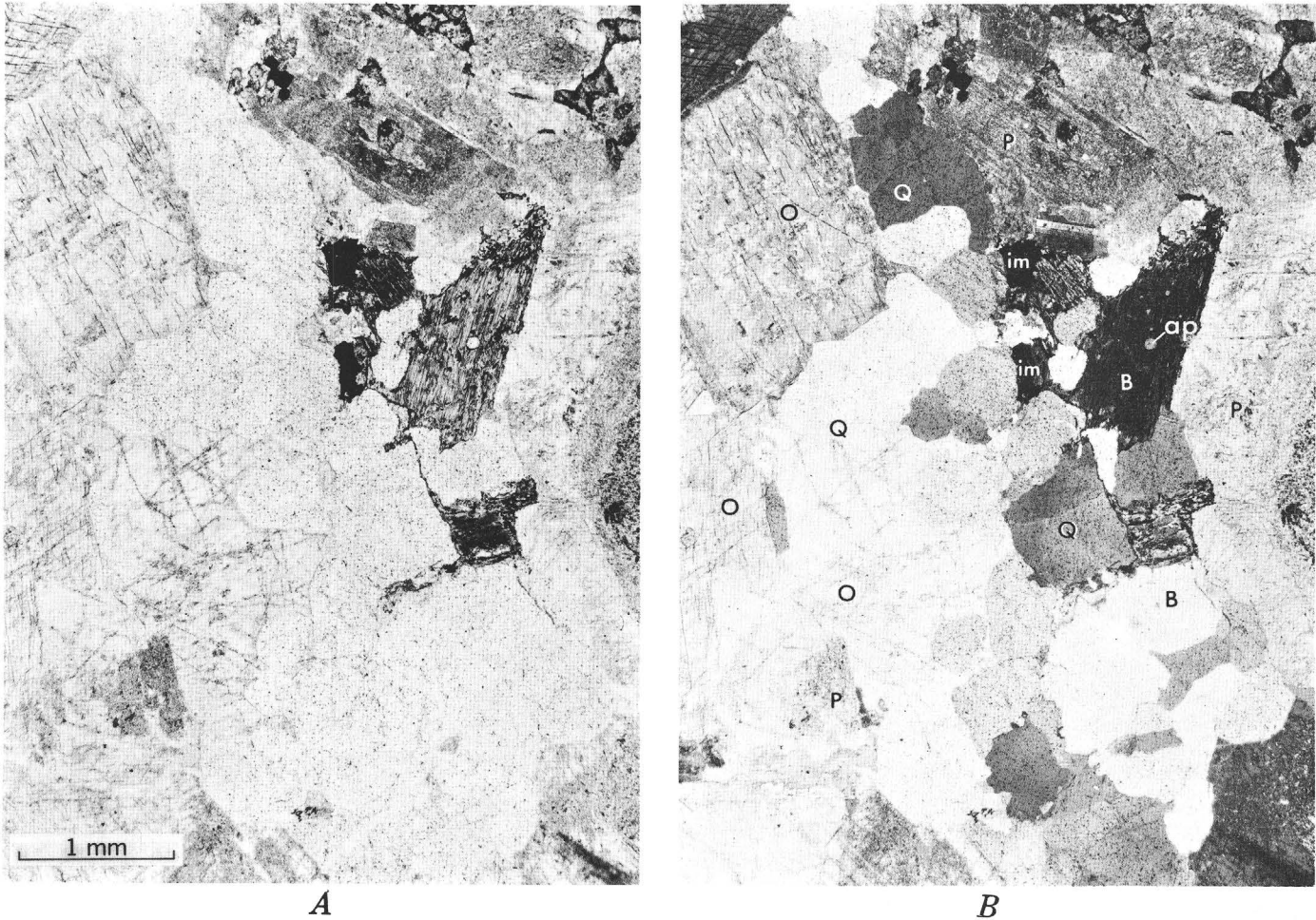


FIGURE 17.—Specimen 45. Squaw Gulch Granite, showing typical texture and mineral assemblage. Crystals: perthitic orthoclase (O), quartz (Q), plagioclase (P), partly chloritized biotite (B), ilmenitic magnetite (im), and apatite (ap). $\times 20$. A, Plain light; B, crossed nicols.

sufficiently abundant in many specimens to make it possible to date the rock by the lead-alpha or fission-track method.

APLITE AND LAMPROPHYRE

Aplite associated with the Squaw Gulch Granite is pale red to pinkish gray in fresh and weathered rock alike. The aplite has a grain size of 0.03–0.3 mm; it typically has a sugary appearance in hand specimens and an idiomorphic-granular texture in thin sections. The texture is commonly granophyric and rarely finely porphyritic.

The mineralogic similarity of the aplite to the Squaw Gulch Granite is indicated by the following estimated mode. Major mineral constituents and their range of abundance, in percent, are quartz (25–35), orthoclase (30–45), and albite plagioclase (15–25). Accessory minerals, in trace amounts, are biotite, ilmenitic magnetite, apatite, and sphene. Kaolinite, sericite, chlorite, epidote, leucoxene, and iron oxide are the alteration minerals which are abundant in some specimens.

Lamprophyre dikes are mostly only 1 to 3 feet thick and are made up of greenish-gray to dark-greenish-gray andesitic or dioritic rock. The dikes form small clusters of parallel bodies in two places along the middle reaches of Josephine Canyon. The dikes of both clusters dip vertically; one group strikes west and the other northwest. Lamprophyre is less resistant to weathering than the adjacent granite and so the dikes rarely crop out.

Under the microscope the lamprophyre is seen to have a felty or ophitic texture. Grain size ranges from 0.1 to 1.0 mm.

The lamprophyre's strong alteration and the fine grain size make it difficult to calculate a mode. Plagioclase is a major constituent and is albitized and strongly sericitized. A pyroxene, which may be augite, and an amphibole are generally represented by pseudomorphs of uraltite, chlorite, and epidote. A little quartz is present in one specimen and magnetite, apatite, and sphene are commonly the accessory minerals. Leucoxene, iron oxide, and penninite occur, along with the alteration minerals already mentioned.

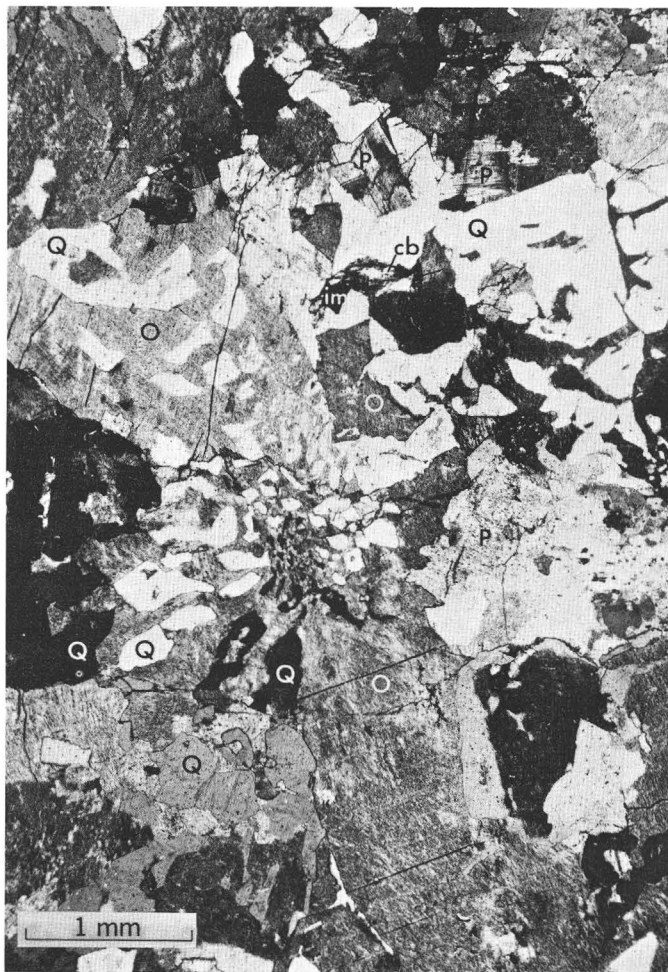


FIGURE 18.—Specimen 48. Squaw Gulch Granite, showing strongly developed granophyric texture and preponderance of orthoclase over plagioclase. Crystals: orthoclase (O), quartz (Q), plagioclase (P), ilmenitic mangetite (im), chloritized biotite (cb). Crossed nicols; $\times 20$.

MODAL AND CHEMICAL SUMMARY

The modified triangular diagram of figure 19 graphically summarizes the modes of the specimens of Squaw Gulch Granite. The solid figure circumscribed around the plotted modes has a discoid shape, centered at a point near the boundary between the granite and quartz monzonite field and 2–3 percent of the distance from the leucocratic face of the composition tetrahedron toward the femic apex. The anomalous mode of specimen 58 is clearly illustrated by its position outside the circumscribed figure, although its composition is included in the calculation of a mean of the modes (table 7). The anomalous composition of specimen 60 from the boulder, also shown, suggests that further study of the composition of the clasts in the conglomerate unit in the Salero Formation might add significantly to the knowledge of the Mesozoic rocks of the area.

Chemical and spectrographic analyses and CIPW norms of four of the moded specimens of Squaw Gulch Granite

are listed in table 8 and the chemistry is compared with that of other plutonic rocks of the area in figure 10. The chemical composition of the granite is very similar to that of the Corona stock and of the Elephant Head Quartz Monzonite (figs. 10I–10L). Chemically the granite also resembles somewhat the granitoid rocks of the Helvetia stocks and the quartz latite porphyry of the Greaterville plugs. The mean chemical composition of the Squaw Gulch Granite is most like that of an alkali granite, such as the muscovite granite, of Nockolds (1954, p. 1012), with a tendency toward the composition of his calc-alkali biotite granite.

AGE AND CORRELATION

The Squaw Gulch Granite is dated as early Mesozoic through its geologic field relations, and it is more precisely dated as Jurassic by radiometric means. With respect to formations dated by their fossil content, the granite post-dates some Permian rocks and predates the Lower Cretaceous Bisbee Group. The age of the granite is further restricted as younger than the Piper Gulch Monzonite, which is radiometrically dated as Triassic and is judged to be of possible Late Triassic age. The granite is also known to be older than the Temporal and Bathtub Formations, both of which underlie the Bisbee Group, and which are assigned to the earliest part of the Early Cretaceous. A Jurassic age is therefore indicated by the combined evidence from the field relations of the granite to other formations whose ages are reasonably well established.

Two specimens (54 and 45 of table 4) are dated by the lead-alpha method of zircon, and one of these is also dated by the potassium-argon method on biotite. The two lead-alpha ages are in excellent agreement at about 160 m.y., and the agreement of these ages with the potassium-argon age determination—145 m.y. from specimen 54—is reasonably good. The biotite concentrate may have given an age that is slightly too young because of chlorite contamination of the biotite. Nevertheless, the combined results of the three radiometric age determinations indicate that the granite is Jurassic or is possibly even restricted to Middle Jurassic.

Granite and quartz monzonite stocks of Jurassic age occur in several other ranges in southeastern Arizona. The Juniper Flat Granite of the Mule Mountains (fig. 1), 50 miles southeast of the Santa Rita Mountains, is dated as Triassic or Jurassic by Ransome (1904, p. 84) and by Gilluly (1956, p. 55) through its geological relations to fossiliferous rocks. Creasey and Kistler (1962, p. D1) dated this granite, using the potassium-argon method, as 163 m.y., or Jurassic. In the Sierrita Mountains the Sierrita Granite of Lacy (1959) was dated by Damon (1966), using the rubidium-strontium method, as 140 m.y. old, and by T. W. Stern (in Marvin and others, 1973), using the lead-alpha method, as 150 m.y.

In the Patagonia Mountains granite and quartz

monzonite stocks mapped by F. S. Simons (1974) are dated by T. W. Stern (in Marvin and others, 1973), using the lead-alpha method, as 160 and 150 m.y., respectively. Biotite and hornblende from another granitic stock mapped by Simons in the hills a few miles north of Nogales is dated as 160 m.y. by the potassium-argon method. The similarity in age and composition of all these rocks is impressive; apparently a distinctive magmatic event affected much of southeastern Arizona at that time.

CRETACEOUS ROCKS

Plutonic rocks of Cretaceous age form a series of stocks and related small masses of aphanitic rocks that were emplaced during the Piman phase of the Laramide orogeny. The Piman phase, lasting from about 90 to 63 m.y. ago (Drewes, 1972b), is the first and more active of two phases of that orogeny. In the Santa Rita Mountains tectonic activity probably peaked shortly before 72 m.y. ago. The Cretaceous plutonic rocks of the area include (1) the granitoid rocks of the Corona stock, which is nearly synchronous with the peak of tectonic activity, (2) the Josephine Canyon Diorite, (3) Madera Canyon Granodiorite, and (4) Elephant Head Quartz Monzonite, all of which slightly postdate the peak of tectonic activity, and (5) a few small intrusive masses of quartz latite porphyry, of somewhat equivocal age and association.

GRANITOID ROCKS OF THE CORONA STOCK

The Corona stock (fig. 20) underlies an area of several square miles at the northern end of the Santa Rita Mountains (Drewes, 1971b). On the basis of recently obtained radiometric dates, the stock is here assigned to the older group of stocks of Late Cretaceous age of the region, rather than to the Helvetia stocks, of Paleocene age, as previously mapped. Only about 1 square mile of stock is exposed within the Sahuarita quadrangle; most of the exposed part underlies the adjacent part of the Empire Mountains quadrangle, where it was mapped by T. L. Finnell (1971), and an unknown amount of the stock underlies gravel deposits on the pediment along the north flank of the mountains. About half the outcrop area of the granitoid rocks shown in figure 20 is on the pediment southeast of the community of Corona de Tucson.

The Corona stock is made up of a variety of granitoid rocks whose mutual relations are not fully known. Most of the rocks in the part of the stock that lies within the Sahuarita quadrangle are quartz monzonite; some of the rocks are granodiorite and others are aplite. According to T. L. Finnell (oral commun., 1971), the rocks of the eastern part of the stock are mainly quartz monzonite and include some quartz diorite phases (not shown in fig. 20). Granodiorite masses found near the collection site of specimen 66 (fig. 20) are enclosed by quartz monzonite and

so may be inclusions, but unequivocal contact data supporting this interpretation have not been found. The relation of other granodiorite from near the collection site of specimen 65 to the quartz monzonite is unknown. The granitoid rocks are intruded by the aplite, as well as by small dikes of lamprophyre and veinlets of quartz.

The outcrop area of the Corona stock is irregular shaped, and the stock contains many inclusions or roof pendants of the host rocks which are comprised of arkosic sandstone and siltstone and of some intercalated thin beds of limestone of the Apache Canyon Formation and the Shellenberger Canyon Formation of the Bisbee Group. The main body of aplite lies within the stock, but many of the small bodies of aplite intrude the host rocks near the stock. The host rocks near the stock, and particularly in the area of aplite intrusives, are contact metamorphosed to hornfels and calc-silicate rocks. Where exposed, the contact is sharp, and the granitoid rocks near the contact seem to lack a chill-zone texture, but they may have a more felsic composition, as described in the third following paragraph.

The quartz monzonite of the pediment area is mostly deeply weathered and that of the hilly terrain forms pinkish-gray to grayish-orange-pink, high, rounded bosses and piles of boulderlike residual blocks that are intermittently veneered by grus. Weathered granodiorite masses are brownish gray and are darker than the quartz monzonite terrain. Aplite commonly weathers to form very pale orange irregular-shaped outcrops, blocky detritus, and some grus. The randomly scattered lamprophyre dikes are dark gray to greenish gray, typical of porphyritic dacite and andesite.

The quartz monzonite is typically hypidiomorphic-granular in texture; some specimens also have a little mosaic, porphyritic or porphyroblastic, and granophyric texture. Grains range in size from 1 to 10 mm and in some specimens, their size distribution is bimodal. The clustering of small grains of some specimens, such as shown in figure 21, may indicate recrystallization. Aplite has an idiomorphic-granular and porphyritic texture. Its groundmass grains are about 0.1 mm across, and its phenocrysts are 0.15 to 2.0 mm across.

Five modes of granitoid rock of the Corona stock are shown in table 9. Specimen 65 is granodiorite; the others are quartz monzonite. Specimens 62 and 63 are from near the margin of the stock, which may be the cause of the abnormally large content of potassium feldspar of specimen 63 and the more felsic composition of specimen 62. Specimens 64 and 66 are, thus, most typical of the main rock type at the western end of the stock, yet their composition deviates but little from the mean of all the modes. The shape and position of the figure circumscribed around the modes plotted on the diagram of figure 22 is probably of slight significance because so few modes are

TABLE 7.—*Modes of Squaw Gulch Granite*

[Field numbers are abbreviated; year of collection and collector's initial omitted. Full field number of specimen 41 thus is 65D915. Symbols:

Rock type.....	Granite (includes quartz monzonite)														
Specimen No.....	41	42	43	44	45	46	47	48	49	50	51	52	53	54	55
Field No.....	915	229	984	906	249	209	237	190	184	167	166	174	446	605	450
Quartz.....	27.5	12.0	11.9	30.0	23.2	31.2	24.0	35.2	37.4	29.4	26.6	22.4	39.6	16.4	38.5
Plagioclase, total.....	9.0	35.2	33.9	16.1	36.1	9.7	24.8	14.6	14.9	22.8	11.9	19.6	27.3	37.6	19.7
(plagioclase in perthite).....	(9.0)	(12.9)	(24.1)	(6.1)	(11.3)	(2.1)	(5.9)	(6.6)	(10.4)	0	(11.9)	(17.6)	(3.5)	(5.3)	(2.6)
Orthoclase.....	63.0	46.2	51.7	52.5	37.6	57.2	48.8	47.9	45.0	46.6	59.0	56.5	30.8	41.3	40.4
Microcline.....	0	0	0	0	0	0	0	0	0	0	0	0	.7	0	0
Biotite.....	.1	2.4	.9	.9	1.9	1.1	1.9	1.4	1.3	.6	1.6	.5	1.2	2.3	1.1
Magnetite.....	.4	.7	1.4	.5	.9	.7	.3	.8	1.0	.6	.9	.5	.4	.9	.3
Apatite.....	0	.6	0	.05	.05	.05	.1	.1	.1	Tr.	Tr.	Tr.	0	.4	Tr.
Zircon.....	0	.05	.1	Tr.	.05	.05	.05	.05	.3	Tr.	Tr.	.05	Tr.	.1	.05
Sphene.....	0	1.7	.1	0	Tr.	0	.05	0	0	0	.05	.5	Tr.	1.0	0
Tourmaline.....	0	0	0	0	.2	0	0	0	.05	0	0	0	0	0	0
Amphibole.....	0	1.1	0	0	0	0	0	0	0	0	0	0	0	Tr.	0
Rutile.....	0	0	0	0	0	Tr.	Tr.	0	0	Tr.	0	0	0	0	0
Total.....	100.0	99.95	100.0	100.05	100.0	100.0	100.0	100.05	100.05	100.0	100.05	100.05	100.0	100.0	100.05
Femic.....	.5	6.6	2.5	1.4	3.1	1.9	2.4	2.3	2.7	1.2	2.5	1.5	1.6	4.7	1.4
Percent anorthite in plagioclase.....	0	0	0—5	0	0	0	0—5	0	0	0	0?	0?	0—5	0—5	0—5
Quartz mixing index (see text).....	.92	.85	.86	.74	.61	.87	.39	.92	.86	.73	.97	.69	.95	.92	.88

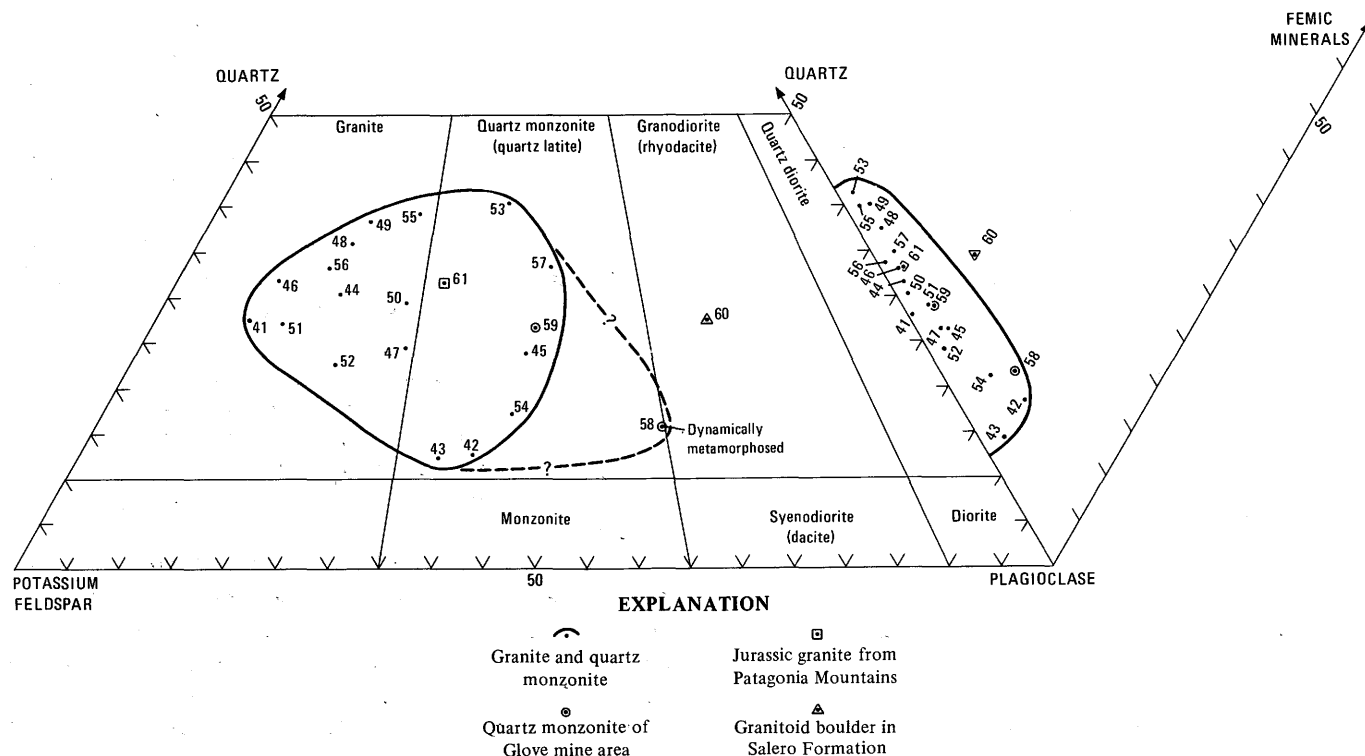
¹Specimen 45 collected almost at same place as chemically analyzed specimen 63D282 (table 8).²Specimen 52 collected from a small wedge of granite, between two small masses of altered rhyolite, that is erroneously shown as Josephine Canyon Diorite (Drews, 1971c).³Specimen 59 dynamically metamorphosed.

FIGURE 19.—Modified triangular diagram showing modal quartz, potassium feldspar, plagioclase, and femic minerals of Squaw Gulch Granite.

available, but the large size of the figure probably reflects the diverse rock types that are characteristic of the stock.

The internal uniformity of the rock, over a span of

several centimetres, seems greater than that of the equally coarse grained Squaw Gulch Granite (compare quartz mixing indexes, tables 5 and 9).

and related rocks

s, standard deviation; Tr, trace; . . . , not determined]

Granite includes quartz monzonite—Continued					Boulder in Salero Formation	Granite, Patagonia Mountains
Quartz monzonite of Glove Mine area				41—59 Mean	60	61
56	57	58	59		395	460
353	920	644	919			
32.9	33.0	14.6	26.0	26.9	20.6	31.2
13.9	34.3	50.7	35.9	24.6	48.0	25.2
(8.8)	(5.4)	(2.7)	(2.7)	(7.8)	(1.3)	(24.7)
52.3	30.5	27.6	35.1	45.8	22.3	41.6
0	0	0	0	Tr.	0	0
.2	2.0	5.3	2.4	1.5	5.8	.8
.6	.2	1.4	.5	.7	1.3	.9
Tr.	0	.3	.05	.1	.4	Tr.
Tr.	Tr.	.1	.05	.06	.07	0
.1	0	0	Tr.	.2	.4	.3
Tr.	0	0	0	Tr.	0	Tr.
0	0	0	0	.06	1.0	0
0	0	0	0	Tr.	0	0
100.0	100.0	100.0	100.0	99.92	100.0	100.0
.9	2.2	7.1	3.0	2.6	9.1	2.0
0?	0	0	0	0—5	0—10	0
.81	.88	.67	.85	.81	.86	.91

The mineral components of granitoid rocks consist of the usual abundant quartz, plagioclase, and potassium feldspar, less abundant biotite, and scarce accessory minerals. The quartz typically is anhedral, has slightly interlocking grain boundaries, and has a moderately strong undulatory extinction. The quartz of some specimens, however, has straight boundaries and no undulatory extinction, and that of others is strongly sutured. Plagioclase forms subhedral grains having a strong normal compositional zoning. The plagioclase is commonly albite, but that of specimen 66 is calcic oligoclase to sodic andesine, and the cores of some crystals of other specimens are sericitized oligoclase. The potassium feldspars are microcline and orthoclase in nearly equal amounts. The grid twinning of the microcline is fairly sharp in the small crystals (fig. 21) and along the edge of some large ones but is indistinct or blurred in the cores of the large grains. Perthitic textures are ubiquitous and range from finely lacy (fig. 21) to moderately coarse lacy types. Biotite is unaltered to partly chloritized and is pleochroic in very pale brown to dark brown. Magnetite is ilmenitic, and zircon grains are fairly abundant but particularly small. Sphene and amphibole occur only in the granodiorite specimen, and allanite occurs in two specimens.

A single chemical and spectrographic analysis and CIPW norm are given in table 10. The chemical analysis closely resembles the analyses of Squaw Gulch Granite and Elephant Head Quartz Monzonite (figs. 10I—10L).

An age of 73.8 m.y. was obtained by the potassium-argon method (Marvin and others, 1973) from quartz monzonite collected by T. L. Finnell about a mile east of the collection site of specimen 66, and another specimen, of a diorite stock that does not extend into the

TABLE 8.—Chemical and spectrographic analyses and CIPW norms of Squaw Gulch Granite

[Chemical analyses by rapid rock method (Shapiro and Brannock, 1962), with analyses of specimen 46, 48, and 55 supplemented by X-ray fluorescence method. Chemical analysts: Lowell Artis, S. D. Botts, G. W. Chloe, P. L. D. Elmore, John Glenn, and H. Smith. Spectrographic analyses by semiquantitative method. Spectrographic analysts: W. B. Crandell, J. C. Hamilton, and Barbara Tobin. Elements looked for but not found: Ag, As, Au, B, Bi, Cd, Eu, Ge, Hf, Hg, In, Li, Nd, Pd, Pr, Pt, Re, Sb, Sm, Sn, Ta, Te, Th, Ti, U, W, and Zn. Symbols: s, standard deviation; <, less than; N, not detected; . . . , not determined]

Granite and quartz monzonite						
Rock type	45	46	48	55	45—55	s
Specimen No.	45	46	48	55	Mean	s
Field No.	282	209	190	450		
Chemical analyses (weight percent)						
SiO ₂	69.1	75.1	75.1	75.5	73.7	3.1
Al ₂ O ₃	15.2	13.3	13.0	12.6	13.5	1.2
Fe ₂ O ₃	1.9	1.0	1.3	1.0	1.3	.4
FeO	1.0	.08	.18	.24	.38	.42
MgO	.55	.55	.05	.23	.35	.25
CaO	1.1	.25	.19	.35	.47	.42
Na ₂ O	4.0	3.0	3.6	3.5	3.5	.4
K ₂ O	5.2	5.9	5.5	4.7	5.3	.5
H ₂ O—	.34	.37	.09	.17	.24	.13
H ₂ O+	.93	.63	.64	.87	.77	.16
TiO ₂	.42	.17	.18	.21	.25	.12
P ₂ O ₅	.16	0	.01	.02	.05	.08
MnO	.03	.03	.02	.02	.03	.01
CO ₂	.19	<.05	.05	.15	.09	.10
Total	100	100	100	100	100	...
Spectrographic analyses (weight percent)						
Ba	0.07	0.02	0.01	0.03	0.03	0.03
Be	.0003	.0003	.0007	.0002	.0004	.0002
Ce	0	0	.015	0	.004	.008
Co	0	0	0	.0003	.0001	.0002
Cr	.00015	0	.00015	0	.00008	.00009
Cu	.0007	.0015	.0015	.0007	.001	.0005
Ga	.002	.002	.003	.001	.002	.0001
La	.005	.003	.007	.007	.006	.002
Mo	.001	0	0	0	.0003	.0005
Nb	.0015	.002	.0015	.001	.0015	.0004
Pb	.002	.0015	.003	.002	.002	.001
Sc	.0007	0	.0005	0	.0003	.0004
Sr	.02	.005	.003	.007	.009	.008
V	.002	.001	0	0	.001	.001
Y	.003	.002	.007	.003	.004	.002
Yb	.0003	N	.0007	.0003	.0004	.0002
Zn	.015	.01	.007	.015	.01	.004
CIPW norms						
Q	23.7	33.7	32.7	36.5		
C	1.8	1.5	.81	1.5		
or	30.7	34.9	32.5	27.8		
ab	33.8	25.4	30.4	29.6		
an	3.2	1.2	.88	.66		
di	0	0	0	0		
fs	0	0	0	0		
hy	1.4	1.4	.12	.57		
mt	2.1	0	.12	.23		
hm	.45	1.0	1.2	.84		
il	.80	.23	.34	.40		
ap	.38	0	.02	.05		
cc	.43	0	0	.34		
Total	98.8	99.3	99.1	98.5		
Femic	5.6	2.6	1.8	2.4		

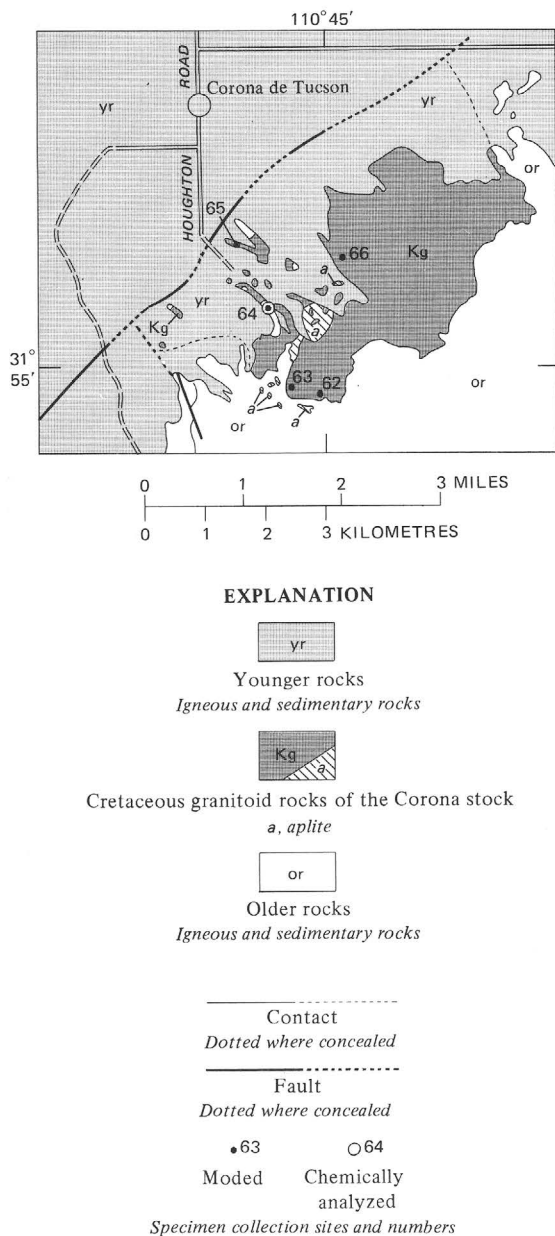


FIGURE 20.—Distribution of granitoid rocks of the Corona stock and specimen collection sites. Geology east of longitude 110°45' mainly adapted from Finnell (1971).

Sahuarita quadrangle, is dated at 73.6 m.y. A nearly identical potassium-argon age of 74.1 m.y. was obtained by S. C. Creasey (1967; and Marvin and others, 1973) from a granodiorite stock in the Whetstone Mountains, 18 miles southeast of the Corona stock. A slightly younger age of 70.3 m.y. was reported by Marvin for the quartz monzonite stock in the Empire Mountains (Marvin and others, 1973). Similar potassium-argon ages—71.4, 72.9, and 75.1 m.y.—were obtained by Bikerman and Damon (1966, p. 1232, 1233) from their Amole Granite and the



FIGURE 21.—Specimen 64. Quartz monzonite of the Corona stock. Zones of small crystals, including subhedral quartz and microcline with fairly sharp grid twinning, may indicate recrystallization. Crystals: perthitic microcline (M), quartz (Q), plagioclase (P), ilmenitic magnetite (im), and biotite (B). Crossed nicols; $\times 25$.

Amole Quartz Monzonite in the northwestern part of the Tucson Mountains.

These three stocks may be genetically related to three fields of rhyodacite volcanics. The eastern part of the Corona stock is shown by Finnell (1971) to cut the exotic block member low in the Salero Formation; an overlying rhyodacite member of this formation is dated at 72.5 m.y. (Drewes, 1971a). Rhyodacite welded tuff dated at 71.9 m.y. (Drewes, 1971a, p. C75) occurs along the San Pedro River, 15 miles southeast of the Whetstone stock, and other rhyodacite welded tuff 3 miles south of Courtland is dated at 72.8 m.y. (Marvin and others, 1973). Similar volcanics about 72 m.y. old occur in the Tucson Mountains (Bikerman and Damon, 1966, p. 1232). The six centers of nearly contemporaneous magmatic activity lie along a northwest-trending line, possibly a fracture in the basement rocks. A similar, possibly genetic, relation between plutonic and volcanic rocks is mentioned in the sections in the present report on the San Cayetano stock.

TABLE 9.—*Modes of granitoid rocks of the Corona stock*

[Field numbers are abbreviated; year of collection and collector's initial omitted. Full field number of specimen 62 thus is 67D1412. Symbols: s, standard deviation; Tr, trace; ..., not determined]

Specimen No.	62	63	64	65	66	62-66	
Field No.	1412	1411	1415	1422	1420	Mean	s
Quartz	41.7	25.9	28.1	24.4	25.2	29.1	7.2
Plagioclase, total	32.2	25.0	34.8	38.3	52.8	36.6	10.3
(plagioclase in perthite)	0	0	(3.1)	(1.5)	(1.8)	(1.3)	(1.3)
K-feldspar, total	20.9	45.8	34.3	35.1	12.0	29.6	13.2
(orthoclase)	(20.9)	(45.8)	Tr.?	0	(12.0)	(15.7)	(19.0)
(microcline?)	0?	Tr.?	(34.3)	(35.1)	0	(13.9)	(19.0)
Biotite	4.0	2.4	2.4	1.1	5.5	3.1	1.7
Amphibole	0	0	0	0	2.8	.6	.3
Magnetite	1.1	.8	.2	.7	1.0	.8	.4
Apatite	.05	.05	.2	Tr.	.3	.1	.1
Sphene	0	0	0	.2	.3	.1	.1
Zircon	.05	.05	.05	.1	.05	.05	.02
Allanite	0	0	0	.1	.05	Tr.	...
Total	100.0	100.0	100.05	100.0	100.0	100.05	...
Femic	5.2	3.3	2.8	2.2	10.0	4.8	...
Percent anorthite in plagioclase	5?	15?	37	37?	...
(plagioclase rims)	(15)	(15)	(15)	(15)	(20)	(15-20)	...
Quartz mixing index (see text)	.94	.98	.98	.96	.98	.97	...

JOSEPHINE CANYON DIORITE

The Josephine Canyon Diorite is a fine- to medium-grained plutonic rock that ranges in composition from diorite, through quartz diorite and syenodiorite, to granodiorite; a subordinate late phase consists of fine-grained quartz monzonite. The lithologic term "diorite," as applied to the Josephine Canyon Diorite, is used to include syenodiorite and quartz diorite as well as diorite, in order to emphasize the general compositional feature that distinguishes this formation from the granodiorites of the area.

TABLE 10.—*Chemical and spectrographic analysis and CIPW norms of the Corona stock, specimen number 64¹*

[Chemical analysis by rapid rock method (Shapiro and Brannock, 1962), supplemented by atomic absorption method. Chemical analysts: Lowell Artis, S. D. Botts, G. W. Chloe, P. L. D. Elmore, John Glenn, J. Kelsey, and H. Smith. Spectrographic analysis by semiquantitative method. Spectrographic analyst: J. L. Morris. Elements looked for but not found: As, Au, B, Bi, Cd, Eu, Ge, Hf, In, Li, Mo, Nd, Ni, Pd, Pr, Pt, Re, Sb, Sm, Sn, Ta, Te, Th, Tl, U, W, and Zn. Symbol: <, less than]

Chemical analysis (weight percent) ²			
SiO ₂	73.9	H ₂ O—	0.07
Al ₂ O ₃	13.3	H ₂ O+	.24
Fe ₂ O ₃	.58	TiO ₂	1.1
FeO	.56	P ₂ O ₅	.04
MgO	.33	MnO	.04
CaO	1.0	CO ₂	<.05
Na ₂ O	3.9	Total	100
K ₂ O	4.5		
Spectrographic analysis (weight percent) ³			
Ag	<0.0001	Pb	0.001
Ba	.07	Sc	.0003
Be	.0002	Sr	.02
Ce	.015	V	.0015
Cu	.0005	Y	.005
Ga	.001	Yb	.0005
La	.01	Zr	.007
Nb	.001		

CIPW Norms			
Q	31.7	hm	.58
C	.41	il	1.3
or	26.7	u	.43
ab	33.1	ap	.10
an	4.4	cc	.11
hy {en	.83	Total	99.7
fs	0	Femic	3.4

¹Field number 1415.

²A replicate analysis shows Al₂O₃, 14.5; H₂O—, 0.13; H₂O+, 0.47; TiO₂, 0.14; P₂O₅, 0.08; and other minor differences.

³A replicate analysis differed only slightly.

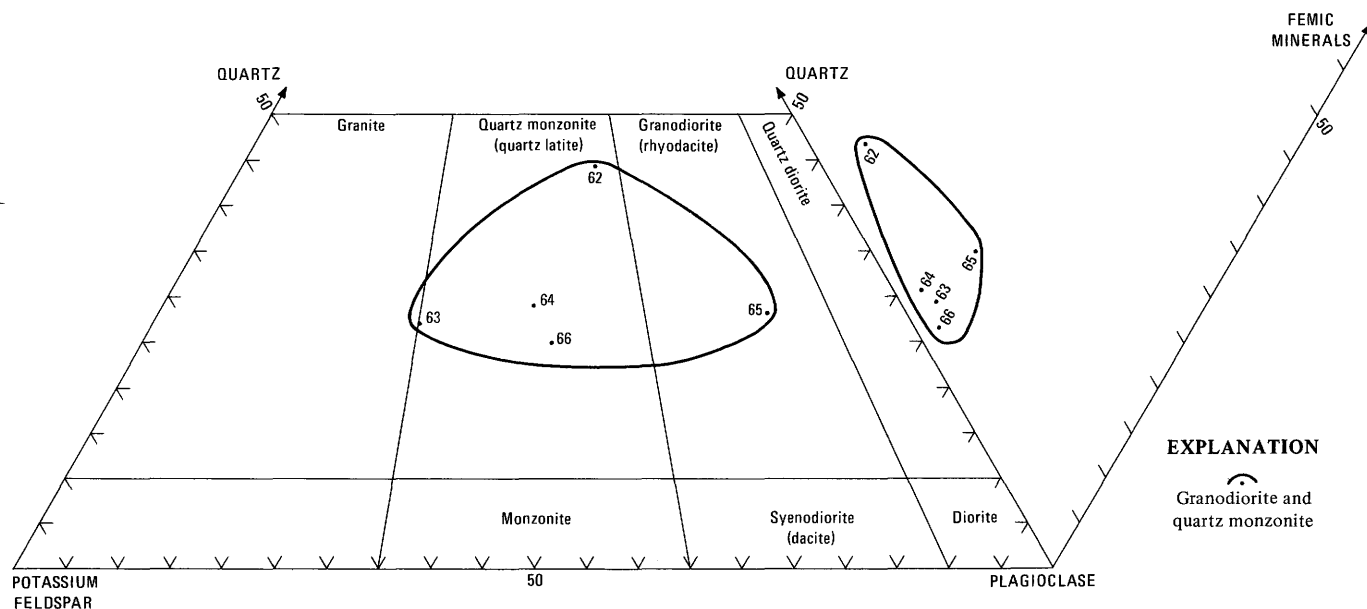


FIGURE 22.—Modified triangular diagram showing modal quartz, potassium feldspar, plagioclase, and femic minerals of granitoid rocks of the Corona stock.

The Josephine Canyon Diorite forms two stocks and several smaller intrusive masses north and west of the stocks (fig. 23). The larger stock is about 15 miles long and consists of two cupolas, each about 2 miles wide, connected by a narrow septum. The direction of elongation of the larger of the stocks is north-northwest, subparallel to the structural grain of the area and diverging 15° to 20° from the trend of the main outcrop area of the Squaw Gulch Granite. The smaller stock of diorite, in the San Cayetano Mountains, also trends north-northwest. Many of the masses of quartz monzonite also trend north-northwest; the larger ones, in the southern cupola of the large stock, cap hills suggesting that they may be remnants of a once fairly extensive sheet of quartz monzonite. The area underlain by the Josephine Canyon Diorite is about 25 square miles; at shallow depths the stocks probably extend over a slightly larger area beneath a cover of roof rocks and younger deposits.

The diorite intrudes rocks as young as the volcanic and arkosic rocks of the Salero Formation of Late Cretaceous age, and it is unconformably overlain by rocks as old as the Gringo Gulch Volcanics of Paleocene (?) age. The grain size of rocks near the contacts of the stocks are as coarse as that farther from the contacts. To the north, the intrusive contacts are fairly sinuous and steep. The host rocks are not demonstrably metamorphosed by the diorite, although some of them were metamorphosed by the Squaw Gulch Granite and so may have been at equilibrium with the thermal conditions accompanying emplacement of the Josephine Canyon Diorite. To the south, the intrusive contacts are less sinuous and dip only moderately steeply outward, or away from the stocks. Locally, as in the southern part of the San Cayetano Mountains, the host rocks are thermally metamorphosed to hornfels, as shown on the geologic map (Drewes, 1971c). Roof pendants and inclusions of metavolcanic rocks and meta-arkose occur in many places and are particularly abundant on the hilltops in the southern part of the southern cupola.

The altered rocks near the Josephine Canyon Diorite are locally mineralized. For example, the base-metal deposits at and near the Hosey mine of the Mansfield Canyon area (Drewes, 1973, pl. 1) are probably a hydrothermal deposit that is, in part, related to the emplacement of the diorite stock. Similarly, the pyrite enrichment of the intensely altered inclusions of volcanic rocks in the upper reaches of Josephine Canyon may be related to the diorite stock. Many of the mineralized quartz veins that cut the diorite (Drewes, 1971c, 1973) are spatially unrelated to the scattered pyrite and stains of secondary copper minerals within the diorite, and for this reason, among others, they are taken to be younger than the scattered pyrite and copper mineralization.

The observations on the distribution of late-phase quartz

monzonite, the dips of the contacts of the stock, and the distribution of inclusions or roof pendants suggest that the present level of exposure of the southern cupola of the large stock is very nearly the top of the stock.

PETROGRAPHY

The diorite rocks that constitute most of the Josephine Canyon Diorite are mapped separately from the late-phase quartz monzonite (Drewes, 1971c). In most places these rocks differ strongly from each other in color and mineralogy; the quartz monzonite resembles the aplite masses of many of the other plutons of the Santa Rita Mountains. But in the northern part of the southern cupola the dioritic rocks are a composite of several rock types that range from typical dark-gray diorite to a light-pinkish-gray granodiorite that resembles the rocks of the late-phase quartz monzonite. The granodiorite was mapped separately on field sheets but is not shown here; where exposures are fairly abundant the map pattern suggests that the granodiorite represents an intermediate phase.

DIORITIC ROCKS

Terrane underlain by the dioritic rocks is typically somber-colored and is commonly more gentle than that underlain by other granitoid rocks in situations of similar local relief. Small light-brownish-gray knobs and other outcrops are irregularly scattered in this terrane and are separated by areas containing dark soil and grus. A discontinuous veneer or lag concentrate of 6- to 10-inch subrounded residual blocks of diorite makes even fairly flat diorite areas deceptively tedious to traverse, a feature that is almost diagnostic of this formation. The more granodioritic rock types of the northern part of the southern cupola, between specimen sites 79 and 97 (fig. 23), form somewhat higher and lighter colored hills than those underlain by the typical diorite.

Specimens of Josephine Canyon Diorite are mostly medium dark gray, but those of granodioritic composition are pinkish gray to light brownish gray. They are typically fine grained and have a speckled appearance (fig. 24) of dark or femic minerals in a background of lighter colored minerals. The lighter color of the granodiorite is due to a smaller amount of femic minerals as well as to a whiter or pinker shade of the background. Tiny flakes of biotite are recognizable in the more granodioritic rocks. Weathered diorite is dark brownish gray, much like the color of the colluvial deposits formed on it.

The dioritic rocks have a subophitic texture that is unique among the plutonic rocks of the area (fig. 25). A few specimens are slightly porphyritic and even fewer have a very fine grained granophyric texture. The grain size of the diorite is commonly 1–3 mm; very few of the grains are outside the range of 0.1–4.0 mm. The phenocrysts of

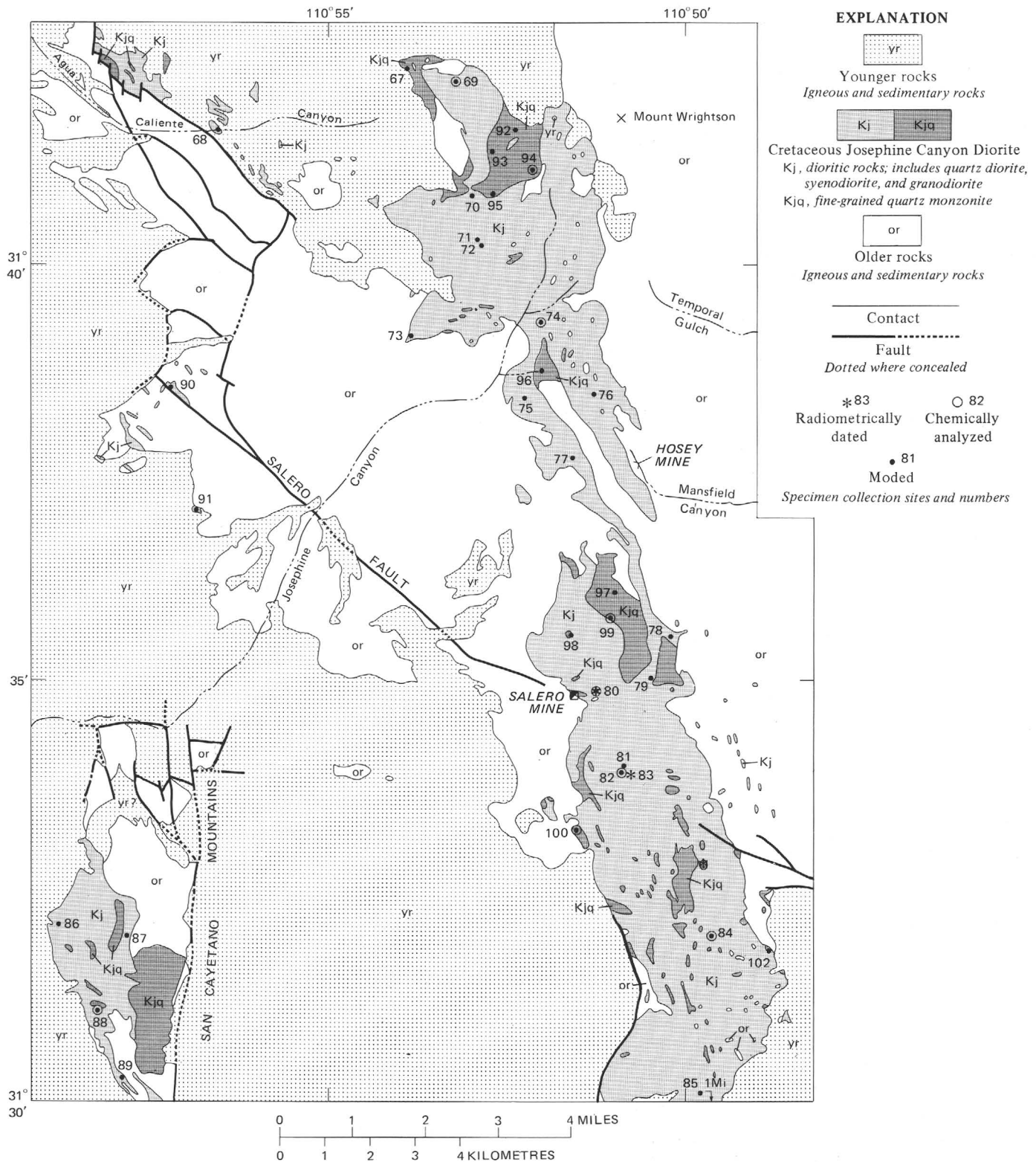


FIGURE 23.—Distribution of Josephine Canyon Diorite and specimen collection sites.

the porphyritic rocks are mostly 1–3 mm long, and the groundmass grains are about 0.1 mm across.

Typical diorite contains (in approximate order of decreasing abundance): plagioclase, amphibole, biotite,

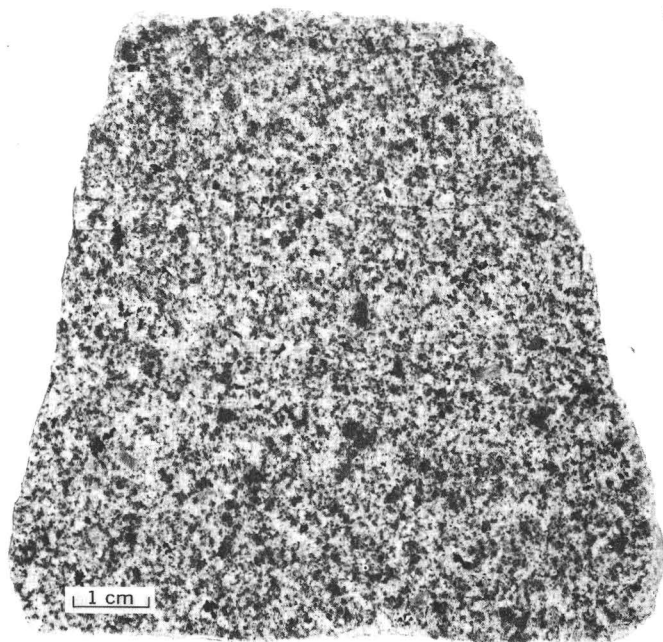


FIGURE 24.—Specimen 80. Josephine Canyon Diorite, showing fine grain size and speckled appearance.

orthoclase, pyroxene, and quartz; all specimens have accessory magnetite, apatite, and zircon, and some also have one or more of such accessory minerals as sphene, hypersthene, tourmaline, allanite, and pyrite. Most plagioclase forms subhedral to nearly euhedral grains, but some nearly anhedral grains lie between the laths and are poikilitic. Plagioclase is only slightly altered to clay minerals and sericite. The anorthite content of most plagioclase is 30 to 50 percent, in the range of andesine, but that of some specimens, particularly specimens containing abundant feric minerals, is 50 to 65 percent, indicative of labradorite. Normal composition zones of calcic oligoclase sheath some grains. Albitized plagioclase appears in only a few specimens. Most of the amphibole is probably a hornblende with mostly very pale yellowish green to pale-green or to pale-bluish-green pleochroism; the pleochroism of some amphibole is pale yellowish green to moderate green. Some amphibole grains are surrounded by biotite grains. Biotite forms anhedral to subhedral grains pleochroic in pale yellow brown to moderate brown. They are only slightly chloritized, or in some specimens altered to penninite and with inclusions of leucoxene. The orthoclase is anhedral, slightly kaolinitized and contains sparse and fine bands of perthitic albite. A specimen from one of the small intrusive bodies contains sanidine instead of orthoclase. The quartz grains are anhedral and have little or no undulatory extinction. The pyroxene is probably augite, which occurs either as subhedral to euhedral grains encased by amphibole or biotite or as grains intricately intergrown with amphibole.

Accessory minerals are more varied and abundant than in other plutonic rocks of the area. Ilmenitic magnetite occurs as subhedral to euhedral grains in amounts ranging from 1 to 5 percent. Euhedral apatite crystals are also fairly abundant, in one specimen exceeding 1 percent, and euhedral to anhedral zircon crystals occur in amounts of as much as about 0.5 percent. Sphene, present in about half the specimens, occurs either as overgrowths around magnetite or as subhedral to euhedral grains. Schorlite tourmaline and pyrite are probably primary minerals but occur in only a few specimens as do hypersthene and allanite.

The Josephine Canyon Diorite contains the same alteration minerals as the pre-Cretaceous plutonic rocks of the area but in less abundance. They include chlorite, penninite, sericite, kaolinite, urallite(?), hydromica(?), epidote, leucoxene, and iron oxide. Veinlets of quartz and calcite and of some of the alteration minerals cut a few of the diorite specimens.

FINE-GRAINED QUARTZ MONZONITE

The quartz monzonite of the late phase of the Josephine Canyon Diorite underlies a terrane slightly more rugged and lighter-colored than that underlain by the dioritic rocks. The rock typically forms small pale-yellowish-gray knobs and ledges which weather to blocky rather than subrounded detritus. Surfaces of fairly fresh quartz monzonite range from pale red to pale reddish brown to light brownish gray; the color varies with the relative abundance of orthoclase and feric minerals.

The correlation of a large mass of fine-grained leucocratic rock in the area of collection sites of specimens 92 to 95, a mile west of Mount Wrightson, with the quartz monzonite member of the Josephine Canyon Diorite rather than with aplite of the Elephant Head Quartz Monzonite is a tenuous one, based more on geographic proximity than on petrographic data.

The texture of the quartz monzonite ranges from faintly porphyritic and subophitic to hypidiomorphic or idiomorphic. Nearly half the specimens contain some granophyric or myrmekitic texture. Argillic alteration is more intense in the quartz monzonite than in the dioritic rocks; as a result, finer features are commonly obscured and staining is invariably needed in preparing specimens for modal analysis.

Major mineral constituents of the quartz monzonite member of the Josephine Canyon Diorite are plagioclase, orthoclase, and quartz. Plagioclase forms lath-shaped crystals, which are less conspicuous than those in the dioritic rocks. Plagioclase of the least altered specimens is andesine, and rarely labradorite, some of the plagioclase is surrounded by a zone of oligoclase. Plagioclase of most of the specimens, however, is albite, presumably as a result of deuteric albitization. This plagioclase is much altered to

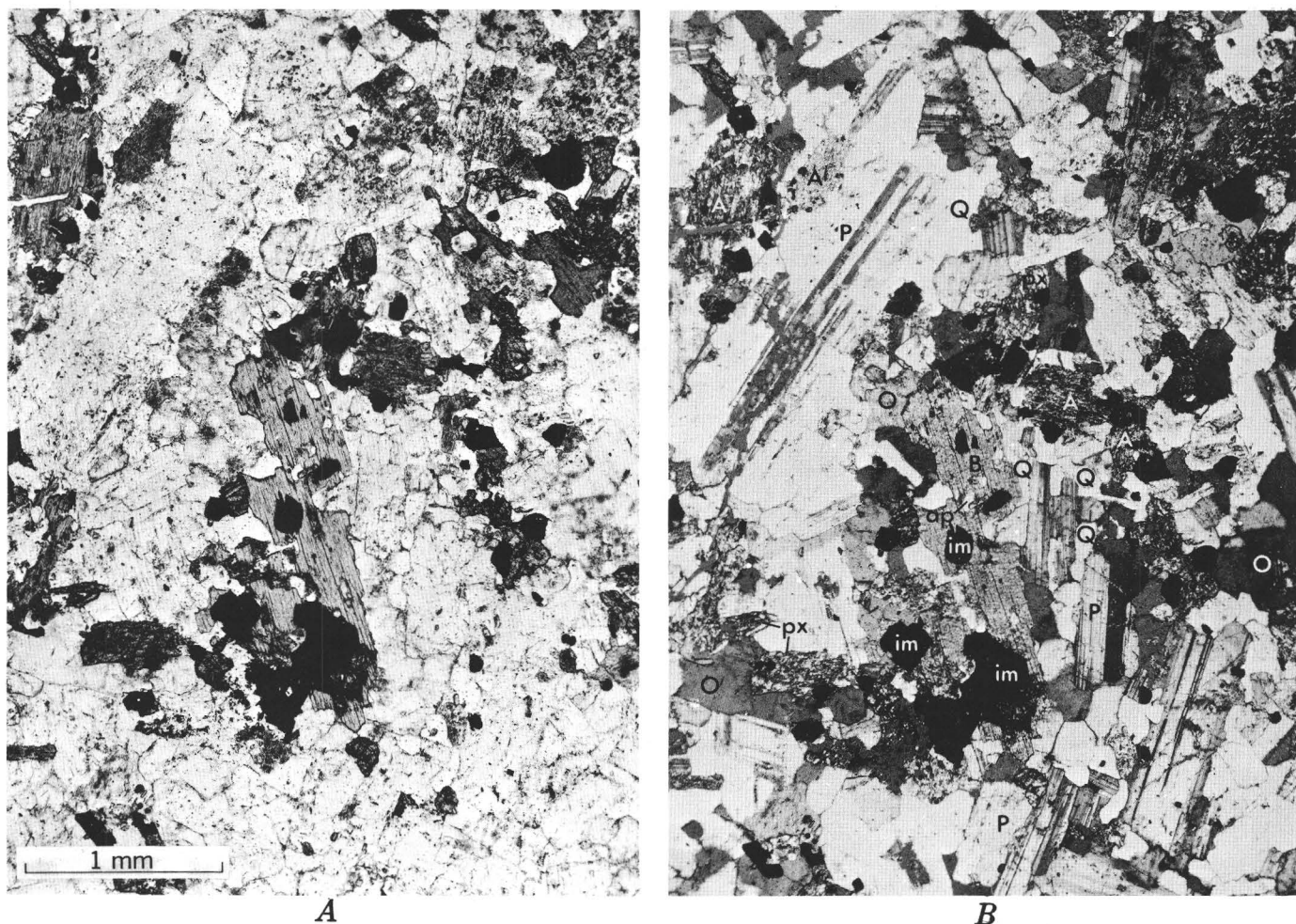


FIGURE 25.—Specimen 81. Josephine Canyon Diorite. Crystals: plagioclase (P), orthoclase (O), quartz (Q), biotite (B), amphibole (A), ilmenitic magnetite (im), pyroxene (px), and apatite (ap). $\times 25$. A, Plain light; B, crossed nicols.

clay minerals and sericite. The orthoclase forms anhedral crystals that are strongly kaolinitized and are perthitic, and the quartz forms interstitial anhedral crystals that have little or no undulatory extinction.

Of the less abundant and accessory minerals, biotite forms partly chloritized subhedral crystals pleochroic in pale greens. Clinopyroxene crystals are colorless and have a $Z \wedge C$ of 40° to 45° , suitable for a magnesium-rich augite. The magnetite is ilmenitic. Schorlite tourmaline forms inclusions in some quartz and biotite, and acicular rutile is sparsely present in some biotite.

MODAL AND CHEMICAL SUMMARY

Modal analyses of 25 specimens of dioritic rocks and of 11 of the quartz monzonite (table 11) illustrate the mineralogical composition of the Josephine Canyon Diorite. The modes of specimens 90 and 91 are excluded from the tabulated mean because they are from small intrusive bodies so rich in femic minerals that their correlation with the other dioritic rocks remains

provisional. The modal analyses are summarized on the modified triangular diagram of figure 26, which shows a good correspondence between the field determination of the two members of the Josephine Canyon Diorite and the rock classification scheme of the diagram.

The figure circumscribed around the plotted modes is an elongated discoid-shaped body that is tilted toward a point lying about a third of the distance from the leucocratic face toward the femic apex of the composition tetrahedron. With the field observation that the more dioritic rocks are intruded by the more quartz monzonitic ones, it seems probable that the magma evolved from one magma approximately represented by the lower edge of the circumscribed or "modal body" to another represented by the upper edge. This trend may be continued with the development of the magmas forming the Madera Canyon Granodiorite and Elephant Head Quartz Monzonite, discussed in some of the following sections of this report.

The mineralogical data (table 11) reflect compositional variations in both geographical distribution and successive

TABLE 11.—*Modes of*
[Field numbers are abbreviated; year of collection and collector's initial omitted. Full field number

Rock type	Dioritic rocks (includes quartz diorite, syenodiorite, and granodiorite)																	
Specimen No.....	167	268	69	70	71	72	73	74	75	76	77	78	79	80	81	82	83	84
Field No.	731	741	780	1579	1580	407	455	351	300	173	271	238	254	361	274	273	292	263
Quartz.....	9.7	3.7	6.8	3.2	4.9	3.9	13.2	10.9	8.6	10.2	4.2	7.9	12.2	10.2	12.1	7.8	11.1	9.3
Plagioclase, total	59.1	60.9	63.6	65.1	59.6	62.8	50.1	55.8	59.1	56.6	63.7	63.1	50.0	47.2	53.1	53.4	51.7	54.3
(plagioclase in perthite).....	0	0	0	0	0	0	0	(6.4)	0	0	0	0	(1.7)	0	0	0	0	0
Orthoclase	7.6	4.9	6.0	3.6	6.3	6.4	23.1	15.7	15.8	14.9	10.9	11.5	21.9	22.5	14.5	20.6	15.1	22.8
Hornblende	11.2	18.5	7.4	13.4	14.0	18.9	0	10.1	6.1	0	10.6	0	0	0	2.4	3.2	1.6	4.9
Pyroxene (augite?)	0	0	4.3	4.8	6.3	1.7	6.5	.05	1.6	6.7	3.5	9.7	6.5	8.7	4.1	5.5	5.9	3.9
Biotite	9.2	6.1	8.0	5.8	5.0	2.1	4.3	3.2	4.8	7.4	3.3	3.7	5.7	6.6	10.7	4.3	10.7	1.4
Magnetite	2.4	3.7	3.5	3.3	3.5	3.7	2.4	3.2	3.0	3.0	3.5	3.4	3.3	2.9	2.5	4.0	2.6	3.2
Apatite1	.5	.3	.8	.3	.4	.4	.4	.6	.4	.05	.6	.3	.7	.5	1.1	.9	.1
Sphene6	1.7	0	0	0	Tr.	0	.4	.1	0	.2	0	Tr.	.1	0	.1	.3	0
Zircon05	Tr.	.1	.05	.05	.05	.05	.2	.2	.1	.05	.1	.05	.1	.1	.05	.05	.05
Allanite	Tr.	Tr.	0	0	0	0	0	0	0	0	0	0	0	0	0	0	0	0
Rutile	0	0	0	0	0	0	0	0	0	0	0	0	0	0	0	0	0	0
Tourmaline	0	0	0	0	0	0	0	0	.1	0	0	0	.1	0	0	0	.05	0
Hypersthene	0	0	0	0	0	0	0	0	0	.7	0	0	0	0	0	0	0	0
Total	99.95	100.0	100.0	100.05	99.95	99.95	100.05	99.95	100.0	100.0	100.0	100.0	100.05	99.0	100.0	100.05	100.0	99.95
Femic	23.6	30.5	23.6	28.1	29.2	26.9	13.6	17.6	16.5	18.3	21.2	17.5	15.9	19.1	20.3	18.2	22.1	13.6
Percent anorthite in plagioclase	49—60	28	37—45	35—40	38—50	40—46	38—49	35—47	33—43	33—36	40—50	43—49	33—39	33—50	37—47	32—49	35—40	47—65
(plagioclase rims)								(28)			(25)		(28)					
Quartz mixing index (see text)89	.83	.94	.68	1.0	.89	.92	.96	.93	.81	.87		.78	.95	.87	.86	.75	.99

¹Specimen 67 collected from dioritic component of a mixed rock, dominantly of the quartz monzonite phase.

²Specimens 68 and 90 contain a little modal calcite.

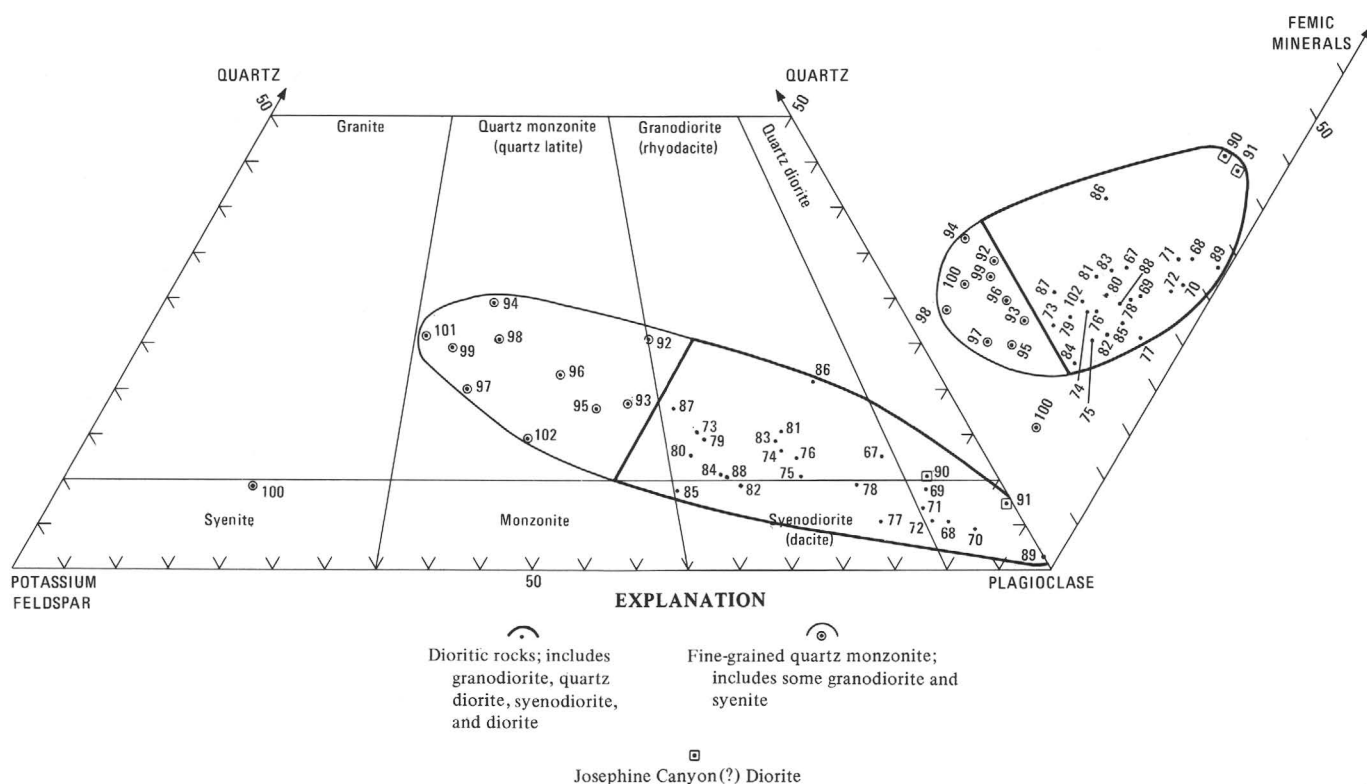


FIGURE 26.—Modified triangular diagram showing modal quartz, potassium feldspar, plagioclase, and femic minerals of Josephine Canyon Diorite.

phases developed in the Josephine Canyon Diorite. Because the sequential order in which the modes are tabulated follows their distribution (fig. 23) from northwest to southeast, geographical variations of modes are readily seen on scanning table 11 from left to right. Toward the southeast, in the large pluton, the abundance

Josephine Canyon Diorite

of specimen 67 thus is 65D731. Symbols: s, standard deviation; Tr., trace; . . . , not determined]

Dioritic rocks (includes quartz diorite, syenodiorite, and granodiorite)—Continued						Josephine Canyon(?) Diorite	Fine-grained quartz monzonite													
³ 85	86	87	88	89	67—89	² 90	91	92	93	94	95	96	97	98	99	⁴ 100	101	102	92—102	
332	571	575	560	545	Mean s	631	621	830	835	404	405	348	234	239	235	330	276	262	Mean s	
6.9	15.6	15.1	8.0	0.9	8.5 3.9	6.2	4.3	22.4	16.2	26.5	16.4	19.5	18.7	24.5	22.3	8.6	24.1	11.8	19.2	5.6
47.7	49.9	46.1	50.3	66.6	56.1 6.3	50.4	55.4	43.3	44.7	28.7	43.4	37.7	31.9	32.9	27.1	17.1	25.0	34.9	33.3	8.6
0	(0.6)	0	0	0	(0.4) (1.4)	0	0	(1.8)	0	0	0	(4.3)	0	0	0	0	0	0	(0.6)	(1.4)
25.2	9.1	23.1	20.5	0	14.0 7.5	4.1	.5	22.8	28.1	34.9	31.8	32.4	43.0	38.4	40.5	66.0	43.4	35.4	37.9	11.2
11.5?	12.9	5.2	0	0	6.6 6.3	16.8	29.2	0	4.7	.05	1.7	3.4	.4	Tr.	.3	.1	0	6.8	1.6	2.4
6.7	2.2	3.8	7.6	22.2	5.3 4.6	0	0	0	0	0	1.6	1.6	0	0	2.1	5.0	4.4	2.4	1.6	1.8
.2	8.6	4.0	10.5	3.8	5.6 3.0	18.0	5.6	10.0	4.0	6.2	3.1	2.4	2.7	2.3	4.4	.6	.7	5.3	3.8	2.7
1.8	.9	2.2	2.6	5.3	3.0 .9	2.0	2.5	1.2	1.6	2.0	1.6	1.8	3.0	1.5	2.4	2.5	1.9	3.2	2.1	.6
Tr.	.4	.5	.3	1.2	.5 .3	.8	.7	.3	.3	.4	.2	.2	.3	.4	.3	Tr.	.3	.2	.3	.1
Tr.	.3	0	.05	0	.2 .4	1.6	1.8	0	.2	1.2	.1	.5	0	0	.5	Tr.	Tr.	0	.2	.4
0	.1	.05	.1	0	.07 .05	.1	0	Tr.	.1	.05	.05	Tr.	Tr.	Tr.	.1	.1	.2	Tr.	.06	.06
0	Tr.	0	0	0	Tr.	0	0	0	.1	0	.05	.3	0	0	0	0	0	0	.04	.09
0	0	0	0	0	0	0	0	0	0	.05	Tr.	0	0	0	0	0	0	0	Tr.
0	Tr.	0	Tr.	0	Tr.	0	0	0	0	0	Tr.	.2	0	0	0	Tr.	0	0	Tr.
0	0	0	0	0	Tr.	0	0	0	0	0	0	0	0	0	0	0	0	0	0
100.0	100.0	100.05	99.95	100.0	99.9	100.0	100.0	100.0	100.05	100.05	100.0	100.0	100.0	100.0	100.0	100.0	100.0	100.0	100.1
20.2	25.4	15.7	21.2	32.5	21.3 5.3	39.3	39.8	11.5	11.0	9.9	8.4	10.4	6.4	4.2	10.1	8.3	7.5	17.9	9.7	3.5

50	45—61	35	41—50	50—65	33—65 (27)	0—28	28—31	25—35	37—35	32—40	38—47	30—33	32—38 (26)	0	39—49 (25)	0?	28—35	50—57 (35)	28—55 (0—28)
.97	.95	.92	.8389 .08	.71	.58	.89	.90	.94	.929592	.83	.91	.04		

³Specimen 85 was collected by F.S. Simons about 1 mile south of the Mount Wrightson quadrangle.⁴Analyses of specimen 100 is omitted from average inasmuch as the specimen is more intensely altered than other rock of this phase.

of orthoclase, and perhaps also of quartz, increases; correspondingly, hornblende and possibly also sphene decrease in abundance. This mineralogical evidence supports field observations of an increasing abundance of more granodioritic rock types in the southern cupola.

Chemical and spectrographic analyses and CIPW norms of nine specimens of Josephine Canyon Diorite are given in table 12, and the chemical data are summarized in the histogram of figure 10C. The compositional range of the analyzed specimens is small (note the low value of the standard deviation of the mean value in table 12). Most analyzed specimens are modal granodiorites (fig. 26), but one, specimen 69, is a modal diorite whose chemical analysis approximates the analytical mean of the five dioritic rocks. Thus, analyses of a suite more representative of the modal varieties included with the dioritic rocks may not significantly alter the mean of the chemical analyses of those rocks. The mean chemical analysis of the dioritic rocks (table 12) compares poorly with the analyses presented by Nockolds (1954, p. 1018, 1019); for a rock of its high alkali content, the Josephine Canyon Diorite is silica poor.

AGE AND CORRELATION

The Josephine Canyon Diorite is dated as Late Cretaceous or early Paleocene (?) on geologic evidence and is dated even more precisely as late Late Cretaceous on radiometric evidence. Field relations show the diorite to intrude rocks as young as the Salero Formation, a middle member of which is dated as 72 m.y. old. The diorite is

unconformably overlain by the Gringo Gulch Volcanics, which are dated as Paleocene (?) and which are probably older than the rocks of the Gringo Gulch pluton (Drewes, 1971c and 1972a), dated as about 60 m.y. old.

Three specimens of Josephine Canyon Diorite are radiometrically dated, one of them by both the potassium-argon method and the lead-alpha method, and the other two only by the lead-alpha method (table 4). The potassium-argon age determination of 67.1 m.y. dates the relatively young part of the southern cupola. Diorite from a deeper part of the stock, in the northern cupola, may well be estimated to be about 69 m.y. old. Should the 69-m.y. estimate prove to be correct, the discrepancy between the ages and the field relations of the Josephine Canyon Diorite with the Madera Canyon Granodiorite and the Elephant Head Quartz Monzonite is clarified. The three lead-alpha ages are consistent with each other at about 62 m.y. despite the fact that this radiometric dating method is usually less reliable than the potassium-argon method. In an age range of about 60 m.y. lead-alpha determinations are generally several million years younger than potassium-argon determinations of the same rock. The true age of emplacement of the quartz monzonite member may thus be about 65 m.y., and it almost certainly is not younger than about 63 m.y. The similarity in the lead-alpha ages of the dioritic rocks with that of the quartz monzonite member, however weak the dating method, lends some support to the interpretation that these rocks are genetically closely related.

Rocks that resemble the Josephine Canyon Diorite in

TABLE 12—Chemical and spectrographic analyses and CIPW norms of Josephine Canyon Diorite

[Chemical analyses by rapid rock method (Shapiro and Brannock, 1962), with analyses of specimens 69, 74, 80, 82, 84, 88, and 94 supplemented by X-ray fluorescence method. Chemical analysts: Lowell Artis, S. D. Botts, G. W. Chloe, P. L. D. Elmore, John Glenn, and H. Smith. Spectrographic analyses by semiquantitative method. Spectrographic analysts: W. B. Crandell, J. L. Finley, J. C. Hamilton, J. L. Harris, A. L. Sutton, and Barbara Tobin. Symbols: s, standard deviation; <, less than; . . . , not determined; N, not detected]

Rock type . . .		Dioritic rocks (includes quartz diorite, syenodiorite and granodiorite)						Quartz monzonite phase				
Specimen No.	69	74	80	82	84	88	69—88	94	99	100	94—100	
Field No. . . .	780	351	316	273	263	560	Mean s	404	235	330	Mean s	
Chemical analyses (weight percent)												
SiO ₂	59.7	61.1	60.2	60.7	58.7	58.8	59.9 1.0	69.9	67.3	67.1	68.1 1.6	
Al ₂ O ₃	17.8	15.5	16.0	15.7	16.6	17.0	16.4 .9	15.0	14.4	15.6	15.0 .6	
Fe ₂ O ₃	2.8	4.0	3.3	3.2	4.3	2.4	3.3 .7	3.1	3.1	2.3	2.8 .5	
FeO	3.1	2.7	3.6	3.2	2.7	3.7	3.2 .4	1.5	1.4	.76	1.2 .4	
MgO	2.9	3.2	3.0	2.4	3.3	2.6	2.9 .3	.60	.65	.10	.45 .3	
CaO	5.2	4.4	5.2	4.8	4.9	5.9	5.1 .5	1.4	2.4	1.7	1.8 .5	
Na ₂ O	3.8	3.4	3.4	3.8	3.8	3.4	3.6 .2	3.3	3.1	3.6	3.3 .3	
K ₂ O	2.5	3.3	2.7	3.3	3.3	2.8	3.0 .4	2.6	4.8	6.6	4.7 2.0	
H ₂ O—18	.15	.26	.28	.27	.19	.22 .05	.18	.38	.29	.28 .10	
H ₂ O+68	.95	1.0	1.1	.71	1.1	.92 .19	.92	.72	.41	.68 .26	
TiO ₂85	.10	.87	.90	.96	.90	.76 .33	.45	.64	.60	.56 .10	
P ₂ O ₅28	.27	.29	.27	.26	.25	.27 .01	.15	.13	.45	.24 .18	
MnO08	.90	.08	.11	.21	.11	.25 .32	.05	.08	.08	.07 .02	
CO ₂08	<.05	.05	.05	.05	.55	.11 .22	<.05	<.05	.05	<.05 .03	
Total	100	100	100	100	100	100	100	99	99	100	99	
Spectrographic analyses (weight percent)												
Ag	0	*0	*0	†0	†0	0	0	0	††<0.0001	††0	0	<0.0001
Ba1	.1	.015	.1	.15	.15	.1 .15	.1	.07	.15	.15	.1 0.4
Be	0	.0002	.0001	0	0	0	.0002 .0002	.0001	.0001	.0003	.0002	.0002 .0001
Ce	0	0	N	0	N	0	0	0	.01	.02	.05	.02 .02
Co002	.003	.003	.002	.007	.002	.002 .003	.003	.002	.0007	.0015	.001 .001
Cr0007	.003	.0015	.005	.003	.0015	.003 .015	.004	.005	.0015	.0015	.0005 .001 .0005
Cu03	.015	.07	.015	.02	.02	.015 .01	.02	.02	.01	.007	.015 .007 .01 .004
Ga001	.005	N	.002	N	.003	.005 .002	.003	.002	.001	.005	.003 .0015 .003 .002
La005	.005	.07	.007	.003	.005	.007 .005	.01	.02	.007	.01	.007 .015 .01 .004
Mo0003	0	0	.0007	0	.007	0 .0007	.001	.002	0	0	0
Nb	0	0	.002	0	.002	.002	0	.0008	.001	.0007	0	.001 .0009 .0008
Nd	0	0	N	0	N	.007	0	.002	.003	0	.007	0 .004 .004
Ni	<.003	.002	.002	.005	.015	.0015	.003 .007	.005	.005	.003	.0015	0 .0015 .001
Pb001	.0015	.003	.002	.001	.002	.002 .002	.002	.001	.001	.003	.002 .003 .001
Sc001	.002	.007	.0015	.002	.001	.0015 .002	.002	.002	.001	.001	.01 .003 .005
Sr1	.15	.015	.1	.015	.05	.15 .1	.09	.05	.05	.1	.05 .03 .06 .03
V015	.03	.02	.02	.03	.01	.02 .02	.02	.007	.01	.01	.01 .005 .009 .003
Y002	.003	.007	.003	.001	.002	.003 .003	.003	.002	.003	.005	.002 .005 .004 .002
Yb0002	.000300030005	.0003 N	.0003	.0001	.0003	.0005	.0003 .0004 .0001
Zr02	.015	.01	.01	.02	.03	.015 .01	.02	.007	.02	.02	.03 .03 .03 .006
CIPW norms												
Q	12.6	14.4	14.9	13.3	10.1	12.7	12.6	37.3	25.2	18.6	37.3	25.2 18.6
C25	0	0	0	0	0	0	4.6	.06	.64	4.6	.06 .64
or	14.8	19.5	16.0	19.5	19.5	16.5	14.8	15.4	28.4	39.1	15.4	28.4 39.1
ab	32.1	28.8	28.8	32.1	32.1	28.8	32.1	27.9	26.2	30.6	27.9	26.2 30.6
an	23.5	17.3	20.4	16.0	18.5	22.9	23.5	6.0	11.1	5.2	6.0	11.1 5.2
di { wo	0	1.2	1.4	2.5	1.7	.54	0	0	0	0	0	0 0 0
en {	0	.77	.99	1.7	1.5	.33	0	0	0	0	0	0 0 0
fs {	0	.30	.34	.57	.04	.18	0	0	0	0	0	0 0 0
hy { en	7.2	7.2	6.5	4.2	6.8	6.1	7.2	1.5	1.6	.25	1.5	1.6 .25
fs {	2.1	2.9	2.3	1.4	.17	3.4	2.1	0	0	0	0	0 0 0
mt	4.1	5.8	4.8	4.6	6.2	3.5	4.1	3.7	2.9	.98	3.7	2.9 .98
hm	0	0	0	0	0	0	0	.55	1.1	1.6	.55	1.1 1.6
il	1.6	.19	1.7	1.7	1.8	1.7	1.6	.86	1.2	1.1	.86	1.2 1.1
ap66	.64	.69	.64	.62	.59	.66	.36	.31	1.1	.36	.31 1.1
cc18	0	0	0	0	1.3	.18	0	0	.11	0	0 .11
Total	99.1	99.0	98.8	98.2	99.0	98.5	99.1	98.2	98.1	99.3	98.2	98.1 99.3
Femic	15.8	19.0	18.7	17.3	18.8	17.6	15.8	7.0	7.1	5.1	7.0	7.1 5.1

*††† Pairs of replicate analyses.

both composition and age have not been reported in mountain ranges immediately adjacent to the Santa Rita Mountains. Somewhat similar rocks, which have been little studied and are poorly dated, occur in the Ruby area, 17 miles southwest of the small stock of Josephine Canyon Diorite, and other such rocks occur in Sonora near Nogales about 15 miles south of that stock (fig. 1).

MADERA CANYON GRANODIORITE

The Madera Canyon Granodiorite is a coarse-grained, light-gray to medium-gray speckled rock in which dark minerals are moderately to very abundant. The granodiorite is in a stock in the Madera Canyon area (fig. 27) that trends northwest and is wedge shaped, tapering to

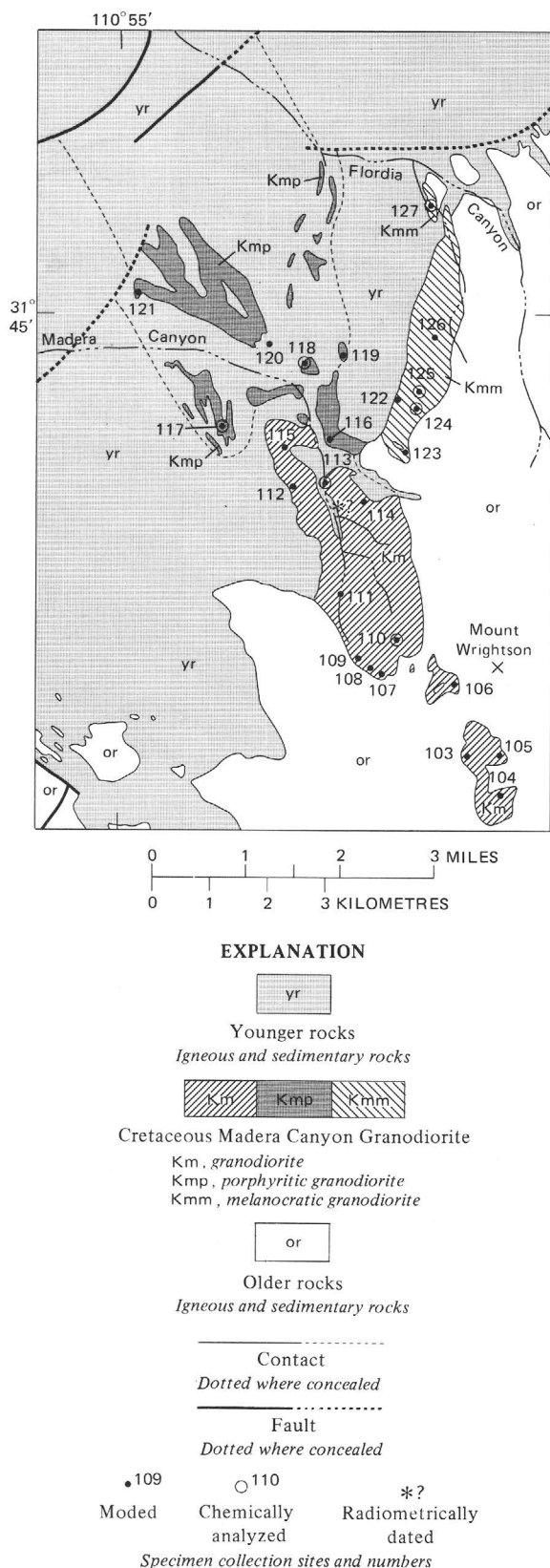


FIGURE 27.—Distribution of Madera Canyon Granodiorite and specimen collection sites.

the southeast. The stock underlies an area of about 10 square miles; about 6 square miles of this area is directly underlain by granodiorite; the remainder is projected beneath a thin gravel cover on the pediment off the mouth of Madera Canyon.

The granodiorite intrudes mainly the Mount Wrightson Formation and the Piper Gulch Monzonite, both of Triassic age, and the southeastern end of the stock intrudes the Josephine Canyon Diorite. Sedimentary rocks intercalated in the Mount Wrightson Formation are strongly contact metamorphosed along the eastern margin of the stock, as shown on the geologic map (Drewes, 1971c), but the volcanic rocks of the formation are no more altered near the stock than they are away from it. The contact zone, as observed at collection site 103 (fig. 27), is narrow and chilled. Inclusions of epidotized and chloritized quartz diorite, probably derived from a nearby Triassic intrusive mass, form inclusions in the granodiorite near the eastern margin of the stock, midway between collection sites 126 and 127. The rocks on both sides of the contact in this area are also slightly pyritized. In general the contact is sharply defined, steeply inclined, and regular in trend; but near the southeastern end of the stock it is steeply to gently inclined and, consequently, irregular in trend. Apparently the southeastern outcrops lie near the top of that part of the stock, whereas the northwestern outcrops lie a considerable distance beneath the original top of the stock.

PETROGRAPHY

The Madera Canyon Granodiorite consists of three rock types each distinctive in texture or in composition. A nonporphyritic granodiorite is the most widespread type; it crops out from the narrow end of the stock almost to the mouth of Madera Canyon, where it appears to grade into a porphyritic granodiorite. The porphyritic granodiorite underlies the northwestern part of the stock, largely in the pediment area. Melanocratic granodiorite underlies an elongate area along the northeastern side of the stock, where it is separated from the other two types of granodiorite by younger intrusive rocks of the Elephant Head Quartz Monzonite and by a prong of the host rocks. The term "melanocratic" will be used hereafter for a rock with an unspecified but relatively large amount of dark minerals.

GRANODIORITE

The nonporphyritic granodiorite, to be referred to hereafter simply as "granodiorite," is much less resistant to weathering than the adjacent rocks, and so it underlies low areas, such as the bottom of Madera Canyon. This weathering characteristic is largely the result of the friability of the rock, which disaggregates readily to form extensive slopes of grus and a few small outcrops. Outcrops of granodiorite are most accessible in the

roadcuts a few hundred feet south of the Santa Rita Lodge (area of specimen 113, fig. 27), as well as along trail cuts and in the bottoms of the narrowest canyons. Rocks from these relatively unweathered outcrops are illustrated by figure 28. The granodiorite typically has a hypidiomorphic-granular texture and a 2- to 5-mm grain size (fig. 29). Near the southeast end of the stock the grain size is slightly smaller and some specimens have a bimodal size distribution of grains, with the smaller ones only 0.1 to 0.5 mm long. Specimens from the northwest end of the granodiorite area, on the other hand, contain some crystals 6 to 7 mm long that resemble underdeveloped phenocrysts. Some granophyric texture is commonly evident in all specimens.

Common minerals of the granodiorite are quartz, orthoclase, plagioclase, biotite, and hornblende (fig. 26). The quartz is anhedral and has little or no undulatory extinction; in rocks whose grains have a bimodal distribution, quartz is commonly among the smaller group of crystals. The orthoclase is anhedral or subhedral and contains a fine lacy perthitic intergrowth of albite. One specimen taken about 2 cm from the contact of the granodiorite with the Josephine Canyon Diorite contains sanidine instead of orthoclase. Plagioclase is subhedral; it generally has a composition of calcic oligoclase to sodic andesine, but in a few specimens it is albitized. The biotite is subhedral and is pleochroic in pale yellowish brown to moderate brown. Hornblende forms euhedral to subhedral crystals pleochroic in pale yellowish green to pale grayish green. In the northern part of the granodiorite body some of the biotite and hornblende are clustered, as they typically are in the nearby melanocratic granodiorite.

Accessory minerals invariably include ilmenitic magnetite, apatite, and zircon, and some specimens also contain a trace of sphene, rutile, and beryl(?). Some magnetite grains are surrounded by sphene. The zircon is moderately abundant and fairly coarse for zircon, reaching a grain size of about 0.4 mm.

Secondary minerals are moderately scarce and consist of kaolinite, sericite, chlorite, leucoxene, and epidote.

PORPHYRITIC GRANODIORITE

Aside from its phenocrysts, the porphyritic granodiorite closely resembles the nonporphyritic type. Indeed, the two units may be gradational, with the porphyritic rock characteristic of the core of the stock and the nonporphyritic rock present along an unrecognized narrow border zone and more extensively present in the narrow southeastern shoulder of the stock. Unweathered, nonfriable outcrops of the porphyritic granodiorite are scarce; some of the freshest material is available in a rock dump along the edge of Madera Canyon nearest to the collection site of specimen 120 (fig. 27).

The texture of the rock is noteworthy for its scattered phenocrysts which are 3 to 5 cm long. Despite the

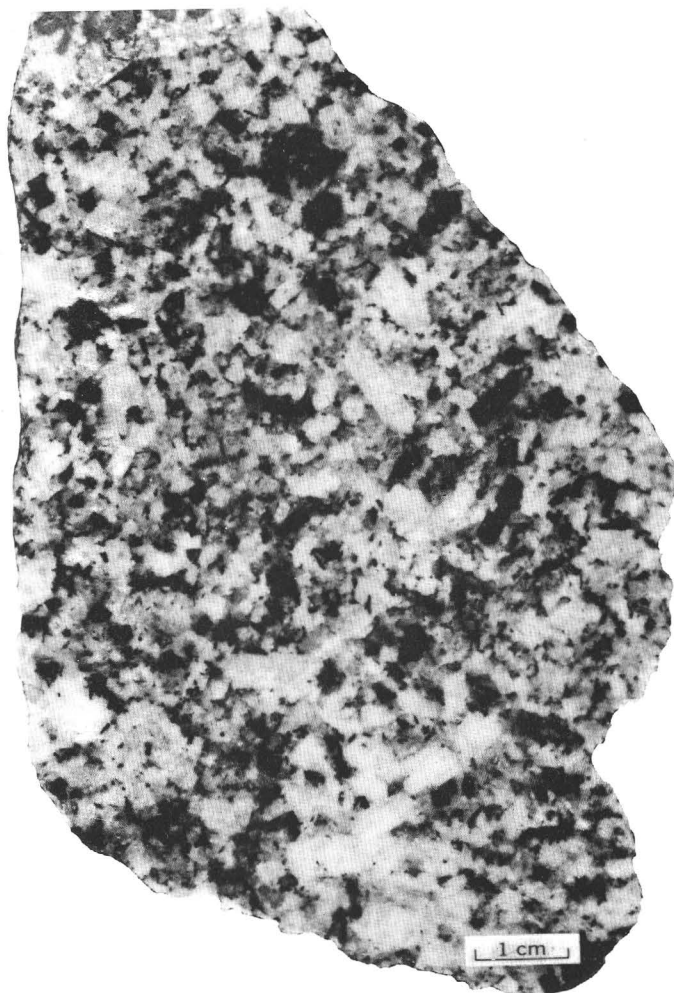


FIGURE 28.—Specimen 113. Nonporphyritic type of Madera Canyon Granodiorite.

occurrence of phenocrysts and the coarse-grained groundmass, the rock differs from the Continental Granodiorite by having fewer phenocrysts and ferromagnesian minerals and being much less altered. Very locally, $\frac{1}{2}$ to 1 mile northwest of collection site 120, the porphyritic granodiorite contains some schlieren of more leucocratic quartz monzonite and some of more porphyritic rocks.

In thin section, the porphyritic granodiorite is seen to differ from the nonporphyritic type in that the potassium feldspar commonly has indistinct or blurred grid twins typical of microcline. One specimen also contains accessory allanite.

MELANOCRATIC GRANODIORITE

The melanocratic granodiorite is a nonporphyritic dark-gray rock that contains abundant hornblende and biotite and a gray plagioclase (fig. 30). Clustered ferromagnesian minerals give the rock a faintly mottled

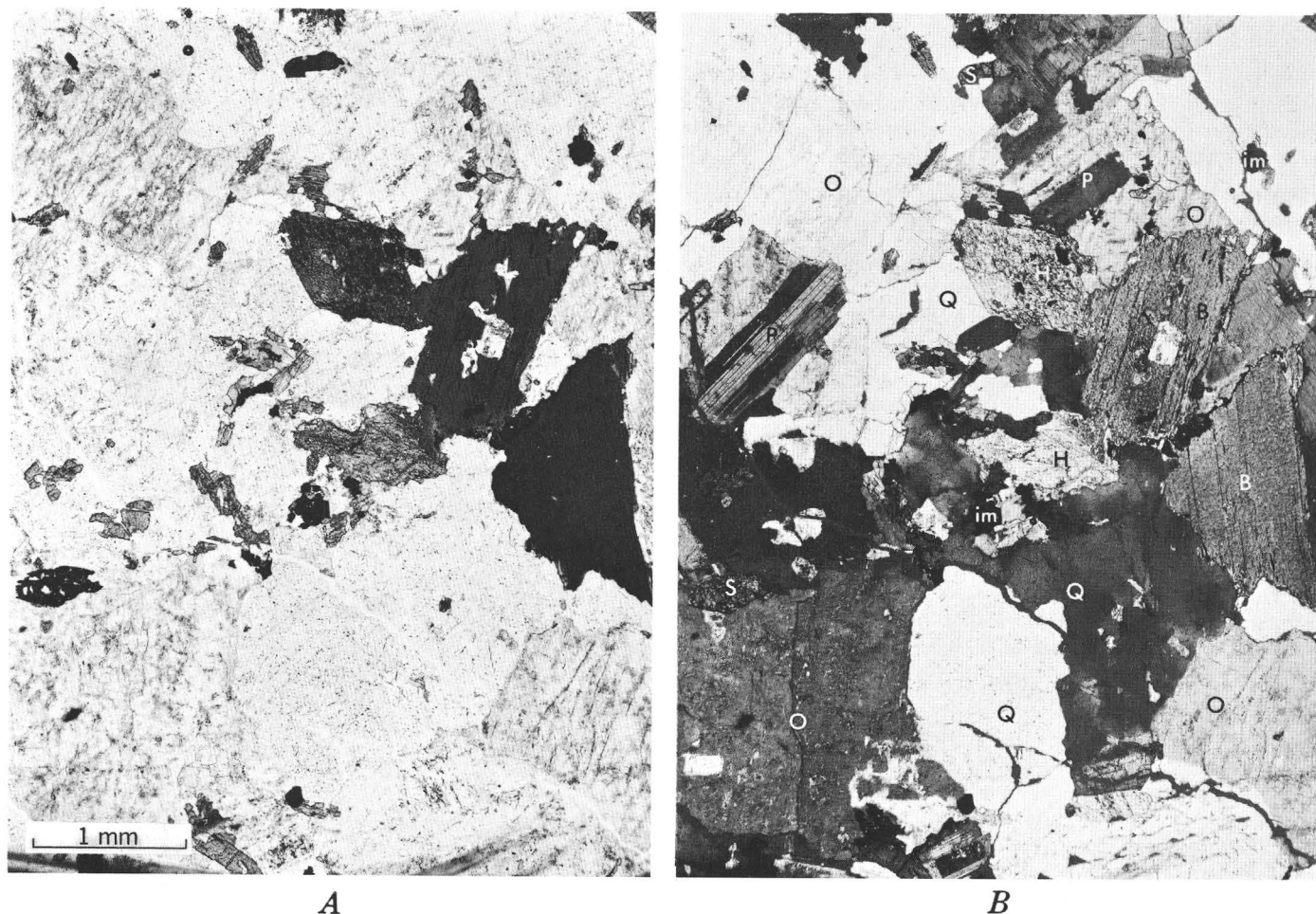


FIGURE 29.—Specimen 113. Nonporphyritic type of Madera Canyon Granodiorite. Crystals: plagioclase (P), quartz (Q), orthoclase (O), biotite (B), hornblende (H), ilmenitic magnetite (im), and sphene (S). $\times 20$. A, Plain light; B, crossed nicols.

appearance. It is most easily accessible near collection site 127 (fig. 27) in the northern part of the outcrop area.

The clustering of small crystals of biotite and the bimodal distribution of grain size in many specimens of melanocratic granodiorite suggest mild recrystallization. Strongly sutured grain boundaries and a peculiar wormy-looking granophyric intergrowth also suggest recrystallization.

The minerals in the melanocratic granodiorite are mostly the same as those in the other types of granodiorite. Most of the plagioclase has the composition of andesine and that of two specimens is calcic andesine, but some of the plagioclase is albitized. The biotite of one specimen is pleochroic in pale olive green to medium olive green, rather than in brown. Schorlite tourmaline is a common accessory mineral, and allanite is a rare one.

MODAL AND CHEMICAL SUMMARY

Modal analyses of 25 specimens of Madera Canyon Granodiorite are shown in table 13. The abundance of femic minerals in the nonporphyritic and in the porphyritic

granodiorite is about 5 percent less than that in the melanocratic granodiorite. Two of the hybridized specimens, 116 and 122, that are excluded from the modal means in table 13 have probably been altered by the nearby intrusive body of Elephant Head Quartz Monzonite. The other hybridized rock, specimen 103, is from a contact chill zone along which there may have been some assimilation. The modes are plotted in a modified triangular diagram, figure 31. Hornblende and biotite together make up about 10 percent of the rock, with substantial amounts of both minerals present in most specimens. However, specimen 104 contains biotite and no hornblende, and specimen 105 contains hornblende and a very minor amount of biotite, suggesting that these minerals may proxy for each other.

An enclosing shell drawn around the plotted modes in figure 31 is subspherical and is centered along the boundary between the granodiorite and quartz monzonite fields and about 15 percent of the way from the leucocratic face of the composition tetrahedron toward the femic apex. The modes for each of the three types of granodiorite

TABLE 13.—*Modes of*

[Field numbers are abbreviated; year of collection and collector's initial omitted. Full field number of specimen

Rock type.....	Granodiorite														104—115	
Specimen No	103	104	105	106	107	108	109	110	111	112	113	114	115	Mean	s	
Field No.	2403	363	765	1581	833	836	828	769	837	843	826	810	847			
Quartz	24.8	24.1	19.1	23.1	21.4	23.7	17.5	21.9	16.0	18.3	22.5	17.9	24.2	20.8	2.9	
Plagioclase, total .	52.7	47.9	40.3	45.2	36.2	39.0	44.6	41.8	42.8	47.5	47.1	48.7	43.4	43.7	3.9	
(plagioclase in perthite).....	0	(1.7)	(1.6)	(2.0)	(1.3)	(2.0)	(0.2)	0	(1.6)	(2.9)	(1.2)	0	(1.9)	(1.4)	(0.9)	
Orthoclase	0	16.1	28.0	19.3	31.8	27.0	25.5	26.2	23.3	21.5	17.8	12.9	21.6	22.6	(5.5)	
Sanidine	10.6	0	0	0	0	0	0	0	0	0	0	0	0	0	
Hornblende	0	0	9.3	3.5	1.8	2.3	6.3	4.9	9.7	3.9	5.7	10.9	2.4	5.1	3.4	
Biotite	10.7	11.4	.5	5.4	6.4	5.7	3.7	3.7	5.6	6.5	4.3	6.2	6.4	5.5	2.5	
Pyroxene	0	0	0	1.3	0	0	0	0	0	0	0	0	0	.1	.4	
Magnetite7	.5	1.9	1.5	1.6	1.5	1.2	1.1	1.4	1.2	1.7	2.2	1.4	1.4	.4	
Apatite3	Tr.	.3	.4	.2	.2	.5	.1	.3	.4	.2	.1	.1	.2	.2	
Sphene	0	0	.6	.3	.5	.6	.6	.3	.9	.7	.7	1.1	.2	.5	.3	
Zircon2	Tr.	Tr.	.05	.1	Tr.	.1	Tr.	Tr.	.05	.05	0	Tr.	.03	.04	
Allanite	0	0	0	0	Tr.	0	0	0	0	0	0	0	0	Tr.	
Rutile	0	Tr.	0	0	0	0	0	0	0	0	0	0	0	Tr.	
Tourmaline	0	0	0	0	0	0	0	0	0	0	0	0	0	0	
Total	100.0	100.0	100.0	100.05	100.0	100.0	100.0	100.0	100.0	100.05	100.05	100.0	99.7	99.93	
Femic	11.9	11.9	12.6	12.4	10.6	10.3	12.4	10.1	17.9	12.7	12.6	20.5	10.5	12.8	3.2	
Percent anorthite in plagioclase...	28	32—42	5—37	35—42	/33—37	28—37	32—34	29—35	33—40	33	32—37	32—37	28—31	28—37	
(plagioclase rims)										(23)	(20)	(20)	(21)	
Quartz mixing index (see text)89	.88	.85	.85	.70	.96	.90	.97	.93	.97	.91	.94	.90	.07	

¹ Specimen is hybridized.² Actual sample collection site is at dump ¼ mile southwest of source site shown on map, figure 27.³ Modal orthoclase includes a microcline (?).⁴ Omits hybridized specimens 103, 116, and 122.

fall within smaller subspherical circumscribed figures. The modal ranges of the nonporphyritic and the porphyritic granodiorite overlap, bearing out the field evidence that these rocks are gradational. No such overlap occurs for the melanocratic figure and those of the granodiorite and the porphyritic granodiorite figures.

The low value of the quartz mixing index of the melanocratic granodiorite relative to the other types may be the result of minor redistribution of quartz; this is compatible with the other evidence suggesting mild thermal metamorphism of the rock.

Chemical and spectrographic analyses and CIPW norms of specimens of Madera Canyon Granodiorite are shown in table 14. The chemical data are summarized in the histogram of figure 10D, which shows the rock to be unique among the several granodiorites of the Santa Rita Mountains in having nearly equal amounts of CaO, Na₂O, and K₂O. The mean of the chemical analyses is fairly close to that of the average of hornblende-biotite granodiorite tabulated by Nockolds (1954, p. 1014).

AGE AND CORRELATION

The Madera Canyon Granodiorite is, on geologic evidence, considered to be younger than the Josephine Canyon Diorite and older than the Elephant Head Quartz

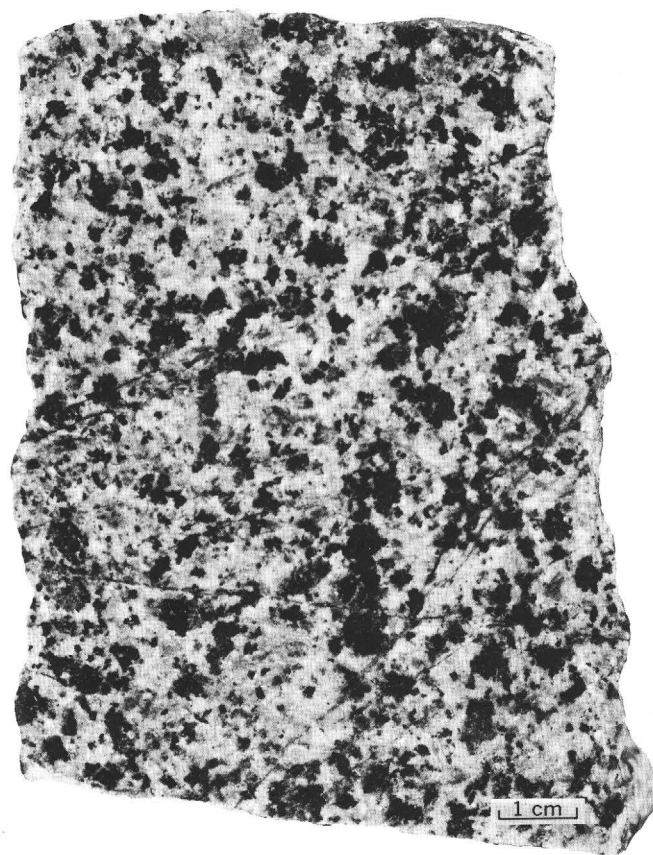


FIGURE 30.—Specimen 127. The melanocratic type of Madera Canyon Granodiorite.

Madera Canyon Granodiorite

103 thus is 63D5103. Symbols: s, standard deviation; Tr., trace;, not determined]

Porphyritic granodiorite									Melanocratic granodiorite								
¹ 116	117	118	119	120	121	117-121			¹ 122	123	124	125	126	127	122-127		⁴ 104-127
873	874	872	865	877	889	Mean	s		825	908	824	867	869	902	Mean	s	Mean
37.5	26.0	21.8	28.5	27.3	20.7	24.9	3.4		16.3	12.2	12.1	8.2	11.0	9.3	10.6	1.8	19.4
28.9	37.8	47.6	46.0	42.0	43.2	43.3	3.8		34.1	37.3	50.1	47.6	45.5	49.0	45.9	5.1	43.8
0	(1.9)	(1.4)	(0.2)	(1.1)	(0.2)	(1.0)	(0.8)		(3.0)	(5.6)	(4.8)	(2.4)	(3.3)	(3.0)	(3.8)	(1.3)	(1.7)
29.9	21.3	18.2	15.3	² 23.7	14.8	18.7	3.8		23.7	34.7	16.9	22.1	23.6	28.6	25.2	6.8	21.7
0	0	0	0	0	0	0		0	0	0	0	0	0	0
.7	4.0	5.5	.05	1.3	8.0	3.8	3.2		11.0	6.5	10.5	11.2	9.2	5.4	8.6	2.5	5.1
2.5	9.2	4.7	9.2	4.6	9.9	7.5	2.6		11.2	4.4	7.3	6.1	7.0	5.4	6.0	1.2	6.1
0	0	0	0	0	0	0		0	0	0	0	0	0	0
.3	.9	.9	.8	.7	1.7	1.0	.4		1.6	2.3	1.2	2.9	1.7	1.6	1.9	.7	1.4
.1	.4	.2	.1	.3	.3	.3	.1		.8	.6	.6	.5	.6	.3	.5	.1	.3
.1	.3	1.1	.05	.1	1.3	.6	.6		1.1	1.9	1.0	1.4	1.3	.4	1.2	.6	.6
Tr.	.1	.05	.05	Tr.	.1	.06	.04		.15	.1	.15	Tr.	.05	.05	.09	.05	.05
0	0	0	0	Tr.	0	Tr.		Tr.	0	.1	Tr.	Tr.	0	Tr.	Tr.
0	0	0	0	0	0	0		0	0	0	0	0	0	0	Tr.
0	0	0	0	0	0	0		0	0	0	0	0	Tr.	Tr.	Tr.
100.0	100.0	100.05	100.05	100.0	100.0	100.16		99.95	100.0	99.95	100.0	99.95	100.05	99.99	98.45
3.7	14.9	12.4	10.2	7.0	21.3	13.1	5.4		25.9	15.8	20.9	22.1	19.9	13.1	18.3	3.8	13.6
0?	30-35	30	27-30	35	28-33	28-35		0?	37	38-49	36	40	27	28-49	28-49
.....	(20)	(21)	(20)	(20)	(20)	(20-23)
.97	.86	1.0	.63	.78	.92	.84	.1		.60	.80	.81	.82	.80	.68	.78	.06	.86

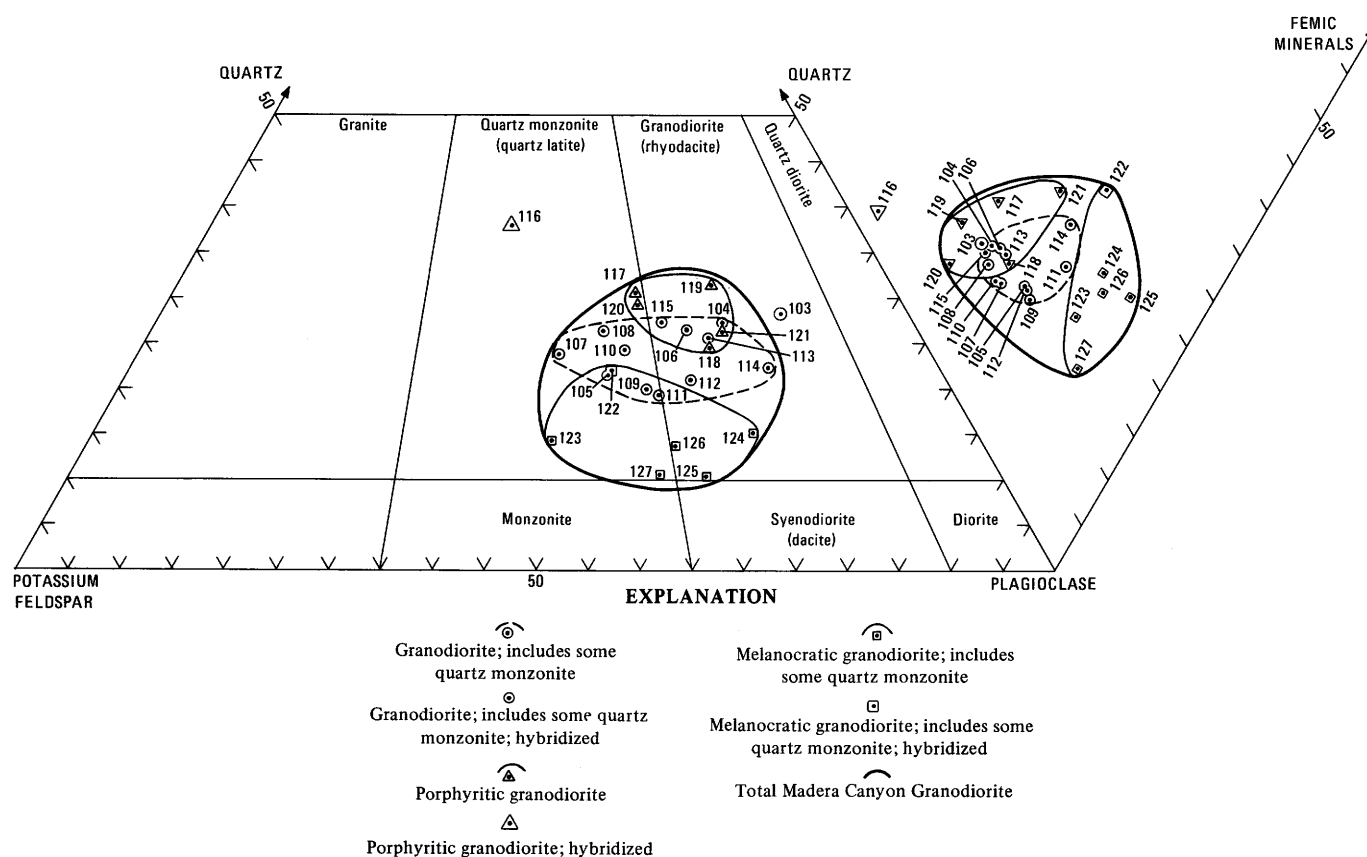


FIGURE 31.—Modified triangular diagram showing modal quartz, potassium feldspar, plagioclase, and femic minerals of Madera Canyon Granodiorite.

TABLE 14.—*Chemical and spectrographic analyses and CIPW norms of Madera Canyon Granodiorite*

[Chemical analyses by rapid rock method (Shapiro and Brannock, 1962), with specimen 113 supplemented by X-ray fluorescence method and specimens 118, 124, and 127 supplemented by atomic absorption method. Chemical analysts: Lowell Artis, S. D. Botts, G. W. Chloe, P. L. D. Elmore, John Glenn, H. Smith, and Dwight Taylor. Spectrographic analyses by semiquantitative method. Spectrographic analysts: W. B. Crandell, J. L. Finley, and J. L. Harris. Elements looked for but not found: Ag, As, Au, Bi, Cd, Eu, Ge, Hf, Hg, In, Li, Nd, Pd, Pr, Pt, Sb, Sm, Sn, Ta, Te, Th, Tl, U, W, and Zn. Symbols: s, standard deviations; <, less than; . . . , not determined; N, not detected]

Rock type.....	Granodiorite			Porphyritic granodiorite			Melanocratic granodiorite				110—127	
Specimen No.....	110	113	110,113	117	118	117,118	124	125	127	124—127	Mean	s
Field No.	769	826	Mean	874	872	Mean	824	867	802	Mean		
Chemical analyses (weight percent)												
SiO ₂	67.9	65.7	66.8	68.6	67.5	68.1	60.5	60.4	60.5	65.1	3.7
Al ₂ O ₃	15.6	16.3	16.0	15.2	15.1	15.2	16.5	16.1	16.3	15.8	.6
Fe ₂ O ₃	1.7	2.1	1.9	2.1	2.2	2.2	2.5	2.8	2.7	2.2	.4
FeO	1.4	1.7	1.6	1.2	1.4	1.3	3.3	3.2	3.3	2.0	1.0
MgO	1.4	1.7	1.6	1.0	1.2	1.1	2.3	2.6	2.5	1.7	.6
CaO	3.1	3.8	3.5	3.5	3.6	3.6	4.5	4.0	4.3	3.8	.5
Na ₂ O	3.6	3.9	3.8	3.6	4.0	3.8	3.7	3.8	3.8	3.8	.2
K ₂ O	3.8	3.0	3.4	3.2	3.3	3.3	4.1	4.6	4.4	3.6	.6
H ₂ O—11	.12	.12	.12	.14	.13	.0907	.08	.11	.02
H ₂ O+81	.62	.72	.51	.52	.52	.7865	.72	.65	.13
TiO ₂42	.55	.49	.58	.66	.62	.9899	.99	.72	.24
P ₂ O ₅13	.23	.18	.17	.19	.18	.4449	.47	.28	.15
MnO06	.05	.06	.05	.07	.06	.1719	.18	.10	.06
CO ₂	<.05	.11	.06	<.05	<.05	<.05	<.05	<.05	<.05	.06	.05
Total	100	100	100	100	100	101	100	100	100	100
Spectrographic analyses (weight percent)												
B	0	0	0	0	0	0	0	0.007	0	0.002	0.001	0.003
Ba07	.1	.09	.1	.1	.1	.015	.015	.015	.015	.06	.04
Be0001	0	.00005	0	.00015	.0001	.0002	.0003	.0003	.0003	.00015	.0001
Ce01	0	.005	.015	.01	.01	N	N	.05	.05	.01	.02
Co0007	.001	.0009	.0005	.0007	.0006	.007	.005	.0015	.005	.002	.003
Cr001	.001	.001	.0007	.001	.0009	.0015	.003	.0015	.002	.001	.0007
Cu002	.02	.01	.0005	.007	.004	.015	.03	.005	.002	.01	.01
Ga001	.001	.001	.0015	.0015	.0015	N	N	.0015	.0015	.0009	.0007
La007	.005	.006	.01	.007	.009	.015	.015	.01	.015	.01	.004
Mo	0	.0003	.00015	0	0	0	0	0	0	0	.0004	.0001
Nb	0	0	0	.0003	0	.00015	.003	.007	.0015	.004	.002	.003
Ni	0	<.003	<.003	0	0	0	.015	.003	0	.006	.003	.006
Pb0007	.0005	.0006	.03	.0007	.015	.002	.001	.002	.002	.005	.01
Sc0007	.0007	.0007	.0007	.0007	.0007	.007	.015	.0015	.008	.004	.005
Sn	0	0	0	.003	0	.0015	0	.0015	0	.0005	.0006	.001
Sr05	.07	.06	.07	.05	.06	.015	.01	.05	.03	.05	.02
V007	.007	.007	.005	.005	.005	.015	.03	.007	.02	.01	.009
Y002	.0015	.002	.0015	.001	.001	.015	.003	.005	.008	.004	.005
Yb0002	.0015	.0002	.00015	.0001	.0001	N	N	.0003	.0003	.0003	.0005
Zr01	.01	.01	.015	.02	.02	.007	.01	.05	.02	.02	.01
CIPW norms												
A	23.9	21.6	27.1	23.4	11.0	9.4
C36	.54	0	0	0	0
or	22.4	17.7	18.9	19.5	24.2	27.2
ab	30.4	33.0	30.5	33.9	31.3	32.2
an	14.2	16.7	15.9	13.5	16.3	13.3
di {wo	0	003	1.2	1.2	1.3
{en	0	003	1.07587
{fs	0	0	0	03537
hy {en	3.5	4.2	2.5	2.0	5.0	5.6
{fs58	.57	0	0	2.3	2.0
mt	2.5	3.0	2.6	2.8	3.6	4.1
hm	0	048	.25	0	0
il80	1.0	1.1	1.3	1.9	1.9
ap31	.5540	.45	1.0	1.2
cc11	.2511	.111111
Total	99.1	99.1	99.6	99.4	99.0	99.6
Femic	7.8	9.6	7.2	9.1	16.2	17.5

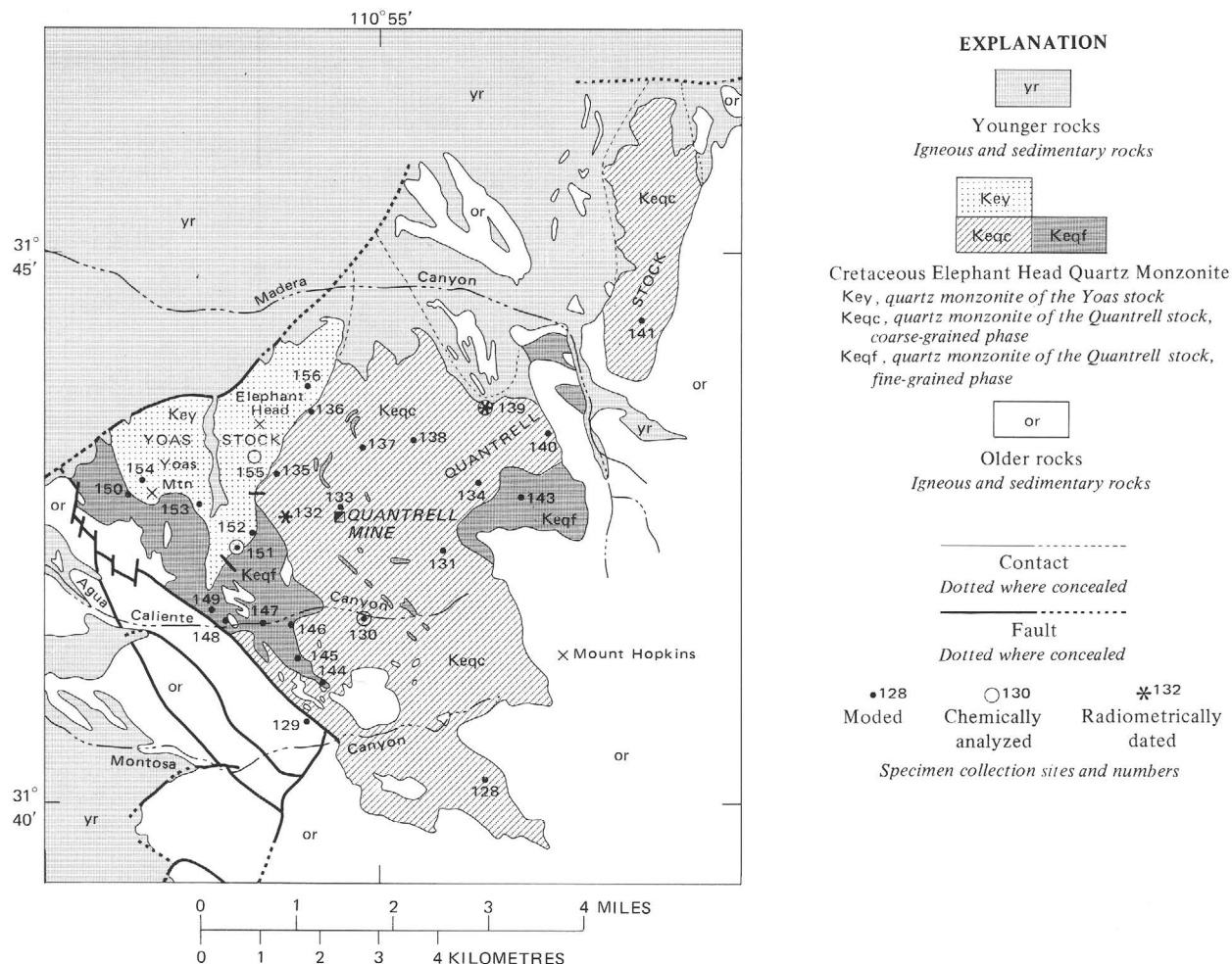


FIGURE 32.—Distribution of Elephant Head Quartz Monzonite and specimen collection sites.

Monzonite, which are radiometrically dated as 67 to 69 m.y. old (table 4). In addition, the nonporphyritic type of Madera Canyon Granodiorite was dated by the potassium-argon method by P. E. Damon (written commun., 1964) as 67.9 ± 2.1 m.y. Because the precise site at which his specimen was collected is uncertain, the rock was not resampled for further dating.

Granodiorite similar in both age and composition to the Madera Canyon Granodiorite has not been reported in ranges adjacent to the Santa Rita Mountains. Other granodiorite stocks of similar appearance occur in both the Sierrita Mountains (Cooper, 1974) and the Patagonia Mountains (Simons, 1973), but they are about 10 m.y. younger.

ELEPHANT HEAD QUARTZ MONZONITE

The Elephant Head Quartz Monzonite is a composite of the Quantrell and Yoas stocks and consists of coarse-grained pinkish-gray leucocratic rock that underlies much of the rugged terrain around Elephant Head and the

mouth of Madera Canyon (fig. 32). It underlies several areas that total about 18 square miles, and it may also underlie a considerable area beneath the piedmont gravel northwest of Elephant Head.

The main mass of quartz monzonite lies west of the upper reaches of Madera Canyon; it is slightly elongate to the northwest, a trend followed by most of the intrusive tongues and inclusions of host rocks in the quartz monzonite. Another mass of quartz monzonite lies northeast of the upper reaches of Madera Canyon and trends north, and small masses crop out between the larger ones.

The attitude of the sides of the present plutonic masses suggests that in most places the original tops of the masses were a considerable distance above the present level of exposure. The trace of the eastern contact of the mass northeast of Madera Canyon is straight and the contact dips steeply outward; the quartz monzonite contact at the southern end of the mass probably also dips steeply outward. The other contacts are concealed by gravel. The

eastern contact of the larger mass of quartz monzonite is irregular but generally is steep. To the north the mass is faulted, and to the northwest it intrudes quartz diorite along a very irregular but mostly steep contact. However, to the south the contact dips gently outward and in places trends irregularly, and several large flat-bottomed roof pendants cap the highest hills. These features suggest that the upper contact of the stock plunges gently southward; to the south the top is exposed near the present surface, and to the north it has been removed by erosion. Small outcrops of quartz monzonite between the two larger masses of identical rock indicates that the septum of granodiorite along Madera Canyon probably does not extend far beneath the surface. Very likely then, the two masses are cupolas of a single stock.

Generally the contacts of the quartz monzonite are fairly sharp and without noticeable chill zones or contact-metamorphosed aureoles, but the exceptions at several places are instructive. At one locality the contact of the smaller cupola, northeast of specimen collection site 141 (fig. 32), forms a gradational zone at least 400 feet wide. The rock toward the quartz monzonite is fine grained and light pinkish gray, and it contains only a few small clots of dark minerals. Toward the granodioritic host the rock gradually is grayer and the clots are progressively larger and more abundant, until they resemble the clusters of felty-textured biotite aggregates of the granodiorite, except that the hybrid rock has a sprinkling of small white feldspar crystals more typical of the quartz monzonite. The biotite in the nearby host rock is recrystallized, probably as a result of contact metamorphism produced by the emplacement of the small cupola of quartz monzonite. At a second locality, between the collection site of specimens 147 and 148 along Agua Caliente Canyon (fig. 32), the quartz monzonite intrudes a quartz diorite that is assigned to the Josephine Canyon Diorite. Not only is the contact very irregular, but also the quartz monzonite contains many small inclusions, and some larger ones of the quartz diorite. Some of these inclusions appear to be incompletely digested granodioritelike rocks. In both of these places, some of the host rocks seem to be assimilated, and in the Agua Caliente Canyon area some stoping may also have occurred along the sides of the stock. At a third locality, near the southern tip of the large cupola along Montosa Canyon, the wallrocks and roof pendants are increasingly intensely altered toward the quartz monzonite. These host rocks are arkose, dacitic volcanic tuff, and breccia of the Salero Formation, which are so widely argillitized and locally are so strongly pyritized that the primary minerals of the rock are almost entirely replaced. This alteration appears to be a hydrothermal rather than a thermal contact effect, but even so the alteration probably is genetically related to the stock, which is the youngest intrusive rock of significant size in the area. Perhaps the alteration was particularly strong in this area of the fairly

flat shoulder on the southern tip of the stock because upward-streaming fluids were more abundant than outward-moving fluids. Finally, a body of fine-grained Elephant Head Quartz Monzonite, erroneously shown as Josephine Canyon Diorite on the geologic map and section A-A' of the Mount Wrightson quadrangle (Drewes, 1971c), intrudes a small unmapped inclusion of tuff breccia north of Montosa Canyon (specimen collection site 144, fig. 32).

PETROGRAPHY

The large cupola is a composite mass of two stocks; the larger and older Quantrell stock underlies a gentler terrain than the smaller and younger Yoas stock. The Quantrell stock includes the rocks of the small cupola, and it contains some fine-grained quartz monzonite, as well as the common coarse-grained kind. Along the east side of the Yoas stock, which is named for Yoas Mountain near the center of the stock (fig. 32), the contrast in weathering characteristics is very striking, as shown in figure 33. Rocks of the Yoas stock underlie some of the most rugged country in the area, including the 2,000-foot-high rock dome of Elephant Head, for which the formation is named, but the eastern part of the stock near the edge of the pediment underlies more gentle terrain. Rocks of part of the Quantrell stock adjacent to the Yoas stock (see geologic map, Drewes, 1971c) also underlie gentle terrain, but some of the Quantrell stock in the high ridges east of the Quantrell mine underlies bold knobs. In most places the contact between the stocks is concealed, but east of Elephant Head it is exposed and the quartz monzonite of the Yoas stock forms a chill zone 5 to 10 feet wide against the Quantrell stock. The trend of this contact is straight and its dip is moderately steep to the east. Biotite in the rocks of the Quantrell stock is recrystallized or contact metamorphosed to felty aggregates of small crystals. The contact southwest of Yoas Mountain is irregular and in places is concealed by small intrusive bodies of lamprophyre and aplite, mostly too small to show on the scale of the geologic map of the Mount Wrightson quadrangle. At this locality the geologic map of the quadrangle erroneously shows two lamprophyre dikes as Josephine Canyon Diorite.

The Quantrell stock is made up mostly of a coarse-grained quartz monzonite, but it also includes masses of fine-grained quartz monzonite or aplite, most of which are intrusive into the coarse-grained rock and are small and tabular. Larger masses of fine-grained rock lie along the edge of the stock on the west side of Madera Canyon and southwest of Yoas Mountain, where a few small bodies of aplite associated with the Yoas stock may have been mapped with the slightly older and petrographically identical aplite of the Quantrell stock.

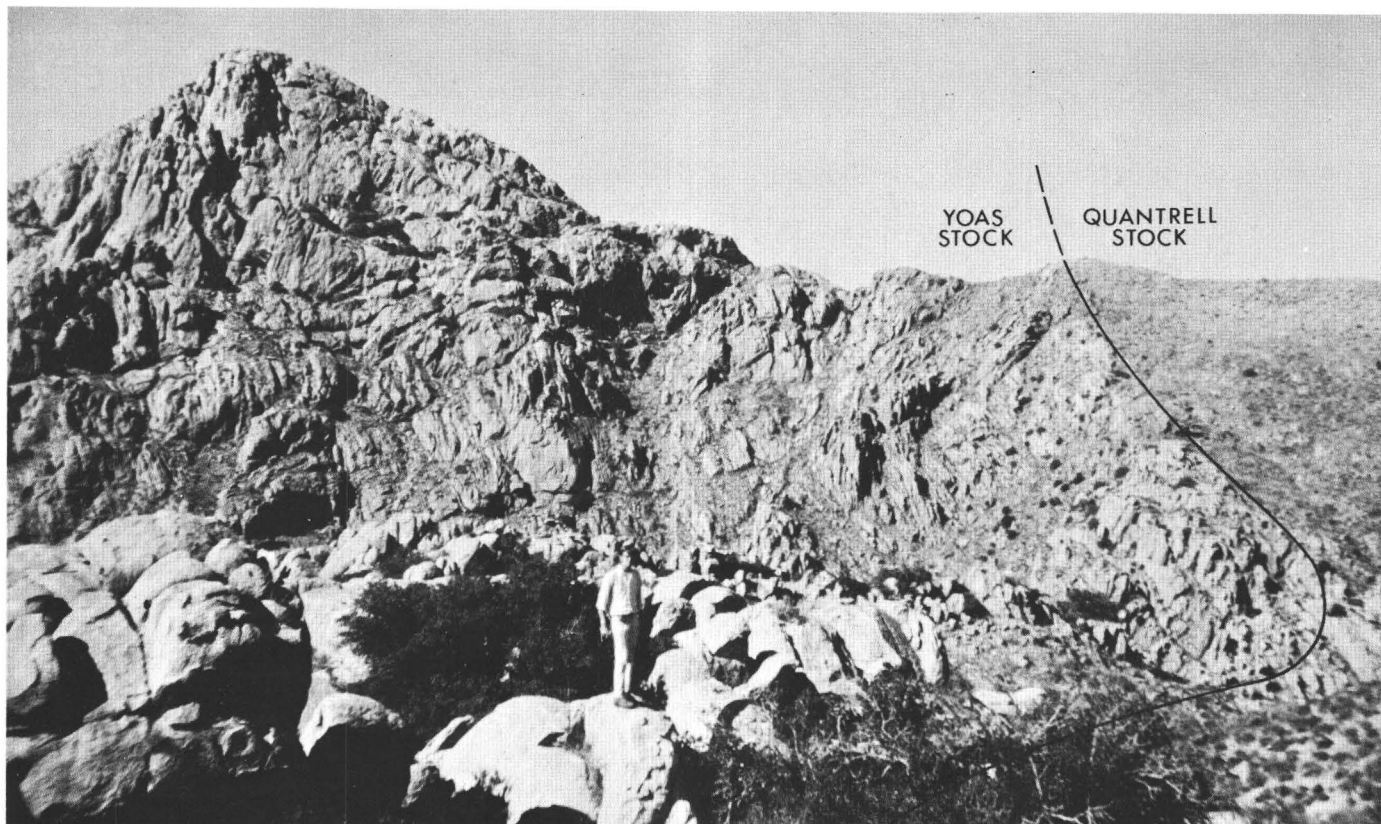


FIGURE 33.—View, toward northeast, of Elephant Head and the east-dipping contact between the Yoas stock, underlying the rugged terrain, and the Quantrell stock, underlying the gentle terrain.

QUANTRELL STOCK,
COARSE-GRAINED QUARTZ MONZONITE

The coarse-grained quartz monzonite of the Quantrell stock underlies a varied terrain of gentle slopes partly veneered by grus and interspersed blocky debris, and of fairly rugged ridges and some chasmlike canyons. The rock is massive and contains at least three prominent sets of widely spaced joints. It is a light brownish gray to light pinkish gray and weathers to brownish gray. Specimens typically are coarsely granular and contain only a sparse scattering of ferromagnesian minerals (fig. 34).

The quartz monzonite has a hypidiomorphic-granular texture and a grain size commonly 4 to 8 mm (fig. 35). Some specimens have poikilitic grains and fine-grained myrmekitic, granophyric, and perthitic textures, but the granophyric intergrowths of one specimen are coarse. Specimen 135 has a weak metamorphic texture superimposed upon the hypidiomorphic-granular one: small crystals of quartz are scattered between the more abundant coarse crystals, crystal boundaries are strongly sutured, and biotite occurs in clusters of small felty crystals. The strong undulatory extinction of quartz crystals in rocks of the Quantrell stock collected near the contact with the Yoas stock may reflect minor intrusive pressure during emplacement of the Yoas stock.

The rock is made up mainly of quartz, plagioclase, orthoclase or microcline and contains small amounts of biotite, magnetite, apatite, sphene, and zircon. Some specimens also have a trace of amphibole, allanite, monazite, pyrite, and tourmaline. The quartz is anhedral and generally has a slight to moderate undulatory extinction. The plagioclase is subhedral, is strongly altered to clay minerals and sericite, and has a composition of albite. About 20 percent of the moded plagioclase occurs as perthitic intergrowths. Potassium feldspar is anhedral to subhedral and is moderately kaolinitized. Patch perthite is more common than lace perthite and is very coarse in some specimens. Biotite is pleochroic in pale yellow brown to moderate brown and is partly altered to penninitic chlorite, sericite, leucoxene, and iron oxide. Magnetite is probably ilmenitic, and zircon is euhedral, fairly large, and abundant when compared to that in most other plutonic rocks of the area. Amphibole is pleochroic in bluish green. Alteration minerals include a trace of epidote, in addition to those already mentioned.

QUANTRELL STOCK,
FINE-GRAINED QUARTZ MONZONITE

The fine-grained quartz monzonite of the Quantrell stock is generally a little more resistant to weathering than the adjacent coarse-grained rock. The rock is closely

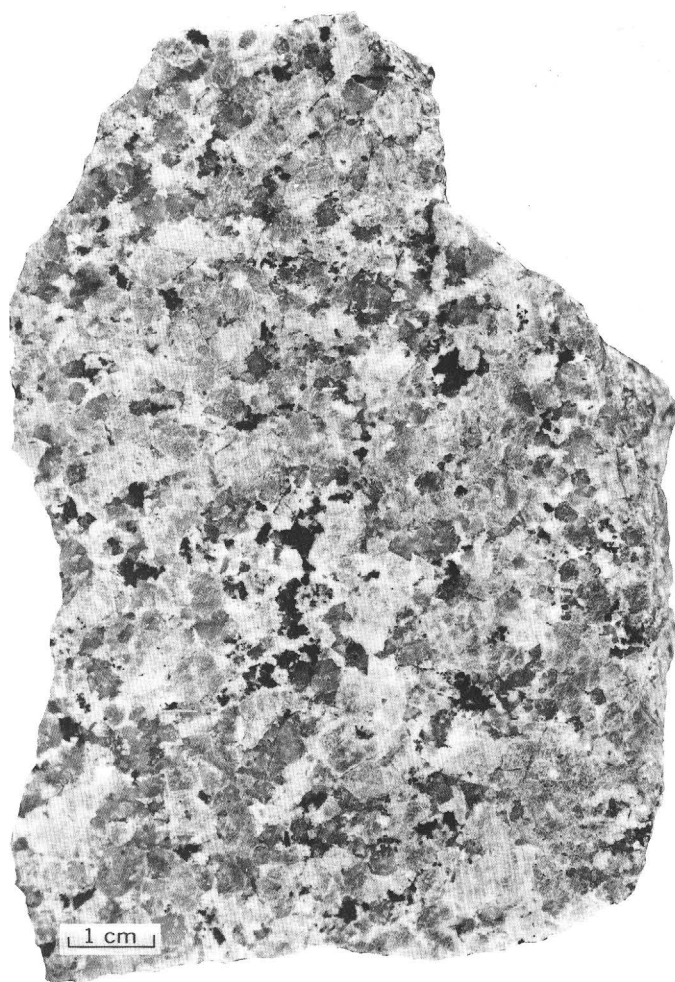


FIGURE 34.—Specimen 134. Elephant Head Quartz Monzonite, a coarse-grained rock of the Quantrell stock.

fractured, and the large mass on the west flank of Madera Canyon also has a weakly developed, steeply eastward dipping flow foliation and is pervasively silicified and pyritized. (See geologic map, Drewes, 1971c.)

Specimens of fine-grained quartz monzonite are very pale grayish orange pink to light pinkish gray. Grain size is mostly 0.2 to 2 mm throughout the suite of specimens, although the range is much less in individual specimens. An idiomorphic- to hypidiomorphic-granular texture is dominant and parts of many specimens have a fine-grained granophyric texture.

The fine-grained rock type contains the same principal minerals as the coarse, but somewhat fewer kinds of accessory minerals are present. The characteristics of the minerals are substantially like those in the coarse-grained quartz monzonite. The alteration minerals are also the same but are more abundant in the fine-grained rock than in the coarse-grained.

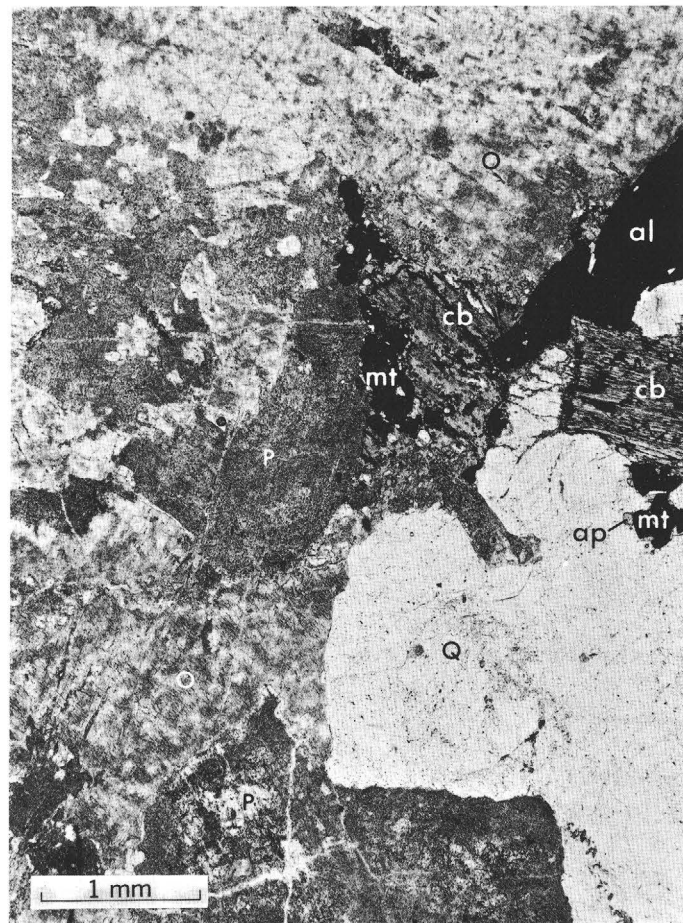


FIGURE 35.—Specimen 132. Coarse-grained Elephant Head Quartz Monzonite from the Quantrell stock. Crystals: orthoclase (O), plagioclase (P), quartz (Q), chloritized biotite (cb), magnetite (mt), apatite (ap), and allanite (al), Plain light; $\times 20$.

YOAS STOCK, COARSE-GRAINED QUARTZ MONZONITE

The quartz monzonite of the Yoas stock is almost entirely coarse grained, and it underlies some extremely rugged terrain. The rock is massive and is cut by several sets of joints, which are strikingly prominent on the many bold outcrops between Elephant Head and the southern end of the stock (fig. 33). Away from the sharp contact on the east side of the stock, the joints are fairly widely spaced, but in a zone 400 to 700 feet wide along this contact the joints are commonly 1 to 3 feet apart, with additional microfractures spaced at intervals of less than an inch. Viewed from a distance, the rock looks slightly pinker than the adjacent quartz monzonite of the Quantrell stock, perhaps because bold outcrops of the Yoas stock are less weathered than the gentler terrain of the Quantrell stock. The quartz monzonite of the Yoas stock is generally free of inclusions, but that in the canyon south of Elephant

Head contains partly assimilated gray andesitic to dioritic inclusions mostly 2 to 12 inches across and rarely many feet across. Quartz veinlets, lamprophyre dikes, and a few aplitic bodies cut the quartz monzonite, apparently at random orientation.

Grain size in quartz monzonite of the Yoas stock is typically 4 to 7 mm and in some specimens is as much as 10 mm. Hypidiographic-granular texture is ubiquitous and a few specimens also have some intergranular texture and some poorly developed granophyric texture. Lace type and patch type of perthitic intergrowths are equally common, and they vary widely in size.

Mineralogically the quartz monzonite of the Yoas stock is indistinguishable from that of the Quantrell stock.

MODAL AND CHEMICAL SUMMARY

Modal analyses of 29 specimens of Elephant Head Quartz Monzonite are listed in table 15. The mean of these modes is much like that of the Squaw Gulch Granite (table 7), except that it has 36 percent (instead of 25 percent) plagioclase, slightly more biotite, and a greater variety of accessory minerals.

The modified triangular diagram of figure 36 graphically summarizes the modal data. A figure drawn around the plotted modes has an hemielliptical shape, flattened against the leucocratic face of the composition tetrahedron and centered in the quartz monzonite field. The ranges of the modes of the coarse-grained rocks of the two stocks are coextensive, and the modes of the fine-grained rock are centered slightly closer to the quartz-plagioclase edge of the composition tetrahedron than those of the coarse-grained rocks.

A comparison of the modal ranges for the three large plutons of late Late Cretaceous age shows systematic changes. Only the figures circumscribed around the three groups of modes—for the Josephine Canyon Diorite, Madera Canyon Granodiorite, and Elephant Head Quartz Monzonite—are shown together in figure 37, along with the estimated positions of the centers of the figures. In the order from the oldest to the youngest pluton, as determined from field relations, the composition of the magma shifted from a femic-plagioclase-rich point to an alkali-quartz-rich point. In direction and amount the shift is similar to that which occurred between the phases of the Josephine Canyon Diorite. The circumscribed figures have also changed from a tilted discoidal body with a near-vertical short axis, to a subspherical body, to a hemielliptical body with a near-horizontal short axis.

The trend of compositional change of the rocks is compatible with the typical model of fractionating magma in which the more "basic" fractions are emplaced before the more "acidic" fractions. However, some of the data on the age of these plutons, discussed in the next section,

indicate that such a model may at least be oversimplified, if it is at all tenable. The change in the configuration of the figures drawn around the plotted modes is intriguing, but no speculation on its possible significance is offered here.

Chemical and spectrographic analyses and CIPW norms of four coarse-grained specimens of Elephant Head Quartz Monzonite are shown in table 16 and are summarized in the histogram of figures 10K–10L. Chemically this rock is very similar to the Squaw Gulch Granite and the quartz monzonite of the Corona stock. The Elephant Head Quartz Monzonite has slightly more K_2O and less CaO and Na_2O than the granite, as reflected by the difference in the abundances of orthoclase or microcline and of plagioclase of rocks (tables 7, 15). Chemically, the rock resembles Nockolds' (1954, p. 1012–1016) biotite adamellite and possibly some of the granite types.

AGE AND CORRELATION

The Elephant Head Quartz Monzonite is given a late Late Cretaceous age on the basis of interpretation of evidence from field relations and radiometric dating, some of which is conflicting. The field relations consistently show that the quartz monzonite is (1) younger than the Salero Formation, which is altered along the contact of the Quantrell stock, (2) younger than the inclusions of quartz diorite, which are correlated with the Josephine Canyon Diorite, and (3) younger than the Madera Canyon Granodiorite, which is metamorphosed near the contact with the small cupola. Because a low grade of metamorphism is a widespread feature in the Santa Rita Mountains, and because contact metamorphic zones are generally indistinct or erratic around stocks of all ages, determining age relations from this evidence requires caution. The evidence of the relationship to the quartz diorite inclusions is weak because it is based on a second interpretation of the identity of the rock. The combined field evidence is thus seen as consistent but not strong.

Radiometric dates of two specimens of Elephant Head Quartz Monzonite, obtained from the coarse-grained rock of the Quantrell stock, are listed in table 4. Separate dates by the potassium-argon method on biotite and by the lead-alpha method on zircon are given for each specimen. The two ages obtained by each method are nearly identical, but the potassium-argon ages are about 68 m.y. and the lead-alpha ages about 180 m.y. The close agreement of the dual results by each method is probably not fortuitous, although further dating information is certainly desirable, particularly in view of the uncertainties besetting the lead-alpha method. Because evidence of recrystallization in the quartz monzonite is lacking, except for the immediate vicinity of the Yoas stock, an explanation involving a late Late Cretaceous thermal

TABLE 15.—*Modes of Elephant*

[Field numbers are abbreviated; year of collection and collector's initial omitted. Full field number

Intrusive mass.....	Quantrell stock																
Rock type.....	Coarse-grained quartz monzonite																
Specimen No.....	128	¹ 129	130	131	132	133	134	135	136	137	138	139	140	141	142	128—142	
Field No.....	579	669	701	734	754	749	846	753	888	880	879	876	844	866	901	Mean	s
Quartz.....	32.1	22.9	23.7	27.2	27.4	32.2	33.3	26.4	24.0	29.4	27.0	18.7	34.8	29.5	27.7	27.8	4.3
Plagioclase, total.....	24.9	37.0	33.4	29.0	40.4	37.8	36.1	32.5	43.3	45.8	20.5	37.7	31.7	35.3	38.1	34.9	6.6
(in perthite).....	(14.7)	(6.1)	(7.5)	(3.0)	(3.9)	(9.2)	(15.1)	(2.3)	(13.1)	(6.9)	(2.2)	(5.0)	(7.6)	(10.3)	(8.2)	(7.7)	(4.2)
K-feldspar, total.....	40.7	38.1	39.0	41.9	29.5	26.6	29.7	37.3	26.8	22.5	49.0	41.8	30.9	32.1	30.3	34.4	7.3
(orthoclase).....	(40.7)	0	(39.0)	(41.9)	(9.9)	(26.6)	(29.7)	(26.1)	(26.8)	(22.5)	(49.0)	0	0	0	0	(20.8)	(17.8)
(microcline?).....	0	(38.1)	0	0	(19.7)	0	0	(11.2)	0	0	0	(41.8)	(30.9)	(32.1)	(30.3)	(13.6)	(16.6)
Biotite.....	.8	1.1	3.3	1.1	1.4	2.2	.8	2.6	4.6	1.3	2.4	1.0	1.4	2.1	2.7	1.9	1.1
Amphibole.....	0	0	0	0	0	.3	0	0	0	0	.6	0	0	0	0	.06	.2
Magnetite.....	1.4	.8	.3	.5	.8	.6	.1	1.1	1.0	.6	.3	.8	.9	.6	.7	.7	.1
Apatite.....	Tr.	.1	.2	.05	.1	.1	Tr.	Tr.	.2	.05	.05	Tr.	.1	Tr.	Tr.	.07	.07
Sphene.....	Tr.	Tr.	Tr.	.2	.3	.1	0	.1	.1	.4	Tr.	0	.2	.2	.4	.1	.1
Zircon.....	.1	.05	.05	.1	.1	.1	Tr.	Tr.	.05	Tr.	.1	Tr.	Tr.	0	.05	.05	.04
Allanite.....	0	0	0	0	Tr.	0	0	0	0	0	0	Tr.	0	.2	.05	Tr.
Monazite(?).....	Tr.	0	0	0	0	.05	0	0	0	0	0	0	0	0	0	Tr.
Pyrite.....	0	Tr.	0	0	0	0	0	0	0	0	0	0	0	0	0	Tr.
Tourmaline.....	0	0	0	0	Tr.	0	0	0	0	0	0	0	0	0	0	Tr.
Total.....	100.0	100.05	99.95	100.05	100.0	100.05	100.0	100.0	100.05	100.05	99.95	100.0	100.0	100.0	100.0	100.0
Femic.....	2.3	2.0	3.9	1.9	2.7	3.4	.9	3.8	5.9	2.3	3.4	1.8	2.6	3.1	3.9	2.9	1.4
Percent anorthite in plagioclase (plagioclase rims).....	0	0—5	0—5	0	0—5	0—5	5—10	0—10	5—10	5	5—10	5—10	10	5—10	5—10	5±
Quartz mixing index (see text).....		.93	.61	.74	.88	.73	.79	.57	.78	.67	.90	.65	.93	.90	.94	.79	.13

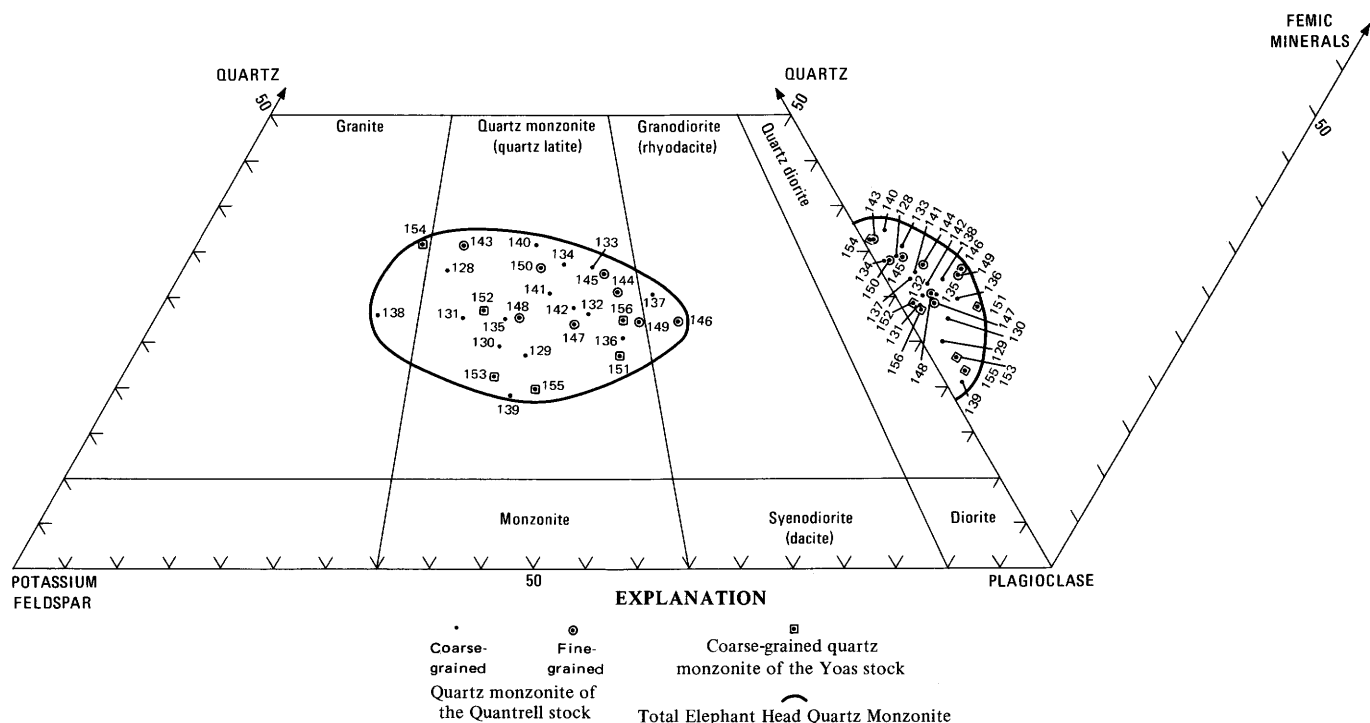
¹ Specimen 129 obtained from mine dump near shaft that bottoms in quartz monzonite.

FIGURE 36.—Modified triangular diagram showing modal quartz, potassium feldspar, plagioclase, and femic minerals of the Elephant Head Quartz Monzonite.

alteration of a Jurassic stock is as unsatisfying as an explanation based on a loss of lead from the zircon. Nevertheless, these conflicting ages may indicate a more

complex history of emplacement and subsequent development of the stock than seems apparent from field evidence alone. This matter deserves further study.

Head Quartz Monzonite

of specimen 128 thus is 64D579. Symbols: *s*, standard deviation; Tr., trace; . . . , not determined]

Quantrell stock—Continued										Yoas stock								128—156 Mean <i>s</i>			
Fine-grained quartz monzonite										Coarse-grained quartz monzonite											
143	144	145	146	147	2 ₁₄₈	149	150	143—150 Mean <i>s</i>		151	152	153	154	155	156	151—156 Mean <i>s</i>		Mean	<i>s</i>		
842	670	698	703	742	740	736	767			747	781	783	785	787	885						
35.4	29.3	31.6	25.2	26.1	26.9	25.3	32.7	29.1	3.8	21.6	28.0	20.6	35.5	19.4	27.0	25.4	6.1	27.6	4.6		
25.2	41.1	39.6	46.7	39.3	33.7	43.5	33.8	37.9	6.8	43.5	30.4	35.0	21.6	39.2	44.6	35.8	8.7	35.9	7.0		
(2.5)	(1.4)	(2.1)	0	(3.6)	(5.0)	(0.4)	(3.9)	(2.4)	(1.7)	(18.5)	(5.7)	(5.4)	(9.0)	(11.4)	(8.6)	(9.8)	(4.9)	(6.6)	(4.7)		
38.5	25.2	26.0	20.3	31.4	35.8	24.1	32.3	29.2	6.3	27.7	39.8	41.9	42.2	38.8	26.7	36.2	7.1	33.3	7.3		
(38.5)	(21.4)	(26.0)	(20.1)	(31.4)	(35.8)	(24.9)	(32.3)	(28.8)	(6.7)	(6.4)	(37.7)	(41.9)	(42.2)	(38.8)	(26.7)	(32.3)	(13.9)	(25.4)	(15.1)		
0	(3.8)	0	(0.2)	0	0	(0.1)	0	(.5)	(1.3)	(21.3)	(2.1)	0	0	0	0	(3.9)	(8.6)	(8.0)	(13.7)		
Tr.	2.5	1.2	5.5	1.7	1.9	5.2	.9	2.4	2.0	2.4	.3	1.2	.6	1.1	1.0	1.1	.7	1.9	1.4		
0	0	Tr.	0	0	.2	0	0	.03	.1	2.9	0	0	0	Tr.	0	.5	1.2	.1	.5		
.8	1.8	.9	1.3	.9	.6	1.3	.1	1.0	.5	1.1	.6	1.1	Tr.	.8	.7	.7	.4	.8	.4		
.1	.1	.1	.2	.2	.3	.2	.1	.2	.1	.2	.05	.1	Tr.	Tr.	.05	.07	.07	.09	.08		
0	Tr.	.4	.8	.3	.5	.3	.05	.3	.3	.6	.3	Tr.	.1	.6	Tr.	.3	.3	.2	.3		
Tr.	Tr.	Tr.	Tr.	.1	.1	.05	.05	.04	.04	Tr.	.05	.05	Tr.	.1	Tr.	.04	.04	.05	.04		
0	0	.2	0	Tr.	0	.05	0	Tr.05	Tr.	0	0	Tr.	0	Tr.	Tr.		
0	0	0	0	0	0	0	0	0	0	0	0	0	0	0	0	Tr.		
0	0	0	0	0	0	0	0	0	0	0	0	0	0	0	0	Tr.		
0	0	0	0	0	0	0	0	0	0	0	0	0	0	0	0	Tr.		
100.0	100.0	100.0	100.0	100.0	100.0	100.0	100.0	100.2	100.05	99.5	99.95	100.0	100.0	100.05	100.1	99.9		
.9	4.4	2.8	7.8	3.2	3.6	7.1	1.2	4.0	2.5	7.2	1.3	2.5	.7	2.6	1.7	2.7	2.3	3.2	1.9		
0—5	0—5	5—10	0—5	5—10	0—5	0—5	0—5?	5±	0—25?	5—10	0	0	0—5	0—5	0—28	5±		

² Specimen 148 obtained from a coarse-grained inclusion in a body of quartz diorite that intrudes a large mass of fine grained quartz monzonite.

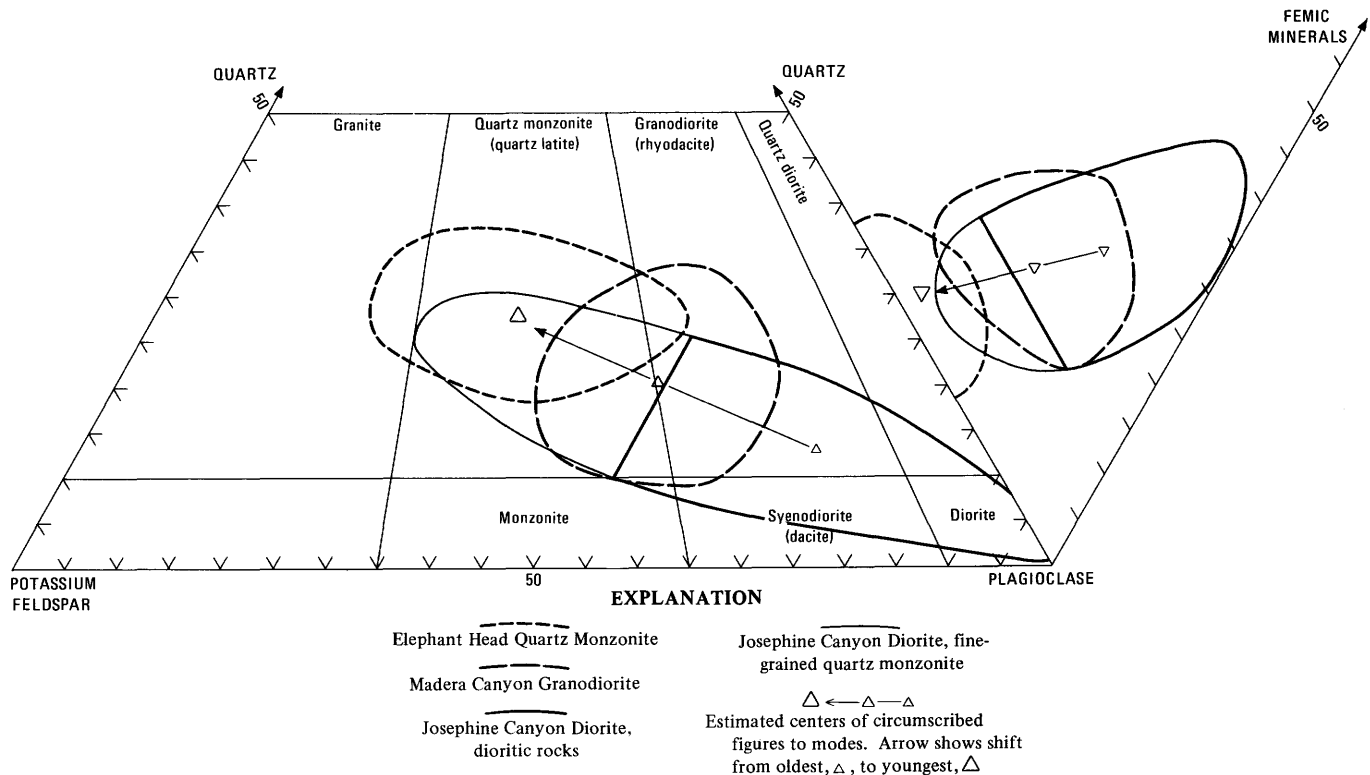


FIGURE 37.—Modified triangular diagram comparing the range of distribution of the modes of the Josephine Canyon Diorite, Madera Canyon Granodiorite, and Elephant Head Quartz Monzonite.

Quartz monzonite stocks around 68 m.y. old are not present in the Sierrita, Patagonia, Empire, and Rincon Mountains, or in the Canelo Hills, adjacent to the Santa

Rita Mountains. Most of the plutonic rocks in these ranges have a granodiorite composition and are either older or younger by 10 m.y.

TABLE 16.—*Chemical and spectrographic analyses and CIPW norms of Elephant Head Quartz Monzonite, coarse-grained rocks*

[Chemical analyses by rapid rock method (Shapiro and Brannock, 1962), with analyses of specimens 139 and 155 supplemented by atomic absorption. Chemical analysts: Lowell Artis, S. D. Botts, G. W. Chloe, P. L. D. Elmore, John Glenn, H. Smith and Dwight Taylor. Spectrographic analyses by semiquantitative method. Spectrographic analysts: W. B. Crandell and J. L. Harris. Elements looked for but not found: Ag, As, Ba, Bi, Cd, Eu, Ge, Hf, Hg, In, Li, Mo, Ni, Pd, Pr, Pt, Re, Sb, Sm, Sn, Ta, Te, Th, Ti, U, W, and Zn. Symbols: s, standard deviation; <, less than, and ..., not determined]

Intrusive mass	Quantrell stock			Yoas stock				
Specimen No.	130	139	130, 139	151	155	151, 155	130 - 155	
Field No.	701	876	Mean	747	787	Mean	Mean	s
Chemical analyses (weight percent)								
SiO ₂	72.2	73.7	73.0	67.2	74.7	71.0	71.6	3.3
Al ₂ O ₃	14.4	13.7	14.1	15.5	13.6	14.6	14.3	.9
Fe ₂ O ₃	1.1	1.5	1.3	1.9	.90	1.4	1.4	.4
FeO74	.56	.65	1.2	.36	.78	.72	.36
MgO40	.13	.27	1.4	.10	.75	.51	.61
CaO75	.70	.73	2.9	.63	1.8	1.2	1.1
Na ₂ O	4.4	2.9	3.7	4.4	4.0	4.2	3.9	.7
K ₂ O	4.7	5.7	5.2	3.8	4.7	4.3	4.7	.8
H ₂ O09	.09	.09	.22	.10	.16	.13	.06
H ₂ O +82	.34	.58	.52	.47	.50	.54	.20
TiO ₂24	.43	.34	.49	.38	.44	.39	.11
P ₂ O ₅	0	.06	.03	.16	.02	.09	.06	.07
MnO ₂13	.05	.09	.10	.05	.08	.08	.04
CO ₂	< .05	< .05	< .05	< .05	< .05	< .05	< .05
Total	100	100	100	100	100	100	100	
Spectrographic analyses (weight percent)								
Ba	0.05	0.07	0.06	0.07	0.05	0.06	0.06	0.01
Be0005	.0015	.0001	.0003	.0003	.0003	.0003	.0001
Ce01	.02	.015	.01	0	.005	.01	.01
Co	0	0	0	.0007	0	.0004	.0002	.0004
Cr	0	0	0	.001	0	.0005	.0003	.0005
Cu0002	.00007	.0005	.01	.00003	.005	.003	.005
Ga001	.0015	.001	.0015	.0015	.0015	.002	.0003
La007	.015	.001	.007	.003	.005	.008	.005
Nb0015	.0003	.0009	.001	.001	.001	.001	.0005
Nd	0	.01	.005	0	0	0	.003	.005
Pb0005	.003	.002	.001	.001	.001	.001	.001
Sc0003	0	.0002	.0007	0	.0004	.0003	.0003
Sr01	.01	.01	.05	.005	.03	.02	.02
V0007	0	.0004	.005	0	.003	.001	.002
Y003	.002	.003	.002	.002	.002	.002	.0005
Yb0003	.0002	.0003	.0002	.0002	.0002	.0002	.0005
Zr03	.003	.03	.03	.01	.02	.03	.01
CIPW norms								
Q	26.4	33.7	19.7	32.1
C84	1.7	0	.95
or	27.8	33.7	22.5	27.8
ab	37.2	24.6	37.3	33.8
an	3.4	2.8	11.3	2.7
di { wo	0	071	0
en { en	0	062	0
fs { fs	0	0002	0
hy { en	1.0	.32	2.9	.25
fs { fs30	.3201	0
mt	1.6	.72	2.8	.22
hm	0	1.0	0	.75
il46	.8293	.72
ap	0	.1438	.05
cc11	.1111	.11
Total	99.1	99.9	99.3	99.5
Femic	3.5	3.4	8.5	2.1

TERTIARY ROCKS

The youngest plutonic rocks and related intrusive rocks in the Santa Rita Mountains are mainly of Tertiary age. They form small intrusive masses, such as small stocks, plugs, and dikes, and some of the rocks have an aphanitic and porphyritic texture, rather than a granitoid one. All these intrusive bodies were probably emplaced fairly close to the surface. Some of them appear to spread downward

and so may well be the tops of larger stocks. Others are probably genetically related to contemporaneous volcanic rocks of nearby areas.

These youngest plutonic rocks consist of four groups; the three oldest were emplaced late during the Laramide orogeny, and the youngest is postorogenic. Rocks of the Gringo Gulch pluton and of some other unrelated masses of quartz latite porphyry, latest Cretaceous or early Paleocene in age, are the oldest group. Granodiorite of the

Helvetia stocks was emplaced next, followed shortly thereafter by quartz latite porphyry of the Greaterville plugs. Granodiorite of the San Cayetano stock, which was emplaced during the late Oligocene, is the youngest rock.

ROCKS OF THE GRINGO GULCH PLUTON AND OTHER ROCKS

Small stocks, plugs, and dikes of microgranodiorite, hornblende dacite porphyry, and quartz latite porphyry crop out at several places in the southern quarter of the Santa Rita Mountains (fig. 38). Many of these rocks are strongly altered; as a result, their original composition is uncertain and their radiometric age is unobtainable. Discussing these rocks together is done for convenience and is not meant to imply a demonstrable genetic association. Indeed, some of the rocks may even be of latest Cretaceous age, as shown on the geologic map of the Mount Wrightson quadrangle (Drewes, 1971c), and other rocks may be as much as 10 m.y. younger.

The least altered and, hence, the most thoroughly studied of these intrusive masses is the Gringo Gulch pluton. In plan it is an elliptical body covering almost half a square mile in the low hills 1 mile north of the junction of Gringo and Temporal Gulches. A smaller plug, cropping out near the Patagonia village garbage dump 2 miles south of that junction, is related to the pluton. The pluton is a composite body; two small areas in the core of the pluton contain light-brownish-gray microgranodiorite, and light-gray to medium-gray hornblende dacite porphyry forms most of the pluton, as well as all of the related plug. The large size, unaltered condition, and abundance of hornblende phenocrysts are the most striking features of this rock, and their uniqueness in the area suggest the correlation of the plug with the rock of the outer part of the pluton.

The rocks of the Gringo Gulch pluton underlie a small basin and form only a few small outcrops as compared to the surrounding host rocks, which are mainly pyroclastic rocks of the Gringo Gulch Volcanics of probable Paleocene age. The plug, however, underlies a small knoll and forms outcrops slightly more resistant to weathering than its host rocks, pyroclastic and epiclastic rocks also of the Gringo Gulch Volcanics. In most places the host rocks next to the pluton and plug are not particularly strongly altered, but those west of the pluton are silicified and intensely argillitized, perhaps owing to the action of fluids from the pluton. The contact of the northern, topographically higher part of the pluton dips gently outward, but that along the southern, lower end of the pluton dips steeply. The southern part of the pluton contains inclusions of altered volcanic rocks. No chilled contact zones have been found along the borders of the hornblende dacite porphyry against the host rocks or on

either side of the contact between the porphyry and the microgranodiorite.

Several large intrusive masses that underlie areas of $\frac{1}{4}$ to 1 square mile and many smaller masses consist of quartz latite porphyry or latite porphyry. A swarm of short dikes and pipes is associated with one large mass near Mansfield Canyon, 2 miles northwest of the Gringo Gulch pluton (fig. 38). Two other large masses of quartz latite porphyry lie between the Salero mine and Josephine Canyon, and a sill-like mass occurs in the northern end of the San Cayetano Mountains. In general, the rocks of these intrusive masses are about as resistant to weathering as the adjacent rocks. They form some small outcrops and a few cliffs, and they disintegrate to a blocky detritus. Both fresh and weathered rocks are mostly pale red to grayish orange pink. They are all finely porphyritic, and phenocrysts are mostly of a pink altered plagioclase and altered mica and, in comparison to other rocks in the area, relatively free of quartz. The edges of these intrusive bodies lack chilled margins, and the host rocks are not contact metamorphosed.

In certain details, however, these intrusive masses differ from each other. The quartz latite porphyry, which intrudes the Mount Wrightson Formation near Mansfield Canyon, is ameoboid shaped, is surrounded by the swarm of small dikes, and contains some bodies of brecciated latite porphyry. This intrusive mass may be a large breccia pipe formed from a highly fluid magma, and it could be of Mesozoic age. The intrusive masses between Salero mine and Josephine Canyon have a subelliptical shape, and they intrude rocks at least as young as the Salero Formation and possibly as young as the Josephine Canyon Diorite. These rocks are flow laminated and in many places the dips of the foliation are steep and the strike seems to be irregular. The contact along the west side of the northernmost of these masses dips moderately eastward and that on the east side is about vertical, so apparently the size of that mass diminishes downward. These intrusive masses were probably formed from a fairly viscous magma, and they may be plugs or laccoliths. The intrusive mass in the northern part of the San Cayetano Mountains forms a thick southward-dipping sheet of gray latite porphyry that intrudes the Salero Formation. Its geologic relations with an adjacent stock of Josephine Canyon Diorite are concealed.

Under the microscope, the microgranodiorite of the Gringo Gulch pluton is seen to be made up of about equally abundant crystals of a larger size (1–4 mm) and a smaller size (0.03–0.1 mm), arranged in a hypidiomorphic-granular texture. The rock contains mostly plagioclase, quartz, orthoclase, biotite, and hornblende, and trace amounts of ilmenitic magnetite, apatite, zircon, and allanite(?), as shown by the modes in table 17. The larger crystals of plagioclase have the composition of calcic

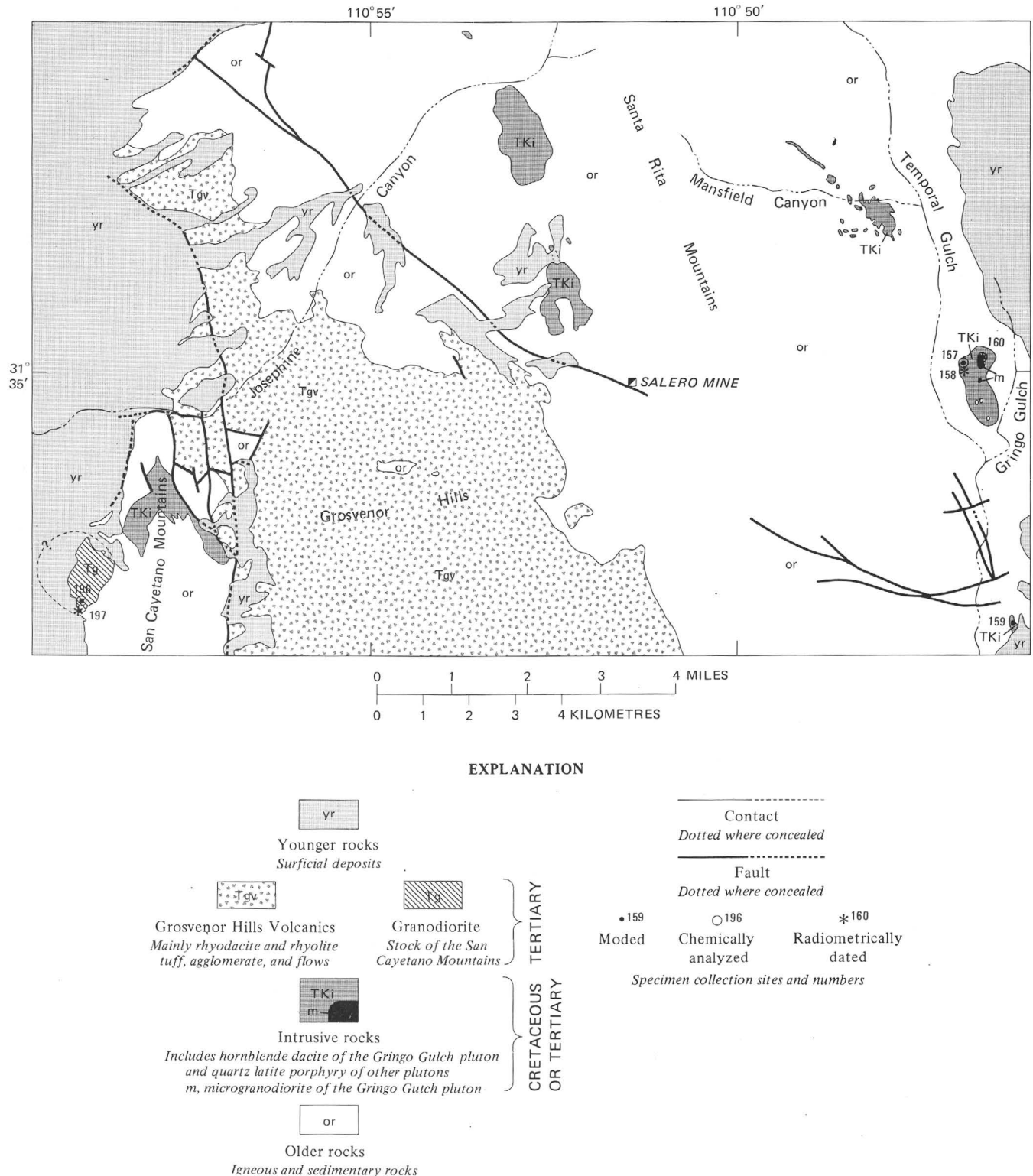


FIGURE 38.—Distribution of rocks of Gringo Gulch pluton and other rocks and specimen collection sites.

andesine and the smaller ones are calcic oligoclase. Biotite is pleochroic in pale yellow brown to moderate yellow brown and is slightly altered to penninite. Hornblende forms fairly long subhedral crystals largely altered to

actinolite and to a rim of iron oxide. Quartz and orthoclase are typically smaller grains.

Hornblende dacite porphyry of the Gringo Gulch pluton and of the associated plug has a felty and granular

groundmass and phenocrysts as much as 1 cm long. Phenocrysts make up 15 to 40 percent of the rock and are chiefly of hornblende and plagioclase, but some are augite and magnetite. The plagioclase phenocrysts have an andesine or labradorite composition, and in some specimens they are partly albitized. The hornblende phenocrysts are mostly euhedral, and in one specimen they form a sheath around a xenocryst of quartz. They are pleochroic in light olive brown to dark olive brown or olive green and are slightly altered to chlorite, epidote, and iron oxide. The groundmass biotite forms small crystals pleochroic in yellowish brown that are largely chloritized, and the pyroxene is probably augite.

The quartz latite porphyry of the other intrusive masses is a strongly altered rock that has an idiomorphic-granular groundmass. Phenocrysts are 4 to 7 mm long and make up 15 to 25 percent of the rock. They are much-albitized plagioclase and some chloritized and sericitized biotite; a few specimens contain a perthitic potassium feldspar. Trace amounts of magnetite, apatite, quartz, sphene, zircon, amphibole(?), and pyroxene(?) are present in various combinations. Alteration minerals are very abundant and include clay minerals, chlorite, sericite, leucoxene, epidote, actinolite(?), calcite, chalcedony, and iron oxide.

The few available modes are plotted on the modified triangular diagram of figure 39. The hornblende dacite porphyry is a modal syenodiorite that is similar to the rocks of the Josephine Canyon Diorite.

The chemical and spectrographic analyses and CIPW norms of two specimens of the Gringo Gulch pluton, which are shown in table 18 and are plotted in figure 10E, suggest the microgranodiorite to be compositionally similar to the granodiorite of the San Cayetano stock (table 23). The chemical analyses show that hornblende dacite porphyry is not simply a fine-grained variety of the microgranodiorite, as in a chilled-border phase. For example, the microgranodiorite contains at least 10 percent more SiO_2 than does the porphyry. Even assuming that this difference is due to a secondary enrichment, and so removing the excess and recalculating the analytical results to 100 percent, the microgranodiorite has much more K_2O and less total iron, MgO , and CaO than the dacite porphyry. The rocks must have been crystallized from separate, but perhaps genetically related, magmas, even though they were contemporaneously emplaced in the same pluton, as is shown by their radiometric ages.

The age of the rocks of the Gringo Gulch pluton is more accurately determined by radiometric methods than by geologic relations. The pluton is known to antedate the Gringo Gulch Volcanics, which are younger than the Josephine Canyon Diorite. Most of the other rocks of the group are found to antedate the Salero Formation, and one of the intrusive masses may antedate the Josephine Canyon

Diorite. An upper age limit cannot be determined from the geologic relations.

Nearly identical radiometric potassium-argon ages of 60 m.y. (Marvin and others, 1973) are obtained from biotite of the microgranodiorite and from hornblende of the hornblende dacite porphyry. No ages were determined on the other rocks of the group.

The Gringo Gulch pluton and the related plug, and possibly also most of the other rocks, are considered to be emplaced penecontemporaneously with the deposition of the Gringo Gulch Volcanics, during the tectonically quiescent interval between the Piman and Helvetian phases of the Laramide orogeny.

GRANITOID ROCKS OF THE HELVETIA STOCKS

During the late Paleocene seven small elliptical stocks, mainly of granodiorite and quartz monzonite, intruded the complexly deformed rocks of the northern part of the Santa Rita Mountains (fig. 40). They underlie areas of about $\frac{1}{4}$ to 2 square miles, and most of them are elongate in a northwest direction. Collectively I refer to the stocks as the Helvetia stocks; individually they include the Helvetia, Shamrod, South Johnson Ranch, and Johnson Ranch stocks of quartz monzonite and granodiorite, the Southeast stock entirely of quartz monzonite, the Huerfano stock wholly of granodiorite, and the Sycamore stock of quartz diorite. Compositionally, most of the rocks are nearly the same despite the different rock names that are applicable, but the quartz diorite is sufficiently different that the Sycamore stock may be a genetically distinct intrusive mass. The stocks were emplaced, approximately contemporaneously, during faulting of the Helvetian phase of the Laramide orogeny (Drewes, 1972b) and before the mineralization of the Helvetia mining district (Drewes, 1973).

The stocks intrude a wide assortment of rocks of Precambrian and Paleozoic ages, and they are covered by much younger gravel deposits. They are also cut by faults, which are intruded by quartz latite porphyry of the Greaterville plugs. The host rocks are metamorphosed, and the zone of metamorphism is wider to the south than to the east, where unaltered Mesozoic rocks have been faulted against the older rocks. Although the intensity of metamorphism does not seem to increase immediately adjacent to the stocks, it does gradually decrease southward about 3 miles away from the stocks. This thermal event may have begun as early as the time of intrusion of the stocks of Helvetia but it probably extended through the time of injection of the plugs of Greaterville as well, and so it is not, strictly speaking, a contact metamorphic effect of one stock.

The intrusive contacts of the Helvetia stocks are mostly straight and are vertical or dip steeply outward. In a few places apophyses of the stocks extend a short distance into

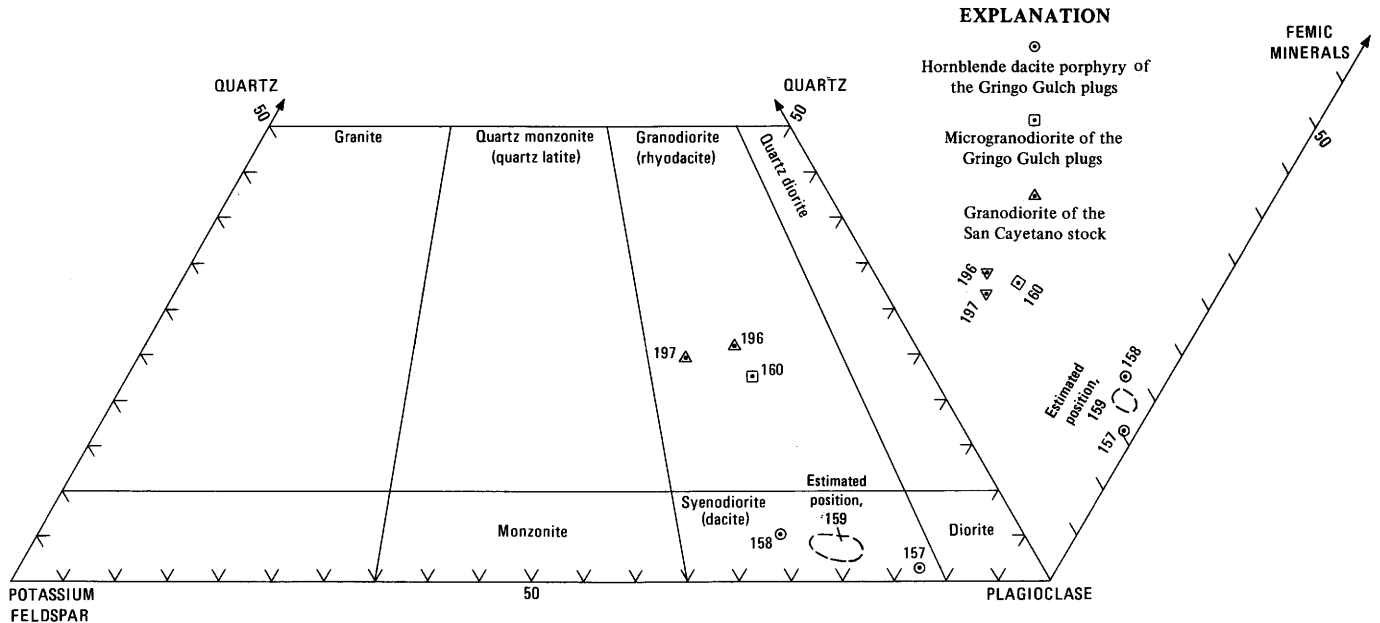


FIGURE 39.—Modified triangular diagram showing modal quartz, potassium feldspar, plagioclase, and feric minerals of rocks of the Gringo Gulch pluton and of the San Cayetano stock.

the host rocks, and, along the east side of the Shamrod stock, a large block of Cambrian Bolsa Quartzite is engulfed in the stock. Chill zones were not found along the margins of the stocks.

PETROGRAPHY

The granitoid rocks of the Helvetia stocks are generally light gray to yellowish gray or light brownish gray, coarse grained, massive, and slightly altered. The quartz monzonite and aplitic rocks of the Southeast stock (fig. 40) are slightly more orange or pink than are the rocks of the other stocks, and the rocks of the Sycamore stock are medium gray to medium greenish gray. Several of the stocks underlie, in part, the pediment at the foot of the mountains where they are deeply weathered. They also underlie some gentle slopes and low hills beneath the more rugged outcrops of Paleozoic rocks. Only the rocks of the Southeast stock and aplitic masses in the Huerfano stock form bold outcrops. The granitoid rocks are cut by widely spaced joints, and, locally, they weather to low rounded bosses or extensive fairly flat surfaces that are separated by abundant grus and overlain by scattered rounded residual blocks. The rocks of most of these stocks are nearly free of inclusions; exceptions are the Shamrod stock, which contains a large engulfed block on the east side, and the Sycamore stock, which contains large masses of Paleozoic rocks and granodiorite. The granitoid rocks are cut by a few widely scattered and mostly small dikes of lamprophyre and aplite (Drewes, 1972b, pl. 5). Huerfano Butte is underlain by the largest of the aplite masses and

the nearby granodiorite is silicified. Other smaller aplite and lamprophyre dikes extend across the contacts of stocks or are entirely within the host rocks near the stocks.

Most of the rocks have a hypidiomorphic-granular texture, a 3 to 7 mm grain size, and slight or no alteration (figs. 41, 42). A trace of microgranophyric texture is present in most specimens, and some of the finer grained rocks are idiomorphic granular or have a mosaic texture. A bimodal distribution of grain size occurs in the specimens of the Southeast stock, in the nearby end of the Helvetia stock, and in the southeast end of the South Johnson Ranch stock. Large irregular intergrowths of quartz in feldspar also are common in specimens from the east end of the Southeast stock. The texture of the Sycamore stock is subophitic and the grain size of the rock is only 0.5 to 3 mm. In a few specimens from the other stocks crystals are as much as 9 mm long, and one specimen has phenocrysts as much as 18 mm long.

The dominant minerals in the granitoid rocks are quartz, plagioclase, potassium feldspar, biotite, and, in the Sycamore stock, hornblende. The quartz is generally anhedral and rarely subhedral, and that of most stocks has little or no undulatory extinction. However, quartz of the South Johnson Ranch stock has moderate to strong undulatory extinction, possibly suggesting that stresses along the faults where the highly elongated stock was emplaced had not been fully relieved at the time of emplacement. The Sycamore stock contains relatively minor amounts of quartz that has a moderate undulatory extinction.

TABLE 17.—*Modes of Gringo Gulch pluton and related plug*

[Field numbers are abbreviated; year of collection and collector's initial omitted. Full field number of specimen 157 thus is 63D199. Symbols: Tr., trace; . . . , not determined]

Rock type	Hornblende dacite porphyry					Micro-granodiorite
Intrusive mass	Pluton			Plug		Pluton
Specimen No.	157		158		159	160
Field No.	199		661		257	281
Quartz	1.3	1.0	4.2	10.8	1.0	19.8
Plagioclase	73.5	5.0	58.6	21.8	10.8	52.1
Orthoclase	9.9	0	18.9	0	0	14.9
Pyroxene (augite?)	5.0	.5	.7	.3	.5	0
Hornblende	3.3	3.3	9.0	5.3	5.8	5.4
Biotite	.9	0	2.4	1.0	0	4.7
Magnetite	5.5	1.2	5.9	2.6	1.4	2.5
Apatite	.6	0	.3	0	0	.4
Sphene	Tr.	0	0	0	0	0
Zircon	0	0	Tr.	0	0	.2
Allanite	0	0	0	0	0	Tr.
Total	100.0	10.0	100.0	31.8	18.5	100.0
Femic	15.3	5.0	18.3	9.2	7.7	13.2
Percent anorthite						
in plagioclase	60—68		0—37		38—55	35—47
(plagioclase rims)	(37)		(24)

¹ Phenocrysts.

The plagioclase varies slightly in habit and composition from stock to stock. It typically forms subhedral grains. Plagioclase of the southern four stocks is slightly and finely perthitic, but that of the other stocks is rarely perthitic. The composition of the plagioclase of the Sycamore stock is andesine, except for the outer zones of some crystals, which are oligoclase. The composition of the plagioclase in the other stocks is oligoclase or albite. Several stocks have only albite or only oligoclase except for the rims of some crystals, but the Helvetia stock has oligoclase in some specimens and albite in others, perhaps suggesting an incompletely diagenetic alteration. Sericite and clay-minerals alteration products are generally sparse.

The potassium feldspar also has variable features in the stocks of Helvetia. It generally forms anhedral to subhedral crystals. The Southeast stock has only orthoclase, the Huerfano and Helvetia stocks have both orthoclase and microcline(?), and the Shamrod, South Johnson Ranch, and Johnson Ranch stocks have only microcline(?). The identity of the microcline is in doubt because the grid twinning is very blurred, perhaps because it is partly obliterated. Both kinds of potassium feldspar occur in accessory amounts in the Sycamore stock. Lace and patch types of perthite are about equally abundant, and kaolinite alteration is typically slight.

The biotite generally occurs in subhedral and partly chloritized crystals that are pleochroic in yellow brown to dark brown. Several specimens from the South Johnson Ranch stock that have a bimodal grain size contain small biotite crystals in aggregates, suggesting that they were probably recrystallized. The biotite of one specimen of the Sycamore stock is pleochroic in yellow brown to dark olive

TABLE 18.—*Chemical and spectrographic analyses and CIPW norms of the Gringo Gulch pluton*

[Chemical analyses by rapid rock method (Shapiro and Brannock, 1962), with specimen 157 supplemented by X-ray method. Chemical analysts: Lowell Artis, S. D. Botts, G. W. Chloé, P. L. D. Elmore, and H. Smith. Spectrographic analyses by semiquantitative method. Spectrographic analyst, J. C. Hamilton. Elements looked for but not found: Ag, As, Au, B, Bi, Cd, Ce, Eu, Ge, Hf, Hg, In, Li, Mo, Nd, Pd, Pr, Pt, Re, Sb, Sm, Sn, Ta, Te, Th, Tl, U, W, and Zn]

Rock type	Hornblende dacite porphyry		Microgranodiorite
	157	160	
Specimen No.	199	281	
Field No.			
Chemical analyses (weight percent)			
SiO ₂	59.0	66.9	
Al ₂ O ₃	16.3	15.9	
Fe ₂ O ₃	3.4	2.7	
FeO	2.8	1.4	
MgO	2.6	1.4	
CaO	4.7	2.8	
Na ₂ O	4.4	4.0	
K ₂ O	2.4	3.2	
H ₂ O–	1.1	.36	
H ₂ O+	1.4	.90	
TiO ₂98	.56	
P ₂ O ₅21	.18	
MnO14	.06	
CO ₂12	.10	
Total	100	100	
Spectrographic analyses (weight percent)			
Ba	0.05	0.15	
Be0002	0	
Co	0	.0007	
Cr	0	.001	
Cu001	.01	
Ga002	.003	
La	0	.005	
Nb003	0	
Ni	0	.0007	
Pb002	.007	
Sc	0	.0007	
Sr003	.07	
V	0	.01	
Y0015	.002	
Yb0003	.0002	
Zr007	.007	
CIPW norms			
Q	11.5	24.1	
C	0	1.0	
or	14.2	18.9	
ab	37.2	33.8	
an	17.6	12.1	
di { wo	1.5	0	
en	1.1	0	
fs17	0	
hy { en	5.3	3.5	
fs80	0	
mt	4.9	3.1	
hm	0	.57	
il	1.9	1.1	
ap50	.43	
cc27	.23	
Total	96.9	98.8	
Femic	16.4	8.9	

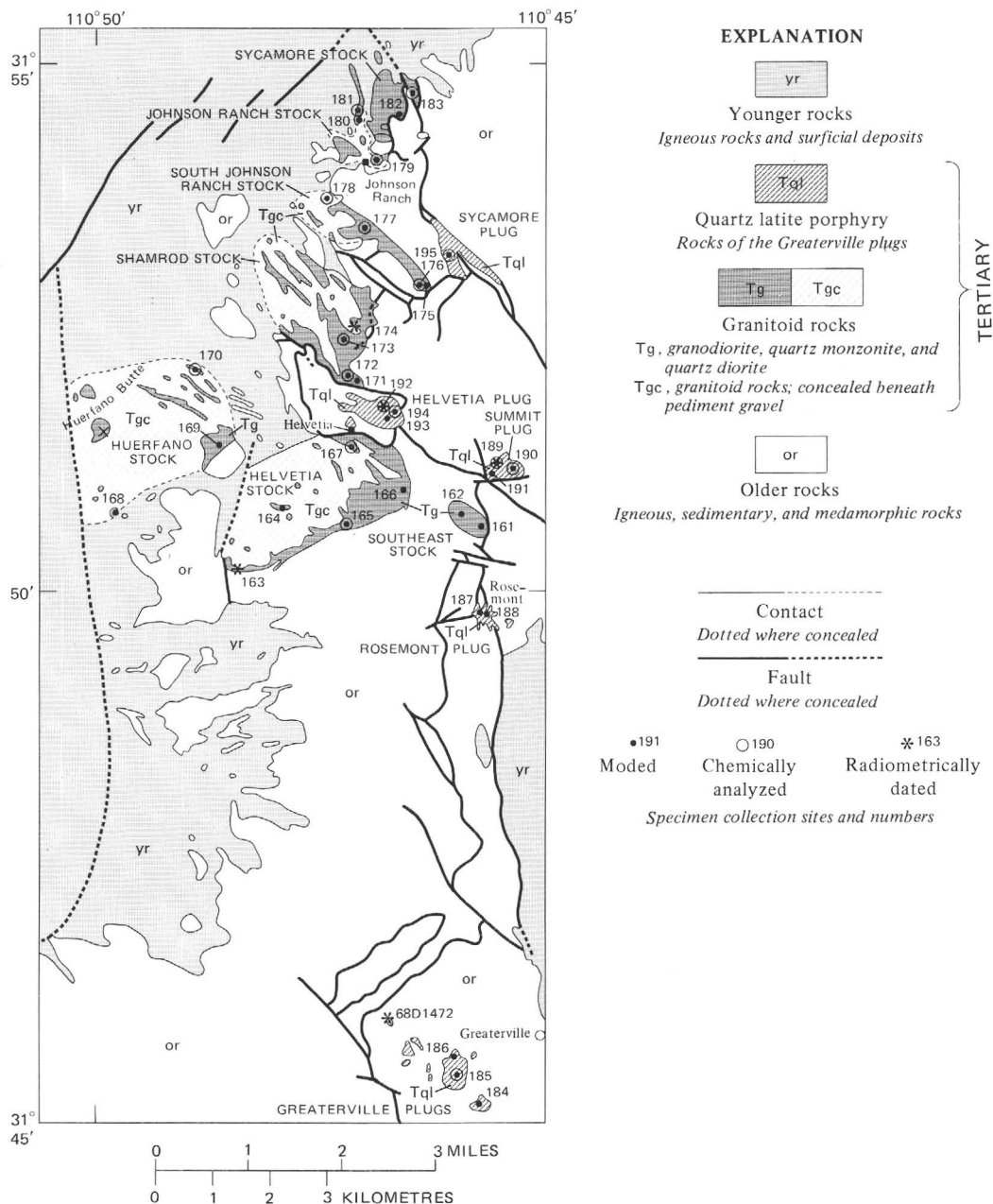


FIGURE 40.—Distribution of granitoid rocks of the Helvetia stocks and Greaterville plugs and specimen collection sites.

brown. Penninitic chlorite alteration seems to be slightly more common in the northern part of the stock than in the southern part.

The hornblende of the Sycamore stock and that of one specimen of the South Johnson Ranch stock is euhedral to subhedral, and it is pleochroic in blue green or moderate green to olive green or olive brown.

Accessory minerals of the Helvetia stocks commonly include magnetite, apatite, sphene, and zircon. These minerals are more abundant in the rocks of the Sycamore stock than in the other rocks. A few specimens from the

Southeast stock and Shamrod stock contain trace amounts of allanite and tourmaline.

MODAL AND CHEMICAL SUMMARY

The modal composition of 23 specimens of the Helvetia stocks are shown in table 19 and are summarized on the modified triangular diagram of figure 43. The figure drawn around the entire suite of modes forms an irregular-shaped flattened body superficially similar to that representing the modes of the Josephine Canyon Diorite

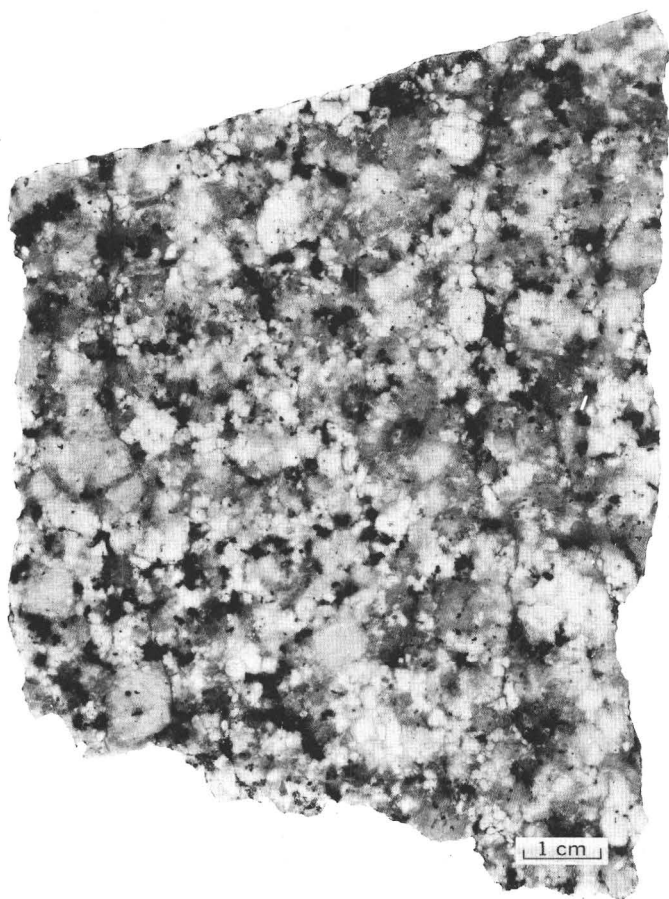


FIGURE 41.—Specimen 174. Quartz monzonite of the Helvetia stocks.

(fig. 26). However, viewed in more detail, the modes of the Helvetia rocks form two clusters, one representing quartz diorite of the Sycamore stock and a second representing the other stocks. The modes of the Josephine Canyon Diorite, in contrast, spread uniformly throughout the circumscribed figure, and so they are believed to be of rocks derived from rather closely associated magmas or perhaps differentiates of a single magma. The Helvetia rocks seem to require a derivation from two magmas that are either unrelated or only distantly related.

A figure drawn around the modes of all the rocks except those of the Sycamore stock forms a nearly hemispherical body flattened against the leucocratic face of the composition tetrahedron and centered along the boundary between the quartz monzonite and granodiorite fields. In shape and position this figure is about midway between those of the Elephant Head Quartz Monzonite (fig. 36) and the Madera Canyon Granodiorite (fig. 31).

Chemical and spectrographic analyses and CIPW norms of 11 of the moded specimens of the Helvetia stocks are assembled in table 20 and are summarized in the histogram of figure 10G. The chemical similarity of these rocks and the quartz latite porphyry of the Greaterville plugs (fig.



FIGURE 42.—Specimen 174. Quartz monzonite of the Helvetia stocks. Crystals: quartz (Q), plagioclase (P), microcline (M), biotite (B), ilmenitic magnetite (im), and sphene (S). Plain light; $\times 20$.

10H) is discussed in the description of that porphyry. In content of total iron and MgO, the rocks of the Helvetia stocks are approximately the same as the granite and quartz monzonites of the Santa Rita Mountains (figs. 10I–10K); the content of Na_2O and K_2O resembles that of some granodiorite (fig. 10D), and the content of CaO is intermediate between that of the two rock groups. The chemistry of these granitoid rocks, exclusive of the quartz diorite of the Sycamore stock, is somewhat similar to Nockolds' (1954, p. 1014) average adamellite and muscovite-biotite granodiorite, but the silica and the calc-alkali components do not closely match.

AGE AND CORRELATION

Through geologic relations with other rocks, the Helvetia stocks are dated as Cretaceous or Paleocene. The stocks postdate the Willow Canyon Formation of the Bisbee Group, for an apophysis of the Johnson Ranch stock intrudes this formation, and it also intrudes some old faults of the Helvetian phase of the Laramide orogeny, one-third mile northeast of the Johnson Ranch (Drewes,

TABLE 19.—*Mode of granitoid rocks*

[Field numbers are abbreviated; year of collection and collector's initial omitted. Full field number of

Rock type	Aplitic quartz monzonite			Dominantly granodiorite						Granodiorite				Dominantly quartz monzonite	
Intrusive mass	Southeast stock			Helvetia stock						Huerfano stock				Shamrod stock	
Specimen No.	161	162	161,162 Mean	163	164	165	166	167	163—167 Mean	168	169	170	168—170 Mean	171	172
Field No.	1143	1155		1051	1107	1054	1190	1163		1426	1109	1403		1168	1313
Quartz	35.2	31.7	33.5	27.7	23.6	31.9	29.5	34.9	29.5	26.1	25.7	34.0	28.6	19.1	23.0
Plagioclase, total	31.8	45.8	38.8	50.9	49.7	43.7	47.7	46.8	47.8	48.8	48.9	47.7	48.5	54.1	42.6
(plagioclase in															
perthite)	(1.9)	(0.2)	(1.1)	(0.4)	(0.9)	(0.6)	0	(1.8)	(0.7)	0	(0.8)	0	(0.3)	(4.4)	(4.5)
K-feldspar, total	30.8	18.4	24.6	19.7	25.2	21.6	20.2	15.4	20.4	21.2	20.8	15.3	19.1	24.6	32.1
(orthoclase)	(30.8)	(18.4)	(24.6)	(18.9)	(25.2)	(21.6)	0	0	(13.1)	(21.2)	¹ (20.8)	0	(14.0)	0	0
(microcline?)	0	Tr.	Tr.	(0.8)	Tr.	0	(20.2)	(15.4)	(7.3)	0	Tr.	(15.3)	(5.1)	(24.6)	(32.1)
Biotite	1.7	2.9	2.3	1.3	1.3	1.8	2.4	2.3	1.8	3.2	3.6	2.0	2.9	1.6	1.3
Amphibole	0	0	0	0	0	0	0	0	0	0	0	0	0	0	0
Magnetite	.3	1.0	.7	.2	.2	.7	.1	.5	.3	.5	.6	.7	.6	.4	.8
Apatite	Tr.	.2	.1	.05	.05	.3	Tr.	.1	.1	.05	.2	.2	.2	.1	.2
Sphene	.1	Tr.	.05	.2	0	.05	.05	Tr.	.05	.05	.1	.1	.1	.05	.05
Zircon	.1	Tr.	.05	Tr.	0	Tr.	.05	Tr.	Tr.	.1	Tr.	Tr.	.05	.05	0
Allanite	0	Tr.	Tr.	0	0	0	0	0	0	0	.1	0	.05	0	0
Tourmaline(?)	0	Tr.	Tr.	0	0	0	0	0	0	0	0	0	0	0	0
Total	100.0	100.0	100.1	100.05	100.05	100.05	100.0	100.0	99.95	100.0	100.0	100.0	100.1	100.0	100.05
Femic	2.2	4.1	3.2	1.7	1.5	2.8	2.6	2.9	2.3	3.9	4.6	3.0	3.9	2.2	2.3
Percent anorthite in plagioclase (plagioclase rims)	0—5?	30		13—30	5—10	(5—10)	25—31	25	25—30	5—10	27	29	27—29 (5—10)		12
Quartz mixing index (see text)				.87	.77	.99	.82	.69	.83	.82	.70	.79	.77	.75	.44

¹ Modal orthoclase, specimen 169, includes some sanidine (?).

1972b, pl. 5). In one place, a half a mile east of Helvetia, and in another place, extending from about a mile southeast to about a mile northeast of the ranch, faults that cut the Helvetia stocks are intruded by plugs of quartz latite porphyry of late Paleocene age.

A more definite age of the stocks is provided by radiometric dating (table 4). Replicate potassium-argon ages of biotite from specimen 163 date the Helvetia stock as 53.5 m.y., or late Paleocene. A single age determination of biotite from specimen 170 dates the Shamrod stock as 53.9 m.y. (Marvin and others, 1973), an age nearly identical to those of the Helvetia stock and well within the limitations of the analytical method.

Plutonic rocks of the same age as the Helvetia stocks have not been identified in the ranges next to the northern part of the Santa Rita Mountains. The batholith-sized body of Ruby Star Granodiorite of the Sierrita Mountains (fig. 1) is somewhat similar to the rocks of the Helvetia stocks but is at least 5 m.y. older (Cooper, 1974). The rocks of the Helvetia stocks, other than the Sycamore stock, are similar to the quartz latite porphyry of the Greaterville plugs in the content of major elements and in age but differ in the content of some trace elements and in texture. These differences apparently have economic significance, for, although these two groups of intrusives are largely coextensive, the Helvetia stocks are not genetically associated with mineralization, whereas the Greaterville plugs are.

The Helvetia stocks were probably emplaced passively from a viscous magma during late Laramide orogenic times. Stopping accompanied the emplacement of the Shamrod and Sycamore stocks, but indications of stopping

are lacking in the others. The viscous or dry aspect of the magma is indicated by the straight-trending contacts and elliptical shape of the stocks, as well as by the absence of signs of mineralizing fluids. The host rocks were probably metamorphosed beginning at the time of emplacement of the Helvetia stocks, and the cooling may have taken place after the the intrusion of the Greaterville plugs. This timing is suggested by the coextensive distribution of much of the metamorphic terrane with the stocks and with most of the plugs, as well as by the widespread occurrence of radiometric dates of 55 m.y. in the stocks, plugs, and recrystallized biotite of the metagranodiorite host rock (table 4, specimen 19). The area may also have been strongly uplifted and deeply eroded concurrently with the Helvetian phase of faulting, for, whereas the Helvetia stocks are coarse grained, only slightly younger rocks of the Greaterville plugs are fine grained.

QUARTZ LATITE PORPHYRY OF THE GREATERVILLE PLUGS

In the northern part of the Santa Rita Mountains, eight plugs and many smaller masses of quartz latite porphyry were intruded during late Paleocene time (fig. 40). This rock is locally known as the "ore porphyry" for its close association with mineralization in the Greaterville and Helvetia mining districts of the Santa Rita Mountains and in the mining districts of other mountain ranges of this part of Arizona. The quartz latite porphyry forms ameboid-shaped masses and is distinctive in its habit and appearance. It is finely granular and porphyritic and contains fairly abundant small biotite (or chlorite) crystals and bipyramidal quartz phenocrysts. The plugs and

of the Helvetia stocks

specimen 161 thus is 66D1143. Symbols: s, standard deviation; Tr., trace; . . . , not determined]

Dominantly quartz monzonite—Continued			Granodiorite and quartz monzonite									Quartz diorite				161—180 Mean s	
Shamrod stock—Continued			South Johnson Ranch stock					Johnson Ranch stock			Sycamore stock						
173	174	171—174 Mean	175	176	177	178	175—178 Mean	179	180	179,180 Mean	181	182	183	181—183 Mean			
1337	1612		1225	1286	1375	1392a		1390	1406a		1406b	1402	1404				
23.0	24.5	22.4	27.5	33.0	29.8	30.8	30.3	37.9	24.2	31.1	10.3	9.1	15.0	11.5	28.1	5.0	
44.0	41.6	45.6	52.9	38.4	45.7	35.9	43.2	33.3	44.7	39.0	50.2	52.1	57.2	53.2	45.4	5.6	
(2.9)	(7.5)	(4.8)	(1.8)	0	0	0	(0.5)	0	0	0	0	0	0	0	(1.4)	(2.1)	
30.0	30.0	29.2	15.1	23.2	13.0	24.9	19.1	26.4	19.7	23.1	1.4	.8	4.0	2.1	22.1	5.5	
0	0	0	0	0	0	0	0	0	0	0	0	0	(4.0)	(1.3)	(6.0)	(10.0)	
(30.0)	(30.0)	(29.2)	(15.1)	(23.2)	(13.0)	(24.9)	(19.1)	(26.4)	(19.7)	(23.1)	(1.4)	(0.8)	0	(0.7)	(16.2)	(11.6)	
2.6	3.3	2.2	4.2	5.0	10.1	8.0	6.8	2.1	8.9	5.5	16.0	0	14.9	10.3	3.6	2.7	
0	0	0	0	0	0	0	0	0	1.0	.5	19.0	34.3	6.7	20.0	Tr.	
.2	.3	.4	.2	.3	1.1	.2	.5	.2	.5	.4	1.2	1.8	1.3	1.4	.4	.3	
.2	.2	.2	.05	.05	.2	.2	.1	.05	.3	.2	.7	.5	.2	.5	.1	.1	
.05	.05	.05	.05	Tr.	0	0	Tr.	.05	.7	.4	1.2	1.4	.6	1.1	.1	.2	
0	.05	Tr.	Tr.	.05	.1	Tr.	Tr.	.05	.05	.05	.05	.05	.05	.05	.03	.03	
0	0	0	0	0	0	0	0	0	0	0	0	0	0	0	Tr.	
Tr.	0	Tr.	0	0	0	0	0	0	0	0	0	0	0	0	Tr.	
100.05	100.0	100.05	100.0	100.0	100.0	100.0	100.0	100.05	100.05	100.2	100.05	100.05	99.95	100.2	99.83		
3.0	3.9	2.9	4.5	5.4	11.5	8.4	7.4	2.4	11.4	7.1	38.1	38.0	23.8	33.4	4.2	3.0	
15	12—15	24—27	24—29	27	14—17	14—29	13	27—30	27—30	50	32?	33—37	32—50	5—30	
.....	(5—10)	(5—10)	(25)	(24)	(25)	(5—10)	
.85	.98	.76	.80	.49	.65	.96	.73	.95	.61	.78	.96	.92	.89	.92	.77	.16	

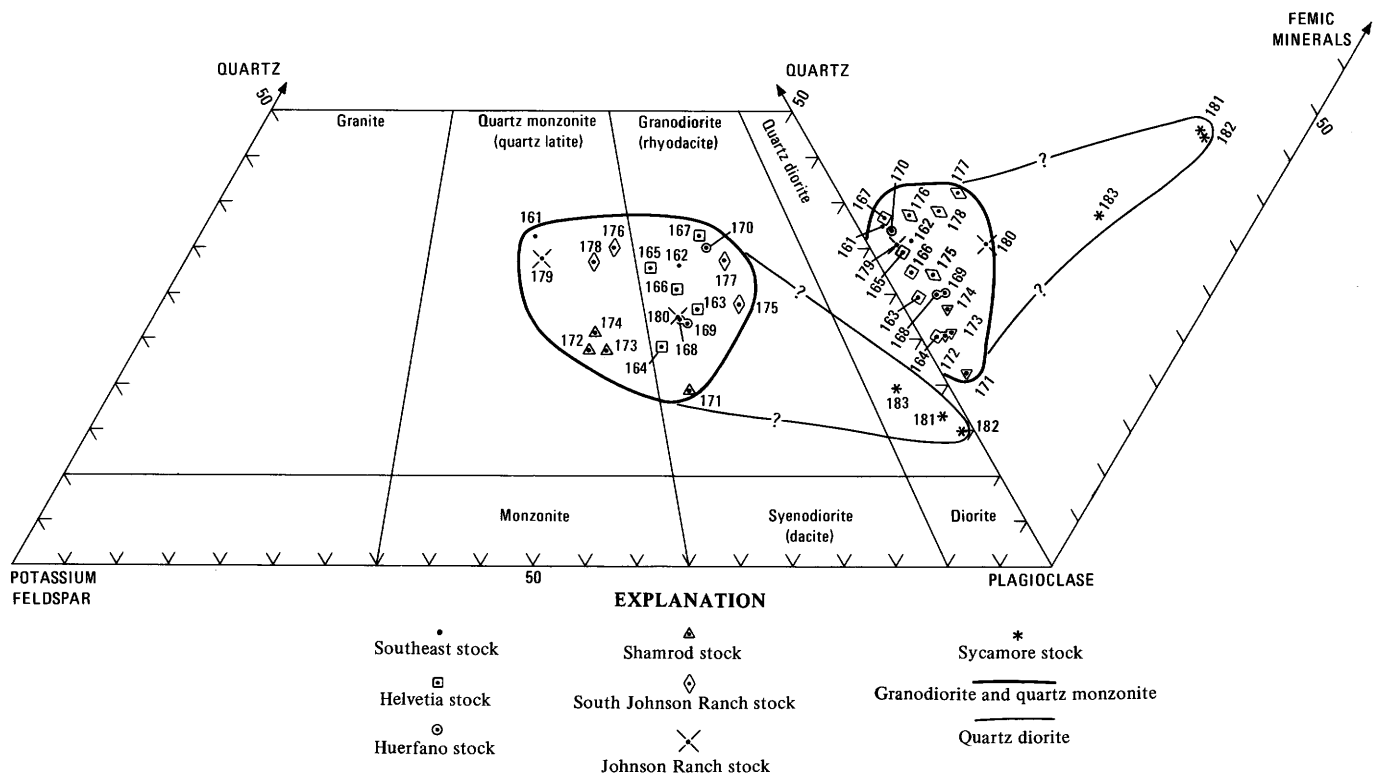


FIGURE 43.—Modified triangular diagram showing modal quartz, potassium feldspar, plagioclase, and femic minerals of the granitoid rocks of the Helvetia stocks

related smaller intrusive masses are collectively herein referred to as the Greaterville plugs.

A cluster of plugs, small pipes, and dikes intrude the Willow Canyon and Apache Canyon Formations of the Bisbee Group in the Greaterville area. The cluster is

elongated with its long axis oriented northwest along the Boston syncline, which is interpreted to be a disharmonic structure within the upper plate of a thrust fault that extends northward beyond the Helvetia area. This cluster of intrusive bodies is surrounded by a zone of contact-

TABLE 20.—*Chemical and spectrographic analyses and CIPW norms of granitoid rocks of the Helvetia stocks*

[Chemical analyses of specimens 167, 173, 178, and 181 by rapid rock method (Shapiro and Brannock, 1962), supplemented by atomic absorption method; other specimens analyzed by single solution method (Shapiro and Massoni, 1968). Chemical analysts: Lowell Artis, S. D. Botts, G. W. Chloe, P. L. D. Elmore, John Glenn, J. Kelsey, and H. Smith. Spectrographic analyses by semiquantitative method. Spectrographic analysts: W. B. Crandell and J. L. Harris. Elements looked for but not found: As, Au, B, Bi, Cd, Eu, Ge, Hf, Hg, In, Li, Nd, Pd, Pr, Pt, Rb, Sb, Sm, Sn, Ta, Te, Th, Ti, U, W, and Zn. Symbols: s, standard deviation; <, less than; . . . , not determined; Tr., trace]

Rock type	Granodiorite and quartz monzonite											Quartz diorite			Granodiorite and quartz monzonite		
Intrusive mass	Helvetia stock			Huerfano stock	Shamrod stock			South Johnson Ranch stock			Johnson Ranch stock	Sycamore stock					
Specimen No.	165	167	165,167 Mean	170	172	173	172,173 Mean	176	177	178	176—178 Mean	179	181	183	181,183 Mean	165—179 Mean	s
Field No.	1054	1163		1403	1313	1337		1286	1375	1392a		1390	1406b	1404			
Chemical analyses (weight percent)																	
SiO ₂	71.1	72.8	72.0	71.9	71.9	71.8	71.9	72.5	71.2	72.3	72.0	73.1	55.4	56.4	55.4	72.9	0.7
Al ₂ O ₃	15.1	14.6	14.9	15.2	15.0	15.9	15.5	14.2	14.3	14.7	14.4	14.8	16.9	16.0	16.5	14.9	.5
Fe ₂ O ₃	.94	.96	.95	.50	.68	.78	.73	.54	1.0	.53	.69	.30	2.9	3.5	3.2	.69	.2
FeO	.60	.40	.50	.64	.56	.56	.56	.96	1.5	.96	1.1	.64	5.7	4.6	5.2	.76	.3
MgO	.43	.33	.38	.35	.25	.36	.31	.58	1.0	.46	.68	.36	4.3	3.3	3.8	.46	.2
CaO	1.6	1.4	1.5	2.3	2.0	1.7	1.9	2.3	3.1	1.9	2.4	1.9	6.2	6.3	6.3	2.0	.5
Na ₂ O	4.5	4.1	4.3	4.3	4.3	4.6	4.5	3.4	3.0	3.6	3.3	3.9	3.4	2.8	3.1	4.0	.5
K ₂ O	4.0	4.0	4.0	3.7	4.1	3.4	3.8	4.0	3.2	4.0	3.7	3.7	2.2	2.8	2.5	3.8	.3
H ₂ O—	.12	.14	.13	.20	.11	.13	.12	.21	2.0	.10	.77	.36	.18	.33	.26	.37	.6
H ₂ O+	1.0	.37	.69	.51	.58	.46	.52	.79	.78	.44	.67	.74	.75	1.5	1.1	.63	.2
TiO ₂	.23	.12	.18	.20	.20	.14	.17	.23	.35	.16	.25	.17	1.1	1.1	1.1	.20	.07
P ₂ O ₅	0	.06	.03	.10	.08	.06	.07	.11	.18	.08	.12	.05	.23	.36	.30	.08	.05
MnO	.11	.05	.08	0	.07	.06	.07	.07	.12	.06	.08	.02	.17	.08	.13	.06	.04
CO ₂	.08	<.05	<.05	<.05	<.05	<.05	<.05	.10	<.05	<.05	<.05	<.05	<.05	.94	.47	<.05	<.05
Total	100	99	100	100	100	100	100	100	100	99	100	100	99	100	99	100
Spectrographic analyses (weight percent)																	
Ag	0	0	0	<0.0001	<0.0001	0	<0.0001	<0.0001	<0.0001	0	<0.0001	<0.0001	0	<0.0001	<0.0001	<0.0001
Ba	.15	.07	.1	.07	.07	.07	.07	.07	.07	.1	.08	.07	.07	.07	.07	.08	.03
Be	.0003	.0002	.0003	.0003	.0002	.0003	.003	.0002	.0002	.0003	.0002	.0003	.0001	.0001	.0001	.0003	.0001
Ce	.01	0	.005	.01	.01	.05	.03	0	0	.02	.01	.01	.01	.01	.01	.01	.02
Co	.0003	0	.00015	0	0	0	0	0	0	0	0	0	.003	.002	.003	Tr.
Cr	<.0003	0	0	0	0	0	0	0	0	.0003	.0001	0	.0015	.0015	.0015	Tr.
Cu	.001	.0002	.0006	.0007	.0003	.0002	.0003	.003	.001	.0001	.001	.0005	.02	.01	.015	.0008	.0009
Ga	.0015	.0015	.0015	.001	.001	.0015	.001	.001	.001	.0015	.001	.001	.002	.001	.0015	.001	.0003
La	.007	0	.004	.007	.007	.02	.015	0	.007	.007	.005	.007	.005	.007	.006	.007	.006
Mo	0	0	0	0	0	0	0	0	0	0	0	0	.0003	0	.0002	0
Nb	.0007	.001	.0009	.002	.001	.001	.001	.001	.001	.001	.001	.001	0	.0007	.0004	.001	.0004
Ni	0	0	0	0	0	0	0	0	0	0	0	0	.005	.003	.004	0
Pb	.0015	.0007	.001	.0005	.001	.0007	.0009	.001	.001	.002	.001	.003	.0003	.001	.0007	0
Sc	.0005	.0003	.0004	0	0	.0003	.0002	.0003	.0003	.001	.0005	0	.002	.001	.0015	.0003	.0003
Sr	.007	.05	.06	.03	.02	.05	.04	.015	.02	.03	.02	.03	.1	.05	.08	.03	.01
V	.0015	.0015	.0015	.0007	.001	.0015	.001	.0015	.002	.002	.002	.0007	.02	.01	.015	.001	.0005
Y	.0015	.002	.002	.003	.002	.002	.002	.003	.003	.003	.003	.003	.005	.003	.004	.003	.0008
Yb	.00015	.0002	.0002	.0003	.0002	.0002	.0002	.0003	.0003	.0003	.0003	.0003	.0005	.0003	.0004	.0003	.00006
Zr	.01	.007	.009	.015	.01	.007	.009	.005	.01	.007	.007	.01	.007	.02	.01	.009	.003
CIPW norms																	
Q	26.0	30.6	27.5	26.8	28.0	31.7	33.3	31.3	31.6	6.3	12.8
C	.41	1.230	.16	1.859	.81	1.3	1.2	0	0
or	23.9	23.8	21.9	24.3	20.1	23.6	18.9	23.8	21.8	13.1	16.5
ab	38.8	34.9	36.4	36.4	38.9	28.8	25.4	30.7	33.0	28.9	23.7
an	8.1	6.3	10.4	9.1	7.7	10.1	13.9	8.6	8.8	24.5	22.8
wo	0	0	0	0	0	0	0	0	0	1.9	.06
en	0	0	0	0	0	0	0	0	0	1.1	.04
fs	0	0	0	0	0	0	0	0	0	.70	.02
hy	1.1	.8387	.62	.90	1.4	2.5	1.290	9.6	8.2
fs	0	043	.27	.26	1.1	1.6	1.268	5.9	3.9
mt	1.4	1.173	.99	1.178	1.5	.7744	4.2	5.1
hm	0	.20	0	0	0	0	0	0	0	0	0
il	.46	.2338	.38	.2744	.67	.3132	2.1	2.1
ru	0	0	0	0	0	0	0	0	0	0	0
ap	0	.1424	.19	.1426	.43	.1912	.55	.85
cc	0	.1111	.11	.1123	.11	.1111	.11	2.1
Total	100.2	99.4	99.3	99.3	99.3	99.0	99.1	99.5	99.0	99.0	98.2
Femic	3.0	2.6	2.8	2.6	2.8	4.2	6.8	3.8	2.6	26.2	22.4

metamorphosed rocks about 1 mile wide and 2 miles long. The shale and siltstone of the Cretaceous formations are hornfelsed, the intercalated calcareous beds are altered to calc-silicate rock, and the arkose and conglomerate beds are also altered.

Other plugs and dikes of quartz latite porphyry intrude complexly faulted Paleozoic and Cretaceous rocks in the

Helvetia mining district (Drewes, 1972b, pl. 5). The plugs of this group are fairly widely scattered and are not controlled by a single structural feature as they are in the Greaterville area, but some of the plugs intrude northwest-trending faults. In plan, the plugs have an irregular shape, and many of their apophyses intrude faults. The host rocks of the intrusives in the Helvetia area

are also metamorphosed, except for the rocks east of the plugs near the Johnson Ranch, near collection sites 183 and 195. Metamorphosed Paleozoic rocks are typically altered to marble or tactite, and the Cretaceous rocks, mostly arkosic siltstone and sandstone of the Willow Canyon Formation, are locally hornfelsed and are widely and strongly argillitized and weakly mineralized.

The larger of the two plugs in the Rosemont area (fig. 40) underlies a basin in which the traces of many faults converge. The many apophyses of this plug and the surrounding dikes suggest that the magma was fairly fluid and that it readily spread along the available planes of weakness. It may also have spread laterally along the thrust fault beneath the Cretaceous rocks, as was suggested in the Greaterville district (Drewes, 1970, p. A10). Both the abundance of tactite and the intensity of mineralization and argillitization increase near the plug, and tactite and mineral deposits occur along the faults in the Paleozoic rocks near the plugs (Drewes, 1973a, figs. 3–13). The rocks in the Rosemont area of the Helvetia mining district have over the years been extensively explored for economic deposits of copper, lead, zinc, and silver.

Another plug in the Helvetia area, the Summit plug, underlies a knoll along the crest of the range near the intersection of many faults. Unmapped roads cross the crest of the range north and south of the plug. Although the Summit plug underlies steep slopes and cliffs, the terrain is less rugged than that underlain by the Precambrian and Cambrian rocks to the south. A breccia pipe lies along a fault on the south side of the plug and an apophysis of the plug extends along part of the fault. Tactite occurs in favorable rock around the plug, and some of the tactite and other rocks along faults near the plug are mineralized. Creasey and Quick (1955) described a small copper deposit in the breccia pipe.

The Helvetia plug intrudes altered Paleozoic and Cretaceous rocks of a large klippe and also Precambrian rocks beneath the klippe near Helvetia townsite. The plug underlies moderately low areas containing small outcrops. The plug is inferred to have intruded a major northwest-trending fault overlain by the klippe, and it probably spread along the thrust fault beneath the klippe. The field relations, described in detail elsewhere (Drewes, 1972b), show that the plug antedates the klippe, although Heyman (1958) and Michel (1959) each interpreted the plug to be part of the klippe and to be rooted 1½ miles to the southeast at the Summit plug. Copper ore has been mined from tactite and from highly mineralized faults at several localities near the Helvetia plug.

The Sycamore plug, not to be confused with the Sycamore stock (fig. 40), differs slightly from the other plugs, but it is categorized with them because the differences could be explained by a local variation in the environment of emplacement. The plug underlies

moderately low hills, where it primarily intrudes a major northwest-trending fault (Drewes, 1972b, pl. 5). Some apophyses of the plug intrude this fault for several miles, and a small pipe of quartz latite porphyry lies along the northern extension of this fault. Some rocks of the dike northwest of the plug are brecciated, indicating minor fault movement after the emplacement of the dike. A few outcrops of tactite lie west of the plug and the rocks of this area contain few visible copper minerals, but analyses show that the content of gold and silver of these rocks is greater than it is in rocks near the other plugs (Drewes, 1973, p. 5).

PETROGRAPHY

The quartz latite porphyry of the Greaterville plugs is a rather distinctive rock, and the local term "ore porphyry" is applied even where the rocks are unmineralized. Indicators of the ore porphyry include fairly abundant, moderately large, doubly terminated or bipyramidal quartz phenocrysts and small biotite or chlorite crystals. The rock is typically pale yellowish brown to light gray, and is closely fractured, and is considerably altered. Because of the rapid weathering favored by this fracture habit, the rock mostly underlies gentle hills or basins in which outcrops are small and the slopes are covered with small blocky detritus. Iron oxides stain many of the fracture surfaces, and scattered grains of pyrite, chalcopyrite(?), and some copper oxides are disseminated in the rock. Although most of the fractured and weakly mineralized rocks are deeply weathered, some are fresh and contain unaltered primary biotite and feldspar crystals with lustrous cleavage surfaces.

The rocks of the Sycamore plug (fig. 40) differ slightly in appearance from the others in that some are pale pink or pale purple and in that they contain fewer phenocrysts and little or no biotite. Furthermore, rocks from the core of the plug are moderately coarse grained rather than aphanitic. The relations between the coarse core rock and the surrounding aphanitic rock are uncertain; as mapped and described herein, they are considered to be gradational, but it is also possible that the plug is a composite body having a core of quartz monzonite related to the Helvetia stocks and a rim of quartz latite porphyry.

Under the microscope the quartz latite porphyry is seen to consist of about 30 percent (common range 20 to 40 percent) phenocrysts 2 to 5 mm, rarely as much as 8 mm, long (fig. 44) and of about 70 percent groundmass, mostly of a 0.02-mm size. The groundmass has an idiomorphic-granular texture and is considerably altered to clay minerals. The texture of the core rocks of the Sycamore plug is hypidiomorphic granular, and its grain size is 2 to 9 mm. The dikes near this plug have a cryptocrystalline texture, and some specimens have a cataclastic texture.

The dominant minerals of the quartz latite porphyry are



FIGURE 44.—Specimen 185. Quartz latite porphyry of the Greaterville plugs showing porphyritic texture and fine-grained groundmass. Crystals: quartz (Q), biotite (B), chloritized biotite (cb), plagioclase (P), potassium feldspar (pf), apatite (ap), and magnetite (mt). Plain light; $\times 25$.

quartz, plagioclase, potassium feldspar, and biotite. The quartz phenocrysts are mostly equant and euhedral, but some specimens also have a few partly resorbed, embayed, and rounded crystals; all are nearly without undulatory extinction. Groundmass quartz is anhedral and also free of undulatory extinction, except in the specimens having cataclastic texture. These specimens also have some quartz in pods along shear or flow bands. Plagioclase occurs as subhedral to euhedral phenocrysts and anhedral groundmass crystals that are much altered to sericite and clay minerals. Compositional zoning is emphasized by variations in the intensity of alteration. The composition of the plagioclase in the plugs in the Helvetia area is mostly andesine with rims of oligoclase. The composition of the plagioclase in the plugs in the Greaterville area is labradorite with rims of andesine; a few specimens are albitized. Plagioclase from the moderately coarse-grained rock of the core of the Sycamore plug is oligoclase; plagioclase from the surrounding rock cannot be

determined petrographically, because of the fine grain size and the intensity of the alteration. Potassium feldspar is mostly in the groundmass as kaolinitized anhedral crystals, but in some specimens it occurs as larger subhedral grains with poikilitic rims. The potassium feldspar in specimens from the Greaterville area and the Rosemont plug is orthoclase, whereas that in specimens from the other plugs is, at least in part, sanidine. About half the specimens contain trace amounts of perthitic intergrowths that commonly form a fine lacy texture; in one specimen such intergrowths form a reticulate texture. Biotite is pleochroic in pale yellow brown to dark brown, and in most specimens it is largely chloritized. Oxybiotite, pleochroic in reddish brown, occurs in two specimens from widely separated plugs.

The accessory minerals are magnetite, apatite, sphene, and zircon, and, in some specimens, pyrite, allanite, and rutile. The pyrite, like magnetite, occurs in scattered crystals, and may be primary, even though in the more mineralized rock it includes secondary grains and veinlets.

Secondary minerals are mainly clay minerals, sericite, and chlorite, and, in lesser amounts, iron oxide, leucoxene, epidote, and, in one specimen possibly tremolite. The more intensely mineralized porphyry contains traces of copper oxides, chalcopyrite, pyrite, galena, cerussite, and possibly sphalerite.

MODAL AND CHEMICAL SUMMARY

Modes of 12 specimens of quartz latite porphyry are listed in table 21 and are summarized on the modified triangular diagram of figure 45. The figure drawn around the tightly clustered plots of the modes of the porphyry resembles an ellipsoid which is centered about a point in the right half of the quartz monzonite field and almost 5 percent of the way from the leucocratic face of the composition tetrahedron toward the femic apex. Specimen 186 seems to be anomalous in plagioclase for this group of modes, but more analyses are needed to properly assess its position on the diagram. The modes of this formation about 5 percent higher in potassium feldspar than those of the Helvetia stocks.

Chemical analyses of six specimens are listed in table 22 and are summarized in the histogram of figure 10H. The slightly greater abundance of CaO and Na₂O and lesser amounts of SiO₂ in specimen 184, from a plug in the Greaterville area, than in the specimens from the plugs in the Helvetia area is reflected in the slight difference in the modes of these rocks. The quartz latite porphyry of these plugs is chemically similar to the granitoid rocks of the Helvetia stocks, aside from the quartz diorite stock. The mean of the analysis of the ore porphyry resembles somewhat the biotite adamellite of Nockolds' (1954, p. 1014) except that it contains more Na₂O and less K₂O, total Fe, and MgO.

The modal data, combined with some petrographic descriptions, suggest that the plugs were emplaced from a fairly hot, fluid magma. The abundant sanidine and rare oxybiotite in the ore porphyry and the concentration of tactite in chemically suitable rocks near some plugs are indicative of a high magma temperature. Magma fluidity is suggested by the ameoboid shape of some plugs, by the abundance of dikes, and by the association with abundant hydrothermal mineralization.

AGE AND CORRELATION

The age of the quartz latite porphyry of the Greaterville plugs obtained through radiometric dating methods is more definitive than that obtained through the observations of geologic relations to dated rocks. The porphyry intrudes rocks as young as the Apache Canyon Formation of the Bisbee Group, and it is unconformably overlain by gravel no older than Pleistocene age. It does not come into contact with the granitoid rocks of the Helvetia stocks, although there are some similarities between the rock in the core of the Sycamore plug and the rocks of the Helvetia stocks.

The porphyry does, however, intrude faults, some of which truncate the Helvetia stocks. For example, the Sycamore plug and nearby dikes and pipes are intruded along faults that cut the Johnson Ranch and Sycamore stocks a half a mile northeast of Johnson Ranch (Drewes, 1972b, pl. 5). Similarly, the Helvetia plug is seen to truncate the east edge of the klippe at Helvetia, which is faulted across the Shamrod and Helvetia stocks. The postulated age relation between the coarse-grained (older) stocks and the fine-grained (younger) plugs is compatible with an environment of emplacement that changed during the brief interval between two times of intrusive activity. The earlier intrusives may have been relatively deep-seated and the later ones relatively shallow, as a result of local tectonic action, uplift, and consequent erosion.

Three potassium-argon ages were obtained from biotite concentrates derived from separate plugs; they are specimens 189, 192, and the unnumbered specimen following 192 in table 4 (field number 68D1472, fig. 40), which has not been modally or chemically analyzed. The ages range from 55.7 to 56.3 m.y., a range sufficiently small to provide considerable confidence in their accuracy. The confidence is only justified, however, if the plugs are known to be emplaced simultaneously. This evaluation of three nearly identical ages is similar to that of the radiometric ages of the Helvetia stocks; the ages support each other only if independent evidence shows that the intrusive events were coeval. There is, indeed, some cause to doubt that either the faulting or the intrusive activity of the Helvetian phase of the Laramide orogeny, or both events, were geologically instantaneous events (Drewes, 1972b, p. 32–33).

One dating problem is obvious: the radiometrically determined ages indicate that the Greaterville plugs are about 2 m.y. older than the Helvetia stocks, whereas their geologic relations suggest that the stocks are older than the plugs. The resolution of this problem may require additional dating of minerals other than biotite and perhaps the dating of more of the stocks and plugs. Additional fieldwork may yet lead to direct evidence of the relationship between these intrusive bodies. Furthermore, controls are needed to measure the range of time that may elapse between the emplacement of an intrusive body and its cooling to a temperature at which the radiometric "clock" is set.

Intrusive rocks resembling the quartz latite porphyry, or ore porphyry, of the Greaterville plugs occur in at least two nearby ranges. The ore porphyry of the Sierrita Mountains (fig. 1) is described by Cooper (1974) as a quartz monzonite porphyry, but its groundmass is clearly aphanitic and of the same size as that of the Greaterville plugs. His quartz monzonite porphyry has the same distinctive bipyramidal quartz phenocrysts and small biotite crystals, and it is spatially and probably also genetically related to the ore deposits at the Sierrita, Esperanza, Twin Buttes, and Pima mines. It is dated as 53.5 m.y. by Damon and Mauger (1966) and as 56.9 m.y. by S. C. Creasey (1964, written commun.), ages suggestive of those of the Helvetia stocks and Greaterville plugs.

Other intrusive rocks resembling the ore porphyry are found in the Empire Mountains and in the hills between them and the Santa Rita Mountains (Finnell, 1971). Some of these intrusive rocks are also associated with copper mineralization, but they are not radiometrically dated and cannot be closely dated by geologic means.

GRANODIORITE OF THE SAN CAYETANO STOCK

A small stock of granodiorite, of late(?) Oligocene age, is the youngest plutonic rock of the Santa Rita area. The stock crops out over an area of about a half a square mile, and it probably extends beneath the piedmont gravel for another half a square mile or more. It appears to have steep contacts and no apophyses or chilled-contact zone. The host rocks are mainly Josephine Canyon Diorite but also include some rhyodacite porphyry dikes; none of the host rocks are contact metamorphosed near the stock. Other rhyodacite porphyry dikes of the same swarm intrude the stock, so dikes and stock may be penecontemporaneous.

The granodiorite is a massive, moderately coarse-grained light-gray rock that weathers to form low knolls, boulderlike residual blocks, and extensive deposits of grus. The rock has a hypidiomorphic-granular texture and a small amount of myrmekitic and lacy perthitic texture and a maximum grain size of 4 mm. As listed in the modal

TABLE 21.—Modes of quartz latite porphyry of the Greaterville plugs

[Field numbers are abbreviated; year of collection and collector's initial omitted. Full field number of specimen 184 thus is 65D894. Symbols: s, standard deviation; Tr., trace; . . . , not determined; a (?) following number indicates uncertainty in the reported value; a (?) preceding number indicates uncertainty in identification of core or rim position within crystal]

Intrusive mass	Plugs at Greaterville				Rosemont plug			Summit plug				Helvetia plug				Sycamore plug	184—195	
Specimen No.	184	185	186	184—186 Mean	187	188	187,188 Mean	189	190	191	189—191 Mean	192	193	194	192—194 Mean	195	184—195 Mean	s
Field No.	894	893	921		1098	1129		1185	1183	1209		1245	1244	1236		1224		
Quartz	20.9	22.9	24.4	22.7	22.8	29.6	26.2	27.9	26.1	21.0	25.0	24.1	30.6	21.8	25.5	25.2	24.8	3.2
Plagioclase, total	47.1	45.2	56.1	49.5	41.5	43.5	42.5	41.9	37.0	47.0	42.0	44.9	43.4	42.0	43.4	45.3	44.6	4.6
(plagioclase in perthite)	(0.3)	(Tr.)	(Tr.)	(0.1)	0	0	0	(Tr.)	(Tr.)	0	(Tr.)	(Tr.)	0	(1.6)	(0.5)	(3.1)	(0.4)	(1.0)
K-feldspar, total	26.6	26.3	13.6	22.2	33.0	23.2	28.1	26.3	31.8	27.6	28.6	27.4	22.4	33.0	27.6	26.2	26.5	5.3
(sanidine)	0	0	0	0	0	0	0	(26.3)?	(31.8)	(27.0)	(28.6)	(27.4)?	(22.4)?	(33.0)	(27.6)	(26.2)	(16.2)	(4.5)
(orthoclase)	(26.6)	(26.3)	(13.6)	(22.2)	(33.0)	(23.2)	(28.1)	0	0	0	0	0?	0?	0?	0	0	(11.6)	(13.7)
(microcline)	0	0	0	0	0	0	0	0	0	0	0	0	0	0	0	(Tr.)	(Tr.)
Biotite	4.2	3.9	4.2	4.1	2.1	2.7	2.4	3.0	3.3	3.5	3.3	2.7	2.2	1.8	1.9	2.9	3.0	.8
Magnetite	.3	1.1	.2	.5	.6	.8	.7	.7	1.3	.8	.9	.3	1.0	1.1	.8	.1	.7	.4
Pyrite	0	0	1.2	.4	0	Tr.	Tr.	0	0	0	0	Tr.	0	Tr.	Tr.	Tr.	.1	.1
Apatite	Tr.	.3	.2	.2	Tr.	.1	.05	.2	.2	.1	.2	.4	.1	.05	.2	.2	.2	.1
Sphene	.8	.2	.1	.4	Tr.	.05	Tr.	Tr.	.2	Tr.	.07	.1	.3	.3	.2	.1	.2	.2
Zircon	.1	.05	Tr.	.05	Tr.	Tr.	Tr.	Tr.	.1	Tr.	Tr.	.05	Tr.	Tr.	Tr.	0	Tr.
Allanite	0	.05	0	Tr.	0	0	0	0	0	0	0	.05	0	Tr.	Tr.	0	Tr.
Rutile	0	0	0	0	Tr.	.1	.05	0	0	0	0	0	0	Tr.	Tr.	0	Tr.
Total	100.0	100.0	100.0	100.05	100.0	100.05	100.0	100.0	100.0	100.0	100.07	100.0	100.0	100.05	99.6	100.0	100.1
Femic	5.4	5.6	5.9	5.7	2.7	3.7	3.2	3.9	5.1	4.4	4.5	3.6	3.6	3.2	3.1	3.3	4.3	1.1
Percent anorthite in plagioclase (plagioclase rims)	20—10	29—37	32—34	29—37	27	27	20—28	23	?12	20—28	25?	12	23—24	23—25	?10	20—37
Quartz mixing index (see text)	.70	.84	.87	.828681	.84	.94	.98	.92	.95	.77	.86	.08

¹ Modes of specimens 187 and 188 are less reliable than the other modes because these specimens are finer grained and more strongly altered. Quartz: K-feldspar ratio of specimen 183 adjusted 15 percent as based on ratios typical of this group of rocks.

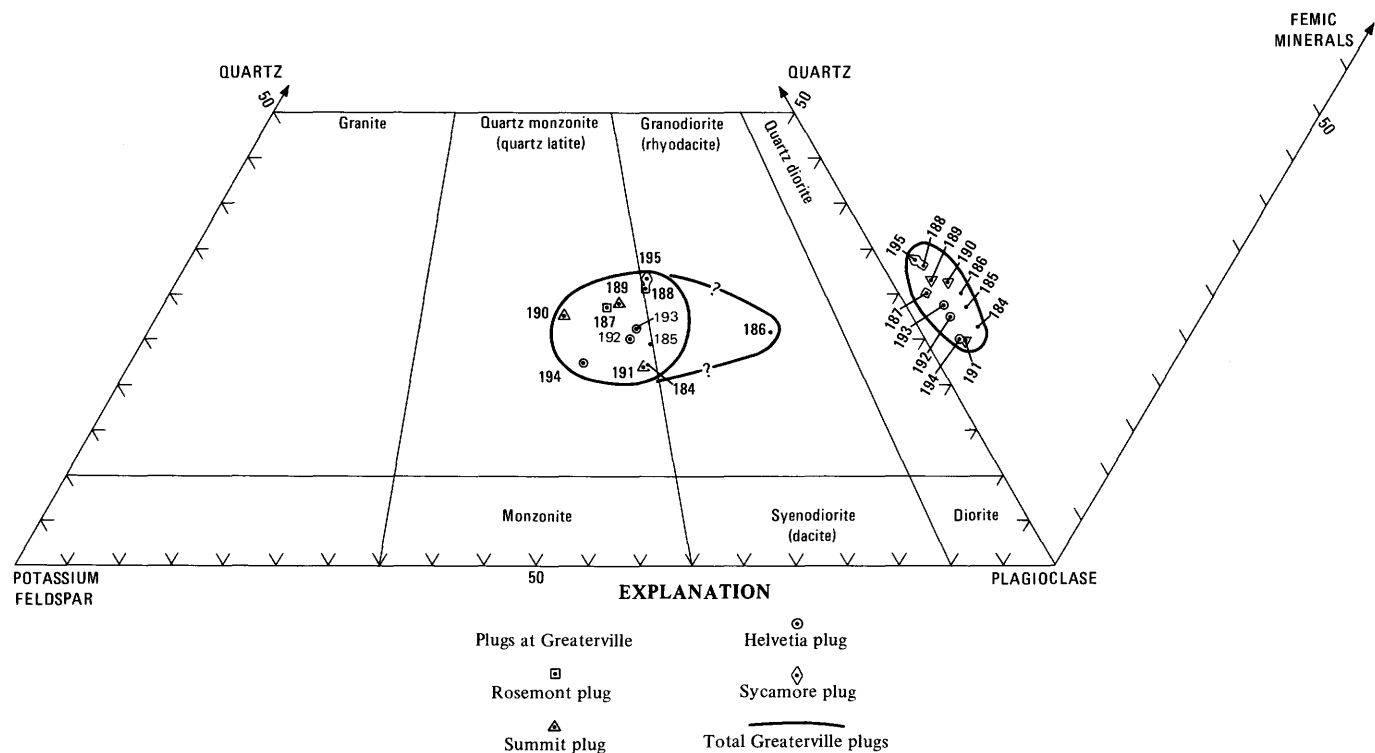


FIGURE 45.—Modified triangular diagram showing modal quartz, potassium feldspar, plagioclase, and femic minerals of quartz latite porphyry of the Greaterville plugs.

TABLE 22.—*Chemical and spectrographic analyses and CIPW norms of quartz latite porphyry of the Greaterville plugs*

[Chemical analysis of specimen 195 by single solution method (Shapiro and Massoni, 1968); other specimens analyzed by rapid rock method (Shapiro and Brannock, 1962), supplemented by atomic absorption method. Chemical analysts: Lowell Artis, S. D. Botts, G. W. Chloe, P. L. D. Elmore, John Glenn, J. Kelsey, and H. Smith. Spectrographic analyses by semiquantitative method. Spectrographic analyst: J. L. Harris. Elements looked for but not found: As, Au, B, Bi, Cd, Co, Eu, Ge, Hf, Hg, In, Li, Nd, Ni, Pd, Pr, Pt, Re, Sb, Sm, Sn, Ta, Te, Th, Tl, U, W, and Zn. Symbol: *s* standard deviation; <, less than;, not determined]

Intrusive mass.....	Plug at Greaterville				Summit plug		Helvetia plug		Sycamore plug	
Specimen No.....	185	189	190	189,190 Mean	192	194	192,194 Mean	195	185-195	
Field No.....	893	1185	1183		1245	1236		1224	Mean	<i>s</i>
Chemical analyses (weight percent)										
SiO ₂	69.4	72.5	72.2	72.4	72.9	72.6	72.8	70.9	71.8	1.3
Al ₂ O ₃	16.0	14.4	14.7	14.6	14.2	14.4	14.3	15.0	14.8	.7
Fe ₂ O ₃	1.8	1.2	1.2	1.2	.86	.94	.90	.78	1.1	.4
FeO82	.36	.52	.44	.76	.60	.68	.84	.65	.2
MgO51	.46	.46	.46	.49	.47	.48	.58	.50	.05
CaO	2.3	1.7	1.2	1.5	1.4	1.6	1.5	2.3	1.8	.5
Na ₂ O	4.2	3.8	3.5	3.7	4.2	4.2	4.2	3.7	3.9	.3
K ₂ O	3.5	4.4	4.6	4.5	4.0	3.9	4.0	3.8	4.0	.4
H ₂ O-21	.17	.08	.13	.04	.05	.05	.22	.13	.1
H ₂ O+89	.67	.74	.71	.51	.51	.51	.98	.72	.2
TiO ₂39	.14	.17	.16	.15	.15	.15	.16	.19	.1
P ₂ O ₃14	.07	.08	.08	.08	.06	.07	.11	.09	.03
MnO06	.02	.07	.05	.03	.04	.04	.16	.06	.05
CO ₂05	<.05	<.05	<.05	<.05	<.05	<.05	.28	.05	.01
Total	100	100	100	100	100	100	100	100	100
Spectrographic analyses (weight percent)										
Ag	0	0	<0.0001	<0.0001	40	<0.0001	<0.0001	<0.0001	<0.0001
Ba1	.07	.1	.09	.07	.07	.07	.07	.08	0.02
Be0001	.003	.0003	.0003	.0003	.0002	.0003	.0002	.0002	.00008
Ce01	.03	0	.015	.02	.03	.03	.01	.02	.01
Cr	0	.0003	0	.00015	.002	0	.001	0	.0004	.0008
Cu0003	.05	.15	.1	.015	.07	.04	.0003	.05	.06
Ga0015	.0015	.0015	.0015	.0015	.0015	.0015	.001	.0015	.0002
La005	.01	0	.005	.007	.01	.009	.007	.007	.004
Mo0003	.0003	0	.00015	0	0	0	.0003	.00015	.00015
Nb001	.001	.001	.001	.001	.001	.001	0	.0008	.0004
Pb0003	.0007	.0007	.0007	.0005	.0003	.0004	.001	.0006	.0003
Sc0005	.001	.0003	.0007	.0007	.0003	.0005	.0003	.0005	.0003
Sr05	.03	.03	.03	.03	.03	.03	.015	.03	.01
V003	.0015	.0015	.0015	.0015	.0015	.0015	.0015	.002	.0006
Y002	.002	.0015	.0002	.0015	.002	.0002	.002	.002	.0003
Yb0002	.0002	.00015	.0002	.00015	.0002	.0002	.0002	.0002	.00003
Zr015	.007	.01	.009	.01	.007	.009	.01	.01	.003
CIPW norms										
Q	26.3	29.6	31.5	29.7	29.5	29.8
C	1.6	.58	2.173	.62	1.5
or	20.6	26.0	27.3	23.7	23.1	22.5
ab	35.4	32.2	29.7	35.7	35.7	31.4
an	10.2	7.7	5.1	6.1	7.3	8.9
di { wo	0	0	0	0	0	0
{ en	0	0	0	0	0	0
{ fs	0	0	0	0	0	0
hy { en	1.3	1.1	1.2	1.2	1.2	1.4
{ fs	0	0	050	.1593
mt	1.7	.82	1.4	1.3	1.4	1.1
hm62	.64	.23	0	0	0
il74	.27	.3229	.2930
ap33	.17	.1919	.1426
cc11	.11	.1111	.1164
Total	98.9	99.2	99.2	99.5	99.5	98.7
Femic	4.8	3.1	3.5	3.6	3.3	4.6

¹Average of two replicate analyses.

²A replicate analysis shows Fe₂O₃, 0.28; FeO, 1.2; MgO, 0.34; CaO, 2.1; P₂O₅, 0.15; and other minor differences.

³A replicate analysis shows Cu, 0.03; Ni, 0.0005; Pb, 0.002; Sc, 0.003; Mo and Be, not detected; and other minor differences.

⁴A replicate analysis shows Ag < 0.0001; La, 0.003; Pb, 0.005; Sc, 0; and other minor differences.

analyses of table 23, the dominant minerals are quartz, plagioclase, orthoclase, biotite, and amphibole. The modes are plotted on the modified triangular diagram of figure 39. The quartz is anhedral and has a slight undulatory extinction, and the orthoclase is subhedral to anhedral. The plagioclase, also subhedral, has a composition of sodic andesine. Biotite is pleochroic in pale yellowish brown to dark brown and is only slightly chloritized. Amphibole, probably a hornblende, is pleochroic in pale yellowish green to pale olive green. Accessory minerals are ilmenitic magnetite, apatite, sphene, and zircon. Secondary minerals are sericite, epidote, kaolinite, iron oxides, and leucoxene, all in small amounts.

Chemical and spectrographic analyses and a CIPW norm are listed in table 24, and the chemical analysis is summarized on the histogram of figure 10F.

The granodiorite of the San Cayetano stock is dated as 27.6 m.y., or late(?) Oligocene, by the potassium-argon radiometric method using a biotite concentrate. The radiometric age is compatible with the age range available through the geologic relations to other rocks.

Granitoid rocks of Oligocene age are not known in nearby ranges, but granodiorite stocks of Oligocene age were found in the Rincon Mountains (Drewes, 1974), which is the next range northeast of the Santa Rita Mountains (fig. 1) and more than 50 miles from the San Cayetano stock.

The granodiorite of the San Cayetano stock is, however, genetically related to a pile of rhyodacite vitrophyre volcanics in the Grosvenor Hills, immediately east of the

San Cayetano Mountains. The volcanic rocks were intruded at shallow depths by several rhyodacite vitrophyre laccoliths, whose feeder dikes extend westward toward a major normal fault at the eastern foot of the San Cayetano Mountains, along which the San Cayetano block was raised a few thousand feet (Drewes, 1971c). The swarm of rhyodacite porphyry dikes of the San Cayetano Mountains which are penecontemporaneous with the stock occupy the same fracture system intruded by the rhyodacite vitrophyre feeder dikes of the laccoliths. The dikes, laccoliths, and volcanic rocks are petrographically and chemically very similar, and these rocks also are chemically somewhat like the granodiorite. Furthermore, the radiometric ages of the stock, the laccoliths, and the lava flows are almost identical. Because of these similarities, the stock is believed to be the remains of a magma chamber, which was the source of a western extension of the volcanic pile, now eroded away. If this interpretation is correct, a similar stock may underlie the volcanic pile at a depth of several thousand feet. Details of this complex magma system are described by Drewes (1972a).

TABLE 24.—Chemical and spectrographic analyses and CIPW norms of granodiorite of the San Cayetano stock, specimen number 196¹

[Chemical analysis by rapid rock method (Shapiro and Brannock, 1962) supplemented by X-ray fluorescence method. Chemical analysts: Lowell Artis, S. D. Botts, and P. L. D. Elmore. Spectrographic analysis by A. L. Sutton, Jr. Elements looked for but not found: Ag, As, Au, B, Bi, Cd, Ce, Eu, Ge, Hf, Hg, In, Li, Mo, Nb, Nd, Pd, Pr, Pt, Re, Sb, Sm, Sn, Ta, Te, Th, Tl, U, W, and Zn. Symbol: <, less than]

TABLE 23.—Modes of granodiorite of the San Cayetano stock

[Field numbers are abbreviated; year of collection and collector's initial omitted. Full field number of specimen 196 thus is 64D570. Tr., trace]

Specimen No.	196	197	196, 197 Mean
Field No.	570	687	
Quartz	23.2	22.4	22.8
Plagioclase, total	50.6	47.7	49.2
(in perthite)	(Tr.)	0	(Tr.)
Orthoclase	15.4	20.7	18.1
Hornblende	4.5	3.2	3.9
Biotite	5.2	5.3	5.3
Magnetite	.8	.4	.6
Apatite	.2	.2	.2
Sphene	.1	.1	.1
Zircon	.05	Tr.	Tr.
Total	100.05	100.0	100.2
Femic	10.8	9.2	10.1
Percent anorthite in plagioclase	32–35	29–32	29–35
Quartz mixing index (see text)	0.99	0.94	0.97

Chemical analysis (weight percent)			
SiO ₂	69.5	H ₂ O—	0.27
Al ₂ O ₃	15.2	H ₂ O+	.58
Fe ₂ O ₃	1.0	TiO ₂	.31
FeO	1.1	P ₂ O ₅	.14
MgO	1.4	MnO	.04
CaO	3.2	CO ₂	<.05
Na ₂ O	4.4		
K ₂ O	2.8	Total	100
Spectrographic analysis (weight percent)			
Ba	0.1	Pb	0.0015
Be	.0002	Sc	.001
Co	.001	Sr	.07
Cr	.007	V	.007
Cu	.0005	Y	.002
Ga	.002	Yb	.00015
La	.003	Zr	.01
Ni	.005		
CIPW norms			
Q	24.6	hy { en	3.0
or	16.5	fs	.66
ab	37.2	mt	1.5
an	13.5	il	.59
di { wo	.62	ap	.33
en	.46		
fs	.10	Total	99.1
		Femic	7.3

¹ Field number 570.

REFERENCES CITED

- Banks, N. G., 1974, Distribution of copper in biotite and biotite alteration products in intrusive rocks near two Arizona porphyry copper deposits: U.S. Geol. Survey Jour. Research, v. 2, no. 2, p. 195–211.
- Bateman, P. C., 1961, Granitic formations in the east-central Sierra Nevada near Bishop, California: Geol. Soc. America Bull., v. 72, no. 10, p. 1521–1537.
- Bikerman, Michael, and Damon, P. E., 1966, K/Ar chronology of the Tucson Mountains, Pima County, Arizona: Geol. Soc. America Bull., v. 77, no. 11, p. 1225–1234.
- Cooper, J. R., 1974, Geologic map of the Twin Buttes quadrangle, southwest of Tucson, Pima County, Arizona: U.S. Geol. Survey Misc. Inv. Ser. Map I–745.
- Cooper, J. R., and Silver, L. T., 1964, Geology and ore deposits of the Dragoon quadrangle, Cochise County, Arizona: U.S. Geol. Survey Prof. Paper 416, 196 p.
- Creasey, S. C., 1967, Geologic map of the Benson quadrangle, Cochise and Pima Counties, Arizona: U.S. Geol. Survey Misc. Inv. Ser. Map I–470.
- Creasey, S. C., and Kistler, R. W., 1962, Age of some copper-bearing porphyries and other igneous rocks in southeastern Arizona, in *Short papers in geology, hydrology, and topography*: U.S. Geol. Survey Prof. Paper 450–D, p. D1–D5.
- Creasey, S. C., and Quick, G. L., 1955, Copper deposits of part of Helvetia mining district, Pima County, Arizona: U.S. Geol. Survey Bull. 1027–F, p. 301–323.
- Damon, P. E., [compiler], 1965, Correlation and chronology of ore deposits and volcanic rocks—U.S. Atomic Energy Comm. Contract AT(11–1)–689, Ann. Prog. Rept. COO–689–50: Tucson, Ariz., Arizona Univ. Geochronology Labs., 157 p.
- _____, 1966, Correlation and chronology of ore deposits and volcanic rocks—U.S. Atomic Energy Comm. Contract AT(11–1)–689, Ann. Prog. Rept. COO–689–60: Tucson, Ariz., Arizona Univ. Geochronology Labs., 154 p.
- Damon, P. E., and Mauger, R. L., 1966, Epeirogeny-orogeny viewed from the Basin and Range province: Soc. Mining Engineers Trans., v. 235, no. p. 99–112.
- Drewes, Harald, 1968, New and revised stratigraphic names in the Santa Rita Mountains of southeastern Arizona: U.S. Geol. Survey Bull. 1274–C, 15 p.
- _____, 1970, Structural control of geochemical anomalies in the Greater-ville mining district, southeast of Tucson, Arizona: U.S. Geol. Survey Bull. 1312–A, 49 p.
- _____, 1971a, Mesozoic stratigraphy of the Santa Rita Mountains, southeast of Tucson, Arizona: U.S. Geol. Survey Prof. Paper 658–C, 81 p.
- _____, 1971b, Geologic map of the Sahuarita quadrangle, southeast of Tucson, Pima County, Arizona: U.S. Geol. Survey Misc. Inv. Ser. Map I–613.
- _____, 1971c, Geologic map of the Mount Wrightson quadrangle, southeast of Tucson, Santa Cruz, and Pima Counties, Arizona: U.S. Geol. Survey Misc. Inv. Ser. Map I–614.
- _____, 1972a, Cenozoic rocks of the Santa Rita Mountains, southeast of Tucson, Arizona: U.S. Geol. Survey Prof. Paper 746, 66 p.
- _____, 1972b, Structural geology of the Santa Rita Mountains, southeast of Tucson, Arizona: U.S. Geol. Survey Prof. Paper 748, 35 p.
- _____, 1973, Geochemical reconnaissance of the Santa Rita Mountains, southeast of Tucson, Arizona: U.S. Geol. Survey Bull. 1365, 67 p.
- _____, 1975, Geologic map of the Happy Valley quadrangle, Cochise and Pima County, Arizona: U.S. Geol. Survey Misc. Inv. Ser. Map I–832.
- Finnell, T. L., 1971, Preliminary geologic map of the Empire Mountains quadrangle, Pima County, Arizona: U.S. Geol. Open-file map.
- Gilluly, James, 1956, General geology of central Cochise County, Arizona, with sections on Age and correlation, by A. R. Palmer, J. S. Williams, and J. B. Reeside, Jr.: U.S. Geol. Survey Prof. Paper 281, 169 p.
- Hayes, P. T., and Landis, E. R., 1964, Geologic map of the southern part of the Mule Mountains, Cochise County, Arizona: U.S. Geol. Survey Misc. Geol. Inv. Map I–418.
- Hayes, P. T., and Raup, R. B., 1968, Geologic map of the Huachuca and Mustang Mountains, southeastern Arizona: U.S. Geol. Survey Misc. Geol. Inv. Map I–509.
- Heyman, A. M., 1958, Geology of the Peach-Elgin copper deposit, Helvetia district, Arizona: Tucson, Ariz., Arizona Univ. unpub. M.S. thesis, 66 p.
- Johannsen, Albert, 1932, The quartz-bearing rocks, V. 2 of *A descriptive petrography of the igneous rocks*: Chicago Univ. Press, 428 p.
- _____, 1939, Introduction, textures, classifications, and glossary, V. 1 [2d ed.] of *A descriptive petrography of the igneous rocks*: Chicago Univ. Press, 318 p.
- Lacy, W. C., 1959, Structure and ore deposits of the East Sierrita area, in *Arizona Geol. Soc. Guidebook 2, 1959*: Arizona Geol. Soc. Digest, 2d Ann., p. 184–192.
- Lovering, T. G., Cooper, J. R., Drewes, Harald, and Cone, G. C., 1970, Copper in biotite from igneous rocks in southern Arizona as an ore indicator, in *Geological Survey research 1970*: U.S. Geol. Survey Prof. Paper 700–B, p. B1–B8.
- Marvin, R. F., Stern, T. W., Creasey, S. C., and Mehnert, H. H., 1973, Radiometric ages of igneous rocks from Pima, Santa Cruz, and Cochise Counties, southeastern Arizona: U.S. Geol. Survey Bull. 1379, 27 p.
- Michel, F. A., Jr., 1959, Geology of the King mine, Helvetia, Arizona: Tucson, Ariz., Arizona Univ. unpub. M.S. thesis, 59 p.
- Nockolds, S. R., 1954, Average chemical compositions of some igneous rocks: Geol. Soc. America Bull., v. 65, no. 10, p. 1007–1032.
- Ransome, F. L., 1904, The geology and ore deposits of the Bisbee quadrangle, Arizona: U.S. Geol. Survey Prof. Paper 21, 168 p.
- Ross, D. C., 1969, Descriptive petrography of three large granitic bodies in the Inyo Mountains, California: U.S. Geol. Survey Prof. Paper 601, 47 p.
- Schrader, F. C., 1915, Mineral deposits of the Santa Rita and Patagonia Mountains, Arizona, with contributions by J. M. Hill: U.S. Geol. Survey Bull. 582, 373 p.
- Shapiro, Leonard, and Brannock, W. W., 1962, Rapid analysis of silicate, carbonate, and phosphate rocks: U.S. Geol. Survey Bull. 1144–A, 56 p.
- Shapiro, Leonard, and Massoni, C. J., 1968, Automatic sample changer for atomic absorption spectrophotometry, in *Geological Survey research 1968*: U.S. Geol. Survey Prof. Paper 600–B, p. B126–B129.
- Simmons, F. S., 1974, Geologic map and sections of the Nogales and Lochiel quadrangles, Santa Cruz County, Arizona: U.S. Geol. Survey Misc. Inv. Ser. Map I–762.
- Turner, F. J., and Verhoogen, Jean, 1951, *Igneous and metamorphic petrology*: New York, McGraw-Hill Book Co., 602 p.
- Wilson, E. D., 1939, Pre-Cambrian Mazatzal revolution in central Arizona: Geol. Soc. America Bull., v. 50, no. 7, p. 1113–1164.
- Wilson, E. D., Moore, R. T., and Cooper, J. R., 1969, Geologic map of Arizona: Arizona Bur. Mines and U.S. Geol. Survey, Special Geologic Map.

INDEX

A	Page
Abstract	1
Age. <i>See</i> Radiometric dates.	
Agua Caliente Canyon	47
Alaskite, Continental Granodiorite	11
Amole Granite	32
Amole Quartz Monzonite	32
Apache Canyon Formation	29, 63
Apache Group	5
Aplitic rocks, Continental Granodiorite	9, 10, 11
Corona stock	29
Elephant Head Quartz Monzonite	48
Helvetia stocks	58
Huerfano stock	58
Pinal Schist	7
Squaw Gulch Granite	25, 27
Yoas stock	51
Artis, Lowell, analyst	16, 23, 31, 33, 40, 46, 54, 59, 64, 69, 70

B	Page
Batholith, Squaw Gulch Granite	24
Bathtub Formation	6
Bisbee Group	6, 29, 61, 63
Bolsa Quartzite	5, 9, 15
engulfed block	58
Boston syncline	63
Botts, S.D., analyst	16, 23, 31, 33, 40, 46, 54, 59, 64, 69, 70
Box Canyon	7, 9
xenoliths	10
Breccia pipe, Mansfield Canyon	55
Summit plug	65

C	Page
Cambrian rocks, Bolsa Quartzite	5, 9, 15, 58
Canelo Hills Volcanics	17
Cave Creek, quartz diorite	23
Chloe, G.W., analyst	16, 23, 31, 33, 40, 46, 54, 59, 64, 69
Continental Granite	5, 7, 9
aplitic rocks	11
correlation	15
granodiorite	9
modal analysis	11, 13
recrystallized	24
Copper Belle Monzonite Porphyry	23
Copper deposit, Summit plug	65
Corona de Tucson	29
Corona stock	6, 29, 31
Correlations, Continental Granodiorite	15
Copper Belle Monzonite Porphyry	23
Corona stock	31
Courtland area	23, 32
Elephant Head Quartz Monzonite	51, 53
Empire Mountains	16, 32, 67
Greaterville plugs	67
Harris Ranch Monzonite	23
Helvetia stocks	15
Josephine Canyon Diorite	39
Juniper Flat Granite	28
Madera Canyon Granodiorite	44
Mule Mountains	28
Nogales	40
Patagonia Mountains	16, 24, 28, 47
Piper Gulch Monzonite	23
Rincon Mountains	15, 70
Ruby area	40

Correlations—Continued	Page
Sierrita Granite	28
Sierrita Mountains	15, 23, 28, 47, 62, 67
Squaw Gulch Granite	28
Tucson Mountains	32
Whetstone Mountains	17, 32
Cottonwood Canyon	7
Crandell, W.B., analyst	16, 23, 31, 40, 46, 54, 64
Cretaceous rocks	28
Bathtub Formation	6
Bisbee Group	6, 29, 61, 63
Corona stock	6, 29, 31
Elephant Head Quartz Monzonite	6, 43, 47, 49
Fort Crittenden Formation	6
Josephine Canyon Diorite	6, 33, 34, 39, 41
Madera Canyon Granodiorite	6, 40
Salero Formation	6, 24, 26, 32, 47, 55
Temporal Formation	6, 24

D	Page
Dikes, Greaterville area	64
Helvetia mining district	64
Helvetia stocks	58
lamprophyre, Continental Granodiorite	13
map error, Yoas Mountain	48
Mansfield Canyon	55
rhyodacite porphyry	67
San Cayetano Mountains	70
Squaw Gulch Granite, lamprophyre	27
Diorites, Josephine Canyon Diorite	33, 34
San Cayetano Mountains	34
<i>See also</i> Quartz diorites.	
<i>See also</i> Syenodiorites.	

E	Page
Elephant Head	47, 48
Elephant Head Quartz Monzonite	6, 47
age	51
correlation	51, 53
intrusion	43
modal analysis	51
Quantrell stock	49
Yoas stock	50
Elmore, P.L.D., analyst	16, 23, 31, 33, 40, 46, 54, 59, 64, 69, 70
Empire Mountains, quartz monzonite stock	32
Enzenberg Canyon, xenoliths	10
Esperanza mine	67

F	Page
Faults, Continental Granodiorite	9, 15
fracture, Corona stock	32
Greaterville area	64
Greaterville plugs, quartz latite porphyry	57
Helvetia stock	67
Johnson Ranch stock	67
Laramide orogeny, Helvetian phase	7, 57, 61
northwest-trending, Helvetia mining district	64
Pinal Schist	7
quartz diorite	23
Santa Rita fault scar	6
Shamrod stock	67
shear zone, Continental Granodiorite	10
South Johnson Ranch stock	58

Faults—Continued	Page
Sycamore plug	65
Sycamore stock	67
thrust, Helvetia area	63
Finley, J.L., analyst	16, 23, 40, 46
Florida Canyon, quartz diorite	23
Fort Crittenden Formation	6

G	Page
Garner Canyon Formation	5
Geologic history	3
Glenn, John, analyst	16, 23, 31, 33, 40, 46, 54, 64, 69
Glove mine	24
Gneisses, granite gneiss	7
Pinal Schist	6
Granite gneiss	7
Granites, Amole Granite	32
Juniper Flat Granite	28
Sierrita Granite	28
Squaw Gulch Granite	24, 26
Granitoid rocks, Corona stock	29
Granodiorites, Continental Granodiorite	9
Corona stock	29
Gringo Gulch pluton	55
Helvetia stock	57
Helvetia stocks	57
Huerfano stock	57
Johnson Ranch stock	57
Josephine Canyon Diorite	33, 34
Madera Canyon Granodiorite	40
microgranodiorite	55
San Cayetano stock	67
Shamrod stock	57
South Johnson Ranch stock	57
Whetstone Mountains	32
Greaterville, Continental Granodiorite	15
Greaterville mining district	62
Greaterville plugs	62
age	67
correlation	67
modal analysis	66
petrography	65
Gringo Gulch	55
Gringo Gulch pluton	6, 55
age	57
modal analysis	57
Gringo Gulch Volcanics	6, 55
Grosvenor Hills, rhyodacite	
vitrophyre volcanics	70
Grosvenor Hills Volcanics	6

H	Page
Hamilton, J.C., analyst	23, 31, 40, 59
Harris, J.L., analyst	16, 40, 46, 54, 64, 69
Harris Ranch Monzonite	23
Helvetia, Continental Granodiorite	15
Helvetia mining district	62
Helvetia plug, copper ore	65
Helvetia stock	58, 67
Helvetia stocks	6
age	61
granitoid rocks	57
granodiorite	57
modal analysis	60
plugs of quartz latite porphyry	62
quartz monzonite	57
Helvetia townsite, klippe	65
Hornblende dacite porphyry	55
Hosey mine	34

	Page		Page		Page
Huerfano Butte	58	Mines, Esperanza	67	Plugs—Continued	
Huerfano stock	57	Glove	24	Rosemont	66
aplitic masses	58	Hosey	34	Summit	65
Hydrothermal deposit,		Pima	67	Porphyries, Gringo Gulch pluton	55
Josephine Canyon Diorite	34	Salero	55	hornblende dacite porphyry	55, 57
J		Sierrita	67	ore porphyry, Greaterville plugs	62
Johnson Ranch, plugs	65	Twin Buttes	67	quartz latite porphyry	55, 57
Johnson Ranch stock	57, 67	Modal analysis	11	rhyodacite porphyry dikes	67
Josephine Canyon	55	Modal tetrahedron	13	Precambrian rocks	6
lamprophyre dikes	27	Modes, Continental Granodiorite	12, 13	Apache Group	5
Squaw Gulch Granite	26	Corona stock	29	Continental Granite	5, 7, 9, 24
Josephine Canyon Diorite	33	Elephant Head Quartz Monzonite	51	granite gneiss	7
age	39	Greaterville plugs	66	Pinal Schist	3, 6
correlation	39	Gringo Gulch pluton	57	Q	
dioritic rocks	34	Helvetia stocks	60	Quantrell mine	48
intrusion	41	Madera Canyon Granodiorite	43	Quantrell stock	48
map error	48	Piper Gulch Monzonite	19, 21	Quartz diorite	23
petrography	34	quartz diorite	24	age	24
Juniper Flat Granite, correlation	28	Squaw Gulch Granite	28	modal analysis	24
Jurassic rocks	17	Sycamore stock	61	Quartz diorites, Helvetia stocks	61
Squaw Gulch Granite	10, 17, 18, 24	Montosa Canyon	47	Josephine Canyon Diorite	33
K, L		map error, Josephine Canyon Diorite	48	Sycamore stock	57
Kelsey, J., analyst	33, 64, 69	Piper Gulch Monzonite	19	Triassic quartz diorite	23
Klippe, Helvetia townsite	65	Monzonites, Piper Gulch Monzonite	17	Quartz latite porphyry	55
Laccoliths, San Cayetano Mountains	70	See also Quartz monzonites		Quartz latite porphyry of the	
Lamprophyre dikes, Yoas Mountain,		Morris, J.L., analyst	33	Greaterville plugs	62
map error	48	Mount Hopkins, Piper Gulch Monzonite	19	Quartz monzonites, Amole	
Lamprophyre rocks, Squaw Gulch Granite	27	Mount Wrightson Formation	5, 18	Quartz Monzonite	32
Lamprophyres, Continental Granodiorite	9, 13	Continental Granodiorite cobbles	15	Continental Granodiorite	9, 11
Corona stock	29	Madera Canyon Granodiorite intrusion	41	Corona stock	29
Elephant Head Quartz Monzonite	48	Mansfield Canyon, intrusion	55	Elephant Head Quartz Monzonite	47
Helvetia stocks	58	Mount Wrightson pile	17	Empire Mountains	32
Pinal Schist	7	Mount Wrightson quadrangle map error,		granite gneiss	7
Squaw Gulch Granite	25, 27	Josephine Canyon Diorite	48	Helvetia stock	57
Yoas stock	51	lamprophyre dikes	48	Helvetia stocks	57
Laramide orogeny	5, 17, 57	O, P		Johnson Ranch stock	57
Helvetian phase	6, 61, 67	Ore porphyry	6, 62	Josephine Canyon Diorite	33, 36
Piman phase	6, 9, 29	defined	65	Patagonia Mountains	28
M		Patagonia Mountains, Squaw Gulch Granite	24	Quantrell stock	49
Madera Canyon	50	Permian rocks, Rainvalley Formation	5	Shamrod stock	57
mouth	47	Petrography, Continental Granodiorite	9, 10, 12	South Johnson Ranch stock	57
Piper Gulch Monzonite	18	Corona stock	29	Squaw Gulch Granite	25, 26
rock dump	42	Elephant Head Quartz Monzonite,		Yoas stock	50
quartz diorite	23	Quantrell stock	49, 50	R	
Madera Canyon Granodiorite	40	Yoas stock	50	Radiometric dates,	
age	44	granite gneiss	9	Continental Granodiorite	15
correlation	44	Greaterville plugs	65	Elephant Head Quartz Monzonite	51
granodiorite	41	Gringo Gulch pluton, hornblende		Greaterville plugs	67
inclusions	41	dacite porphyry	56	Gringo Gulch pluton	57
melanocratic granodiorite	42	microgranodiorite	55	Helvetia stocks	62
modal analysis	43	quartz latite porphyry	57	Josephine Canyon Diorite	39
petrography	41	Helvetia stock	58	Madera Canyon Granodiorite	47
porphyritic granodiorite	42	Huerfano stock	58	Piper Gulch Monzonite	23
quartz diorite recrystallized	24	Josephine Canyon Diorite	34	quartz diorite	24
Magma development, Elephant		Madera Canyon Granodiorite	41	San Cayetano stock	70
Head Quartz Monzonite	51	Pinal Schist	7	Shamrod stock	62
Gringo Gulch pluton	57	Piper Gulch Monzonite	19	Squaw Gulch Granite	28
Josephine Canyon Diorite	37	Shamrod stock	58	Rainvalley Formation	5
Mansfield Canyon	34	Southeast stock	58	References cited	71
dikes	55	South Johnson Ranch stock	58	Rhyodacite welded tuff, San Pedro River	32
Piper Gulch Monzonite	19	Squaw Gulch Granite	25	Rosemont plug	65
Map errors discussed	48	Sycamore plug	66	Ruby Star Granodiorite	62
Mavis Wash, Continental Granodiorite	15	Sycamore stock	58	S	
Mazatzal Revolution	7	Pima mine	67	Salero Formation	6, 24
Microgranodiorite	55	Pinal Schist	3, 6	argillitized	47
Mineralization, Elephant Head		petrography	7	boulder	26
Quartz Monzonite	48	Pipe, Sycamore plug	65	exotic block	32
Helvetia plug	65	Piper Gulch Monzonite	6, 17	intrusion	26, 55
Josephine Canyon Diorite	34	age	23	Salero mine	55
Piper Gulch Monzonite	19	intrusion	41	San Cayetano Mountains, rhyodacite	
Rosemont area	65	modal analysis	19, 21	porphyry dikes	70
Summit plug	65	petrography	19	sill-like mass	55
Sycamore plug	65	Plugs, Greaterville area	64	San Pedro River, rhyodacite welded	
		Helvetia	65	tuff, age	32
		Helvetia stocks	62		
		Johnson Ranch	65		

